Effect of biomass variability on catalytic fast pyrolysis to produce renewable transportation fuels

by

Ravishankar Mahadevan

A dissertation submitted to the Graduate Faculty of
Auburn University
In partial fulfillment of the
Requirements for the Degree of
Doctor of Philosophy

Auburn, Alabama
December 10th, 2016

Keywords: Pyrolysis, biomass, catalyst, bio-oil, lignin torrefaction, *in-situ* upgrading

Approved by

Sushil Adhikari, Chair, Associate Professor of Biosystems Engineering
Oladiran Fasina, Professor of Biosystems Engineering
Jeremiah Davis, Associate Professor of Biosystems Engineering
Maria Auad, Associate Professor of Chemical Engineering

Abstract

The paradigm shift in recent years towards the use of renewable sources of energy to fuel economies around the world is primarily due to the limited availability of conventional sources such as fossil fuels, coal and methane. Global concern about climate change and air pollution related to the use of these fuels has also created the need to identify and utilize carbon-neutral sources of energy. Lignocellulosic biomass is one such carbon-neutral source of energy, which could be converted through catalytic fast pyrolysis (CFP) to produce energy in the form of syngas, hydrocarbon fuels and chemicals that can significantly reduce our dependence on crude oil and greenhouse gas emissions. However, economical conversion of biomass to produce fuels and chemicals of consistent quality is affected due to the innate variability in different types of biomass, specifically due to changes in its moisture content, bulk and particle density, carbohydrate content (cellulose and hemicellulose), lignin content and ash composition (alkali and alkaline earth metals or AAEMs) among other factors. This dissertation is an effort to understand some of the sources of variability in biomass and its ultimate impact on the downstream conversion process to produce renewable transportation fuels. A brief introduction to the background information of this study, including the motivation to pursue renewable bio-based resources and the rationale behind this work is discussed in Chapter 1.

The effect of variability in the ash composition of biomass on the primary breakdown of its constituents (cellulose, hemicellulose and lignin) and its subsequent influence on catalytic fast pyrolysis is elaborated in Chapter 2. In order to understand the individual influence of different AAEMs, biomass was doped with various levels of these metals and was subsequently converted to various products of pyrolysis in a micro-reactor. From this study, Mg was revealed to be relatively inert, while Ca, K and Na showed a stronger catalytic activity by influencing the pathways of thermal degradation of biomass. CFP product distribution was also influenced due to the presence of higher levels of Ca, K and Na in the biomass, resulting in changes in the selectivity of the products towards the formation of undesirable side-products (thermally-derived char and non-condensable gases) at the expense of the yield of aromatic hydrocarbons.

During biomass pyrolysis, the fate of various AAEMs after pyrolysis has been studied extensively and these metal species have been reported to volatilize and accumulate on the surface of the catalyst. Chapter 3 discusses the influence of these individual AAEMs on the functionality of the CFP catalyst during pyrolysis. ZSM-5 catalyst was deactivated by different levels of Ca, K and Na and the resulting changes in the properties of the catalyst are reported. Changes in the surface area and acidity of the catalyst due to deactivation by the individual AAEMs were correlated to the observed loss in activity when the catalysts were used in CFP experiments. Higher levels of deactivation (2, 5 wt.% of K or Na) were observed to render the catalyst completely inactive and resemble an inert material during CFP.

Lignin, one of the major components of biomass, varies in composition between different biomass species. Chapter 4 discusses the effect of thermal pretreatment (torrefaction) on lignin as

well as the resulting structural changes and its influence on the product distribution from pyrolysis. Organosolv lignin extracted from woody biomass (pine) and herbaceous biomass (switchgrass) was torrefied at different temperatures (150 ºC – 225 ºC), and the torrefied lignins were characterized to study the changes in the structure, which revealed the polycondensation and de-methoxylation of the aromatic units of lignin. Significant changes to the product distributions and selectivity from non-catalytic pyrolysis as well as CFP experiments are also reported in this chapter, which revealed that torrefaction could be detrimental to achieving a higher aromatic hydrocarbon yield from lignin. Finally, an overall summary and directions for future research in this field are presented in Chapter 5.

Dedicated to my dear Appa (Dad) and Amma (Mom)

Acknowledgements

I would like to express my gratitude to everyone who has been associated with my research during my time at Auburn. The past four years have been some of the most enriching experiences of my life. I consider myself fortunate and thankful to have had the opportunity to learn and work with my guru - Dr. Sushil Adhikari, who was a source of motivation, guidance and strong support through difficult personal and professional periods during my Ph.D. pursuit.

I would also like to thank Dr. Oladiran Fasina, Dr. Jeremiah Davis, Dr. Maria Auad and for serving as committee members as well as the graduate school representative Dr. Allan David for their time, interest and helpful comments. I am greatly indebted to Dr. David Dayton and Dr. Kaige Wang for their guidance during my internships at RTI International and for their support by providing the research infrastructure that made this work possible. I would like to acknowledge US Department of Agriculture-National Institute of Food and Agriculture (USDA-NIFA-2015-67021-22842) and National Science Foundation (NSF-CBET- 1333372) for their support by funding this study.

I am also thankful to all my friends and colleagues especially Rajdeep Shakya, Sneha Neupane and Zhouhong Wang for their invaluable support and collaboration on various projects. I consider myself very lucky to have met some great people who became family during my years in Auburn – Anshu Shrestha, Bharath Ramakrishnan, Nakul Kothari, Shantanu Deshpande and Shyamsundar Chattanathan.

Lastly, I would like to thank my family for all their love and encouragement. To my brother Prakash, thank you for sharing your love of science, and for constantly supporting and encouraging throughout all my pursuits. To my parents who provided me an education, none of this could have been possible without you. And to my grandfather, thank you for the continuing motivation to pursue my dreams.

Table of Contents

List of Figures

List of Tables

1. Introduction

Transportation fuels produced from renewable sources of energy can significantly reduce the stress on fossil fuels to power the global economy. The drive to identify and develop cost-effective and carbon neutral alternatives to fossil fuels has resulted in the increased interest in solar, hydroelectric, wind, geothermal and nuclear power plants. However, hydrocarbon-based fuels are still required to meet our growing demands for transportation, specialty chemicals, lubricating oil, hydraulic fluids. Biomass is one of the solutions primarily due to its carbon neutral nature, since the carbon dioxide released into the atmosphere during combustion is offset by the absorption of carbon dioxide by plants through photosynthesis during their growth. It is a sustainable and renewable source capable of yielding petroleum like hydrocarbon products for liquid fuels and for conversion into chemicals, which can meet the energy demand without having adverse effects on the environment [2]. It is seen as an excellent renewable feedstock because it is both abundant and inexpensive [3]. The billion-ton study by the United States Department of Energy states that biofuels produced from renewable sources such as biomass could replace one-thirds of the annual consumption of fuels in the United States [4]. Further, the United States Energy Independence and Security Act of 2007 mandates the production of 36 billion gallons of biofuels per year by 2022.

Several pathways (thermochemical, biochemical and catalytic) have been proposed for the conversion of biomass to produce hydrocarbon fuels (Figure 1.1). Although the biochemical conversion pathway of biomass to ethanol through fermentation has become commercially viable and is being developed in a large scale, achieving the targeted 36 billion gallons per year requires utilizing all the available biomass resources such as forest residues, energy crops, herbaceous

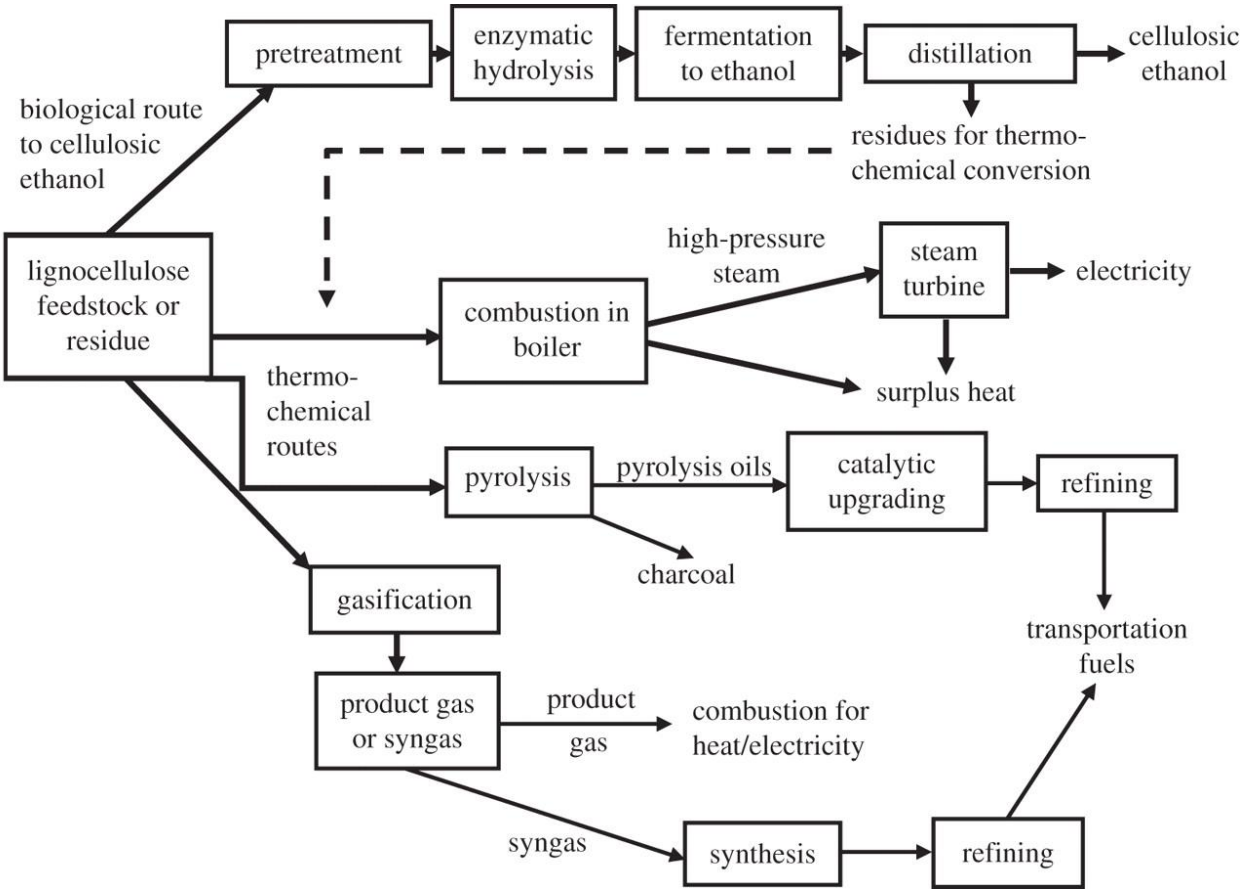

Figure 1.1. Technologies for conversion of biomass to biofuels, energy and chemicals

grasses, etc. It is also imperative that other supporting cost-effective technologies are developed, which can convert these wide range of biomass feedstocks into liquid fuels. Another disadvantage of producing biofuels through the fermentation pathway is the competition between food and energy needs, leading to a high demand for arable land and directly contributing to the rise in food prices. Increasing prices of sugarcane and corn in the Brazil and US have been attributed to the demand for these crops for food and energy production simultaneously [5]. This creates a need to produce renewable biofuels from fast growing forest based biomass resources which does not compete with the availability of land for food cultivation [6]. The thermochemical pathway, particularly pyrolysis and gasification are attractive in this regard since they can utilize a wide

range of biomass species as feedstocks and can be developed throughout the world without over dependence on a particular biomass.

Among the thermochemical processes, conversion through fast pyrolysis has been touted as one of the most promising technologies, since it directly produces a high yield of liquid product known as bio-oil or bio-crude [7-9]. In fast pyrolysis, biomass is converted in the absence of oxygen to produce bio-char, non-condensable gases and bio-oil as products. A detailed literature review, including the classification of types of pyrolysis, influence of various operating parameters (residence time, temperature, heating rate, particle size), reactor configurations and catalytic upgrading has been described in literature as part of a master's thesis of the author [10]. This process has been investigated extensively by researchers, since the bio-oil could potentially be upgraded to produce renewable transportation fuels by using existing infrastructure in the hydrotreating, hydrocracking and catalytic cracking operations in the petroleum industry [11, 12].

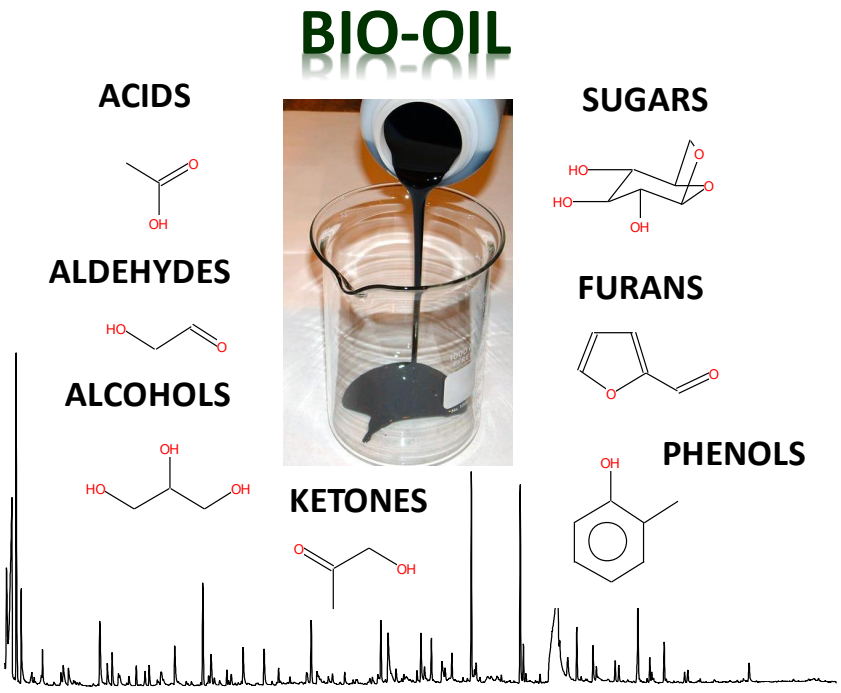

Figure 1.2. Functional groups typicaly observed from GC-MS analysis of bio-oil from pyrolysis

However, one of the key challenges to biomass pyrolysis is the complex chemical composition of bio-oil. During pyrolysis, rapid heating and fragmentation of the individual biomass components (cellulose, hemicellulose and lignin) produces a pyrolysis vapor composed of active free radicals, which subsequently condense to form the bio-oil with a wide range of compounds with functional groups such as phenols, carboxylic acids, esters, furans, ketones, aldehydes and water. The physical and chemical properties of bio-oil, listed in Table 1.1, are also different from the conventional fuels, primarily due to the complex chemical composition of bio-oil, whose component species tend to react further until they reach thermodynamic equilibrium [13]. Operating parameters such as temperature, heating rate, residence time, reactor configuration as well as the composition of biomass can influence the properties of bio-oil obtained.

Table 1.1. Propeties of bio-oil compared to conventional fuels

Properties	Unit	Bio-oil	Diesel	Heavy fuel oil
Density	kg/m^3 at 15˚C	1220	854	963
Typical composition	% C	48.5	86.3	86.1
	% H	6.4	12.8	11.8
	% O	42.5	-	-
	% S	-	0.9	2.1
Viscosity	cSt at 50˚C	13	2.5	351
Flash point	˚C	66	70	100
Water	% wt	20.5	0.1	0.1
LHV	MJ/kg	17.5	42.9	40.7
Acidity	pH	3	-	-

Potential applications are limited for bio-oil due to its high oxygen content, viscous and corrosive nature as well as due to it low heating value and poor stability, which creates the need to deoxygenate bio-oil (upgrade) to produce a product with greater heating value, better stability [14]. A review of the major upgrading techniques, including the use of various chemical catalysts such as zeolites and metal oxides has been described previously [7, 10, 13, 15-18]. Catalytic upgrading of the pyrolysis vapor enables the conversion of bio-oil to different end products, including value added chemicals such as alkanes, olefins, hydrogen, gasoline range aliphatic and aromatic hydrocarbons [19]. Catalytic upgrading is considered promising, since it involves low operating costs and also due to the wide range of catalysts available to produce high quality fuel and chemical products through pyrolysis.

1.1. Rationale

Figure 1.3 shows the projected supply of biomass resources in the USA by the year 2022. It is clear that the average price for the biomass feedstocks, depicted by the black line is significantly lower than the price of obtaining equivalent quantities of just a particular feedstock. It is quite clear that there is a strong need for biorefineries to use multiple feedstocks for conversion at the same time, as the cost per dry ton of using a single feedstock increases. Also, it reduces the dependency of the biorefinery on the availability of any one particular biomass and thus enables continuous supply of feedstock throughout the year. However, the use of different biomass feedstocks could have an impact on the bio-oil yield as well as the composition, thereby affecting the ability of the biorefinery to produce a product of consistent characteristics. There is a clear need to understand how important parameters that vary between different biomass species affect the overall conversion of biomass to the end-products.

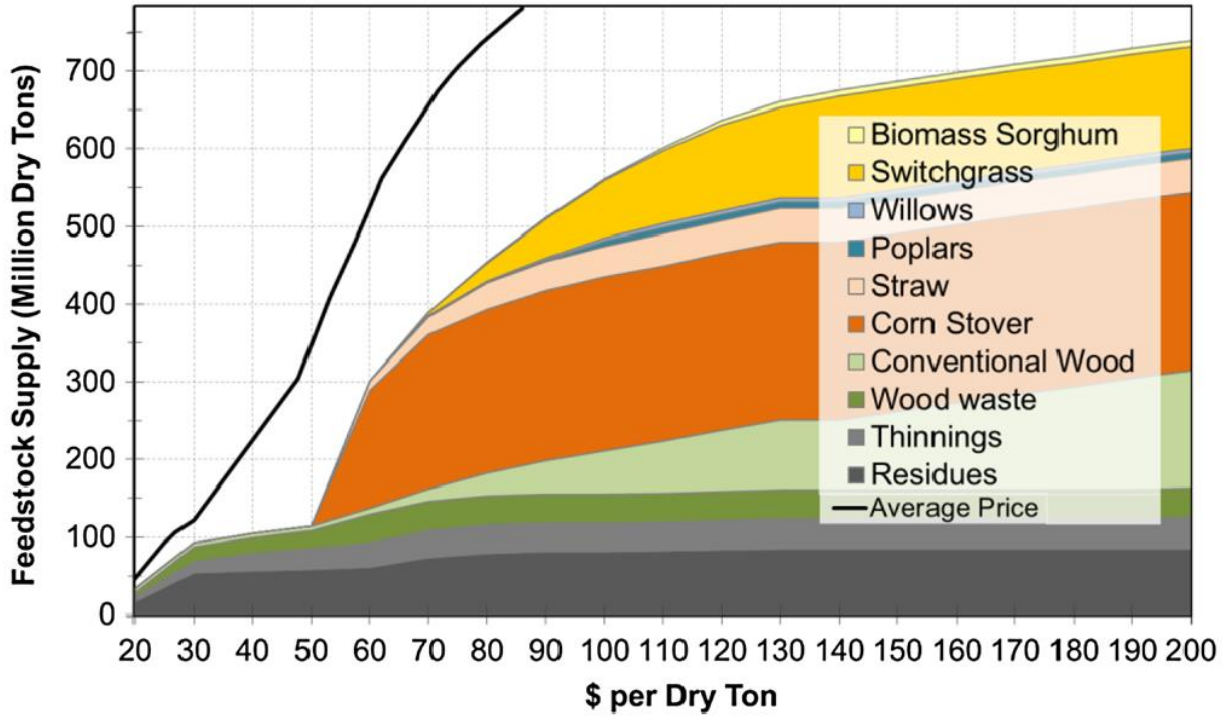

Figure 1.3. Biomass supply projections for feedstock prices between $20 and $200/dry ton in 2022 [1]

The fraction of hemicellulose, cellulose and lignin naturally varies from one biomass type to another and since they undergo pyrolysis differently and make varying contributions to the gas, liquid and char yield, it has a significant effect on the pyrolysis yield with respect to the product composition [20]. The physical properties of the biomass such as particle size, shape also have an influence due to their effect on heating rate [21]. The size of biomass particles in pyrolysis also varies according to the type of reactor in use [22-24]. Auger reactors, circulating fluidized bed reactors and ablative pyrolyzer can handle larger size feedstock (upto 6mm) whereas fluidized bed and entrained flow reactors require a smaller particle size (< 2mm) [25]. When biomass pyrolysis is employed at a commercial scale process, some of these parameters such as particle size, bulk density, particle density, heating rate and moisture content could be normalized in such a way that it does not vary between different biomass feedstocks before they are converted.

However, the composition of biomass with respect to its carbohydrate and lignin content, ash content and composition are factors that are not controlled and can seriously impact the economics of conversion to produce useful end products. For example, the ash content of woody biomass feedstocks is generally low (~0.5-1.0 %) whereas the herbaceous feedstocks such as switchgrass can have much higher ash contents (up to 5%), which could influence the yield and quality of the bio-oil. Concurrently, herbaceous feedstocks also have lower lignin content (~15 %) than woody biomass (~30%), which could change the properties of the bio-oil produced [1]. Further, the changes in composition of biomass could also impact its behavior during pretreatment processes before pyrolysis. For instance, biomass torrefaction has been reported recently by several researchers as a promising pretreatment technique to improve the O/C ratio of biomass and also improve the yield of aromatic hydrocarbons from catalytic fast pyrolysis. However, while the behavior of cellulose and hemicellulose during torrefaction is widely understood, the influence of this thermal pretreatment on lignin is not clear and it is possible that this process could also be affected by the natural variation in biomass.

1.2. Research Objectives

The overall objective of this study was to study the impact of variations in ash content, composition as well as lignin content on the pyrolysis and catalytic pyrolysis of biomass to produce renewable transportation fuels. This overall objective was accomplished by three specific objectives listed below:

1.2.1. Objective 1 – To understand the effect of alkali and alkaline earth metals on in-situ catalytic fast pyrolysis of biomass

1.2.2. Objective 2 - Influence of biomass inorganics on the functionality of HZSM-5 catalyst during in-situ catalytic fast pyrolysis of biomass

1.2.3. Objective 3 - Effect of torrefaction temperature on lignin macromolecule and product distribution from fast pyrolysis of biomass

These objectives were studied and presented in the chapters 2, 3 and 4 respectively. Based on th findings from these studies, an overall summary and directions for future research in this field are presented in Chapter 5.

1.3. References:

1. Williams, C.L., et al., *Sources of Biomass Feedstock Variability and the Potential Impact on Biofuels Production.* BioEnergy Research, 2016. **9**(1): p. 1-14.
2. Sims, R.E.H., et al., *An overview of second generation biofuel technologies.* Bioresource Technology, 2010. **101**(6): p. 1570-1580.
3. Wyman, C.E., et al., *Coordinated development of leading biomass pretreatment technologies.* Bioresour Technol, 2005. **96**(18): p. 1959-66.
4. Perlack, R.D., *Biomass as feedstock for a bioenergy and bioproducts industry the technical feasibility of a billion-ton annual supply.* United States. Dept. of, E.; United States. Dept. of, A.; Oak Ridge National, L., 2001.
5. Raele, R., et al., *Scenarios for the second generation ethanol in Brazil.* Technological Forecasting and Social Change, (0).
6. Hayes, D.J., *An examination of biorefining processes, catalysts and challenges.* Catalysis Today, 2009. **145**(1–2): p. 138-151.
7. Bridgwater, A.V., *Review of fast pyrolysis of biomass and product upgrading.* Biomass and Bioenergy, 2012. **38**(0): p. 68-94.
8. Effendi, A., H. Gerhauser, and A.V. Bridgwater, *Production of renewable phenolic resins by thermochemical conversion of biomass: A review.* Renewable and Sustainable Energy Reviews, 2008. **12**(8): p. 2092-2116.

9. Czernik, S. and A.V. Bridgwater, *Overview of Applications of Biomass Fast Pyrolysis Oil.* Energy & Fuels, 2004. **18**(2): p. 590-598.
10. Mahadevan, R., *Experimental Study of Biomass Pyrolysis in a Fluidized Bed Reactor: Effect of Biomass Blending and In-situ Catalysis*. 2015, Auburn University.
11. Lødeng, R., et al., *Chapter 11 - Catalytic Hydrotreatment of Bio-Oils for High-Quality Fuel Production*, in *The Role of Catalysis for the Sustainable Production of Bio-fuels and Bio-chemicals*, K.S. Triantafyllidis, A.A. Lappas, and M. Stöcker, Editors. 2013, Elsevier: Amsterdam. p. 351-396.
12. Baker, E.G. and D.C. Elliott, *Catalytic hydrotreating of biomass-derived oils.* Pyrolysis Oils from Biomass, 1988. **376**: p. 353.
13. Zhang, Q., et al., *Review of biomass pyrolysis oil properties and upgrading research.* Energy Conversion and Management, 2007. **48**(1): p. 87-92.
14. Lu, Q., W.Z. Li, and X.F. Zhu, *Overview of fuel properties of biomass fast pyrolysis oils.* Energy Conversion and Management, 2009. **50**(5): p. 1376-1383.
15. Dickerson, T. and J. Soria, *Catalytic Fast Pyrolysis: A Review.* Energies, 2013. **6**(1): p. 514-538.
16. Al-Sabawi, M., J. Chen, and S. Ng, *Fluid Catalytic Cracking of Biomass-Derived Oils and Their Blends with Petroleum Feedstocks: A Review.* Energy & Fuels, 2012. **26**(9): p. 5355-5372.
17. Butler, E., et al., *A review of recent laboratory research and commercial developments in fast pyrolysis and upgrading.* Renewable & Sustainable Energy Reviews, 2011. **15**(8): p. 4171-4186.
18. Huber, G.W., S. Iborra, and A. Corma, *Synthesis of transportation fuels from biomass: chemistry, catalysts, and engineering.* Chem Rev, 2006. **106**(9): p. 4044-98.
19. Vispute, T.P. and G.W. Huber, *Production of hydrogen, alkanes and polyols by aqueous phase processing of wood-derived pyrolysis oils.* Green Chemistry, 2009. **11**(9): p. 1433-1445.
20. Carole Couhert, J.-M.C., Sylvain Salvador, *Is it possible to predict gas yields of any biomass after rapid pyrolysis at high temperature from its composition in cellulose, hemicellulose and lignin?* Fuel, 2009. **88**(3): p. 408-417.
21. Beaumont, O. and Y. Schwob, *Influence of physical and chemical parameters on wood pyrolysis.* Industrial & Engineering Chemistry Process Design and Development, 1984. **23**(4): p. 637-641.
22. Kang, B.-S., et al., *Fast pyrolysis of radiata pine in a bench scale plant with a fluidized bed: Influence of a char separation system and reaction conditions on the production of bio-oil.* Journal of Analytical and Applied Pyrolysis, 2006. **76**(1-2): p. 32-37.
23. Onay, O. and O. Kockar, *Pyrolysis of rapeseed in a free fall reactor for production of bio-oil.* Fuel, 2006. **85**(12-13): p. 1921-1928.
24. Şensöz, S., D. Angın, and S. Yorgun, *Influence of particle size on the pyrolysis of rapeseed (Brassica napus L.): fuel properties of bio-oil.* Biomass and Bioenergy, 2000. **19**(4): p. 271-279.
25. Bridgwater, A.V., D. Meier, and D. Radlein, *An overview of fast pyrolysis of biomass.* Organic Geochemistry, 1999. **30**(12): p. 1479-1493.

2. Effect of alkali and alkaline earth metals on *in-situ* catalytic fast pyrolysis of lignocellulosic biomass – A micro-reactor study

Abstract

In-situ catalytic fast pyrolysis (CFP) is considered as a promising pathway to produce aromatic hydrocarbons from lignocellulosic biomass. However, the presence of variable amounts of inorganic ash in biomass in the form of alkali and alkaline earth metals (AAEMs) is a concern while using *in-situ* catalysts because AAEMs could influence product distribution from CFP while also being a major reason for catalyst deactivation. In this study, the effect of four alkali and alkaline earth metals (K, Na, Mg and Ca) commonly found in biomass was investigated to understand their individual influence on the fate of primary pyrolysis products as well as their effect on the selectivity of products from *in-situ* CFP using ZSM-5 catalyst. Experiments were performed in a micro-reactor (Py-GC/MS) with ZSM-5 catalyst using AAEM-impregnated biomass. It was found that the type of AAEM as well as the concentration were significant, with Mg appearing to be relatively inert when compared to the stronger catalytic activity of K, Na and Ca. The influence of AAEMs on the formation of pyrolysis products from cellulose, hemicellulose, lignin and its subsequent influence on CFP is discussed. From non-catalytic pyrolysis experiments, even the lowest concentration of AAEMs (0.1 wt.%) was observed to have a significant influence on the thermal decomposition behavior of biomass, promoting the formation of lower molecular weight cellulose and lignin-derived products. AAEMs were found to be influencing CFP product distribution by reducing the carbon yield of desired aromatic hydrocarbons and olefins, while it accelerated pathways resulting in increased yields of thermally-derived char and non-condensable gases. The effect of AAEMs on CFP followed the order: Na > K > Ca > Mg.

Keywords: *Biomass, Catalytic Fast Pyrolysis (CFP), Ash, AAEM, In-situ*

2.1. Introduction

Lignocellulosic biomass is a renewable source of organic carbon which has been studied extensively in recent years to produce biofuels and biochemicals [1-4]. The abundance of different types of biomass around the world gives it the potential to augment as well as compete with conventional sources of fuels and chemicals [5]. Fast pyrolysis is a process which involves thermal breakdown of biomass constituents (cellulose, hemicellulose and lignin) utilizing high temperature (400-600 ˚C), short vapor residence time (<2s) and high heating rates in an oxygen free atmosphere to produce high yields of liquid (commonly known as bio-oil) along with gas phase products and solid char [6]. However, bio-oil from pyrolysis suffers from several drawbacks such as high water content (15-30%), oxygen content (30-40%), high viscosity and a relatively lower heating value (17-20 MJ/kg) when compared to fossil fuels [7].

In-situ catalytic fast pyrolysis (CFP) using zeolite catalyst is considered as a promising pathway to obtain aromatic hydrocarbons from biomass, which can subsequently be upgraded with relative ease using conventional hydrotreating techniques for producing "drop-in" transportation fuel [8-11]. Zeolite catalysts suppress reactions during pyrolysis that result in oxygenated compounds such as sugars, acids and PAHs (polyaromatic hydrocarbons) by eliminating oxygen through decarbonylation, decarboxylation and dehydration reactions, while promoting the reactions that result in products such as aromatic hydrocarbons. The actual composition of bio-oil produced from CFP is highly dependent on a number of factors such as operating temperature, catalyst to feed ratio and the properties of the catalyst such as acidity, pore size and the presence

of promoters. In addition, the properties of biomass feedstock used can affect the chemistry as well as operability of a CFP process.

Despite the numerous advantages offered by the process, commercial scale-up to produce bio-oil economically is faced with a major challenge due to the rapid deactivation of the catalyst used in CFP. While conventional FCC (fluid catalytic cracking) catalysts are regenerated by burning off the coke through high temperature oxidation, CFP catalysts are additionally deactivated by the deposition of alkali and alkaline earth metals (AAEMs) [12]. Deactivation usually occurs due to the coke and metals blocking the pores of the catalyst or poisoning the active sites on the surface of the catalyst in addition to chemical and mechanical degradation of the catalyst. Thus, conventional FCC-type regeneration only restores partial activity of the CFP catalyst, and it results in a gradual loss of activity and selectivity for the desired CFP products [10, 13, 14]. The AAEMs (e.g. Ca, K, Mg and Na) that cause this deactivation are contained in the biomass feedstock and are important to the plant as nutrients during the growth phase. These mineral nutrients are a part of the biomass structure, bound at hydroxyl and/or phenolic groups in the form of cations or as a salt [15]. Depending on the type of biomass, the inorganic content could range from 0.5% upto 15% [16, 17]. The operating temperatures used in CFP is not sufficient to volatilize the AAEMs, and they are retained on the char/catalyst surface in the reactor [18]. In addition to contributing to catalyst deactivation, AAEMs are also known to influence the product distribution from pyrolysis, by affecting the fate of primary biomass decomposition products and secondary vapor phase reactions during CFP [19-22]. Sodium and potassium have also been known to impact slagging, fouling and corrosion characteristics. Although biomass washing with water or acids has been suggested among other methods as pre-treatment techniques to reduce the effect of these minerals, it has been shown to influence the chemical composition of bio-oil while

more severe pretreatments of biomass have been known to cause hemicellulose degradation [23-25].

Several studies over the last decade have investigated the influence of these AAEMs on biomass. However, broad classification of the products as bio-oil, char and non-condensable gases accompanied by the influence of secondary reactions makes it hard to systematically understand the influence of AAEMs on pyrolysis chemistry. Shafizadeh et al. [26] observed that higher content of inorganics in the biomass promoted secondary reactions resulting in the breakdown of higher molecular weight compounds during pyrolysis, while also affecting the yield of volatiles, gas and char. Studies using model compounds for cellulose have reported high levels of alkali metal content promoting cellulose ring scission, resulting in the formation of lower molecular weight compounds such as hydroxyacetaldehyde, formic acid, furaldehyde, HMF, whereas the removal of alkali metals has been shown to favor the formation of levoglucosan through depolymerization of cellulose [19, 27, 28]. While there have been some studies which have focused on the effects of these inorganic minerals on non-catalytic pyrolysis, there are very few studies in the literature on the effect of these AAEMs on *in-situ* CFP of biomass [14, 28]. This study was performed with the hypothesis that different inorganic minerals (Ca. K, Mg, Na) would have a distinct influence on the product distribution of *in-situ* CFP, depending on their abundance in the biomass feedstock used. Non-catalytic fast pyrolysis and *in-situ* CFP experiments were performed in a micro-reactor with Ca, K, Mg and Na added to the biomass at different concentrations (0.1, 0.5, 1 and 2.0 wt.%) to understand their effect on product distribution and composition of bio-oil produced from pyrolysis.

2.2. Materials and methods

2.2.1. Materials

The biomass used in the experiments was southern pine. Pine wood chips were obtained from a local wood chipping plant in Opelika, Alabama. The wood chips were first air dried for 72 h and a hammer mill (New Holland Grinder Model 358) fitted with a 1.58 mm (1/16 in.) sized screen was used to grind the samples. The sawdust was sieved using a 200 mesh (74 µm) and the fraction that passed was used for pyrolysis experiments in this study. Four concentrations (0.1, 0.5, 1, and 2 wt.% of biomass) of metals were loaded in the biomass. To obtain the required concentration of Na, K, Mg and Ca on biomass, appropriate quantities of the metal oxides (NaOH, KOH, MgO and CaO) were dissolved in 100 ml of DI water and added to 3g of biomass in a plastic centrifuge tube. Once the biomass samples were thoroughly soaked, they were frozen using liquid nitrogen. The frozen samples were kept in a freeze drier for several days to remove the moisture. The dried samples were then used for all subsequent analysis and experiments in this study.

The volatile matter, moisture and ash content were performed according to ASTM standards E871, E872 and E1755, respectively. An oxygen calorimeter (IKA, model C2000) was used for measuring higher heating value (HHV) of the biomass. Elemental composition of the biomass was analyzed using a CHNS/O analyzer (Perkin-Elmer, model CHNS/O 2400). Component analysis to measure the extractives, cellulose, hemicellulose and lignin contents of the biomass was performed according to Laboratory Analytical Procedure (LAP) developed by National Renewable Energy Laboratory [29]. Alkali and alkaline earth metals (AAEM) was analyzed for the biomass samples using ICP analysis. The catalyst used in the *in-situ* CFP experiments was a commercially available HZSM-5 catalyst (CBV 2314 with a SiO_2/Al_2O_3 ratio of 23:1, Zeolyst, USA). The catalyst was sieved using a 200 mesh (74 µm) sieve, and the fraction

that was retained on the sieve was discarded. Catalyst particles that passed through the sieve was then calcined for 5 hours at 550 ˚C in a muffle furnace to convert the catalyst to the acid form prior to use. To prepare the biomass/catalyst mixture for *in-situ* CFP experiments, 50 mg of the biomass and 450 mg of the catalyst were mixed using an ultrasonic bath (VWR Scientific, catalog no. 97043-960) to get a mixture having a biomass to catalyst ratio of 1:9. A microbalance with sensitivity of 0.001 mg (Metller Toledo, XP6) was used to measure the sample weight.

2.2.2. Experimental procedure

Pyrolysis experiments were performed on a Tandem micro-reactor system (Frontier Laboratories, Rx-3050 TR) connected to a gas chromatograph (Agilent Technologies, 7890A). Figure 2.1 shows a schematic diagram of the system used in this study, with two quartz pyrolysis tube reactors (4.7 mm ID, 114 mm length) arranged in series with independent temperature control between 40-900 ˚C. It is also equipped with an independent temperature controlled interface between the two reactors to prevent condensation of pyrolysis products. Deactivated stainless steel sample cups were used to load the samples into the reactor. The sample cups were purged in helium gas flow for 45 seconds and then dropped into the pyrolysis reactor (drop time of 15-20 milliseconds [19]). Helium was used as the carrier gas to sweep the products of pyrolysis from the first reactor into a GC-MS for analyzing the product composition. In the non-catalytic experiments, 0.5 mg biomass was pyrolyzed in the first reactor, and the second reactor was empty. For *in-situ* CFP experiments in this study, approximately 5 mg of the biomass/catalyst mixture (biomass:catalyst – 1:9) was pyrolyzed in the first reactor and the second reactor was empty. The second reactor was also maintained at the same temperature as the interface at 350 ˚C in order to prevent condensation of pyrolysis vapor.

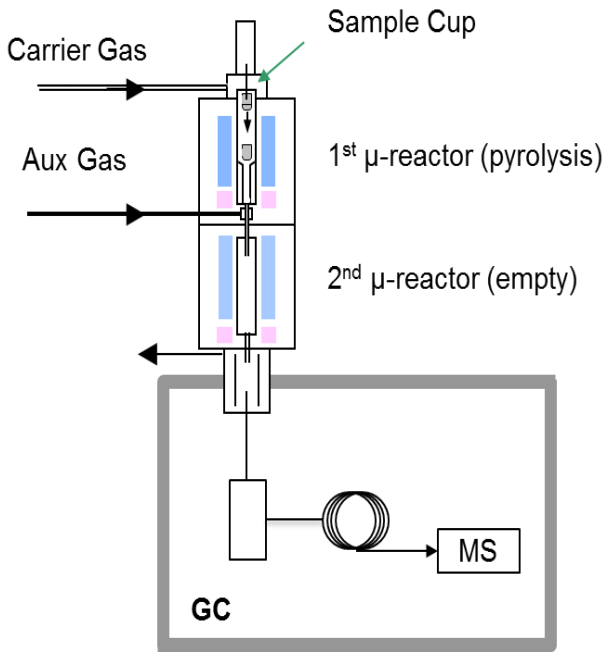

Figure 2.1. Schematic of tandem µ-reactor and GC/MS setup used in this study

The pyrolysis products were analyzed by a gas chromatograph (Agilent Technologies, 7890A) equipped with an Agilent DB 1701 capillary column (60 m × 0.250 mm and 0.250 µm film thickness) to separate condensable compounds from pyrolysis. The GC inlet was maintained at 250 ˚C and a split ratio of 1:100 was used for sample injection into the column. The GC oven was programmed to start at 40 ˚C and hold for 3 min, after which it was ramped at 5 ˚C/min up to the final temperature of 270 ˚C. The final temperature was held for 6 min, and the overall time of the oven program was 55 min. The column was connected to a mass spectrometer (Agilent Technologies, 5975C) for compound identification and quantification by using calibration standards. Some of the major aromatic hydrocarbons identified were quantified using pure compounds purchased from Sigma-Aldrich (St. Louis, Missouri). Three different concentrations of the standards were prepared to obtain calibration factors for quantification. To analyze the composition of non-condensable gas (NCG) products (CO, CO_2, CH_4, C_2H_4, C_2H_6, C_3H_6, C_3H_8

and C_4H_8), a Porous Layer Open Tubular (PLOT) column (Agilent Technologies, GS-GasPro) was used, and a standard gas mixture of these NCG was used to calibrate the yield of non-condensable gases. Char yield was determined gravimetrically by measuring the weight of the sample cup before and after the experiment. However, since *in-situ* CFP experiments were performed with the catalyst mixed along with the biomass in the sample cup, it was not possible to distinguish between pyrolysis char and catalytic coke. Carbon content of the carbonaceous residue was quantified using an elemental analyzer (Perkin-Elmer, model CHNS/O 2400).

All the experiments for measuring the non-condensable gases, carbonaceous residues as well as the condensable pyrolysis vapor were performed at least in duplicates to obtain a standard deviation for the results and verify the reproducibility of the data. Three factors of interest at various levels – 1) Type of inorganic mineral added to biomass (K, Na, Mg, Ca); 2) Amount of AAEM added to biomass (0.1, 0.5, 1.0, 2.0 wt.%) and 3) Catalyst (with / without) – were the focus of this study. The samples are labelled with their name followed by its metal loading in the biomass. For example, MG 0.1 refers to magnesium 0.1 wt.% loading in the biomass. Results labelled as 'control' are from experiments performed using biomass without any added AAEMs. Results labelled as CFP are from experiments using ZSM-5 as the *in-situ* catalyst. Statistical analysis of the results was performed (ANOVA, Tukey's HSD) at 95% confidence interval using JMP software (SAS Institute, Cary, North Carolina). However, since the standard deviation of the results from the micro-pyrolyzer was less than 5%, it is not shown. The product distribution from CFP experiments is reported in terms of carbon yield, which is the ratio of carbon in a specific product or group to the carbon contained in the feedstock. Selectivity of a particular aromatic hydrocarbon is defined as the ratio of moles of carbon in that product to the total moles of carbon in all aromatic hydrocarbons produced. The overall carbon balance for most of the experiments

was close to or above 90 % with the remaining fraction including large molecular weight compounds not identified by the GC.

2.3. Results and Discussion

2.3.1. Biomass Characterization

Elemental composition, ash, moisture content and higher heating value (HHV) of the biomass used in this study are summarized in Table 2.1. The biomass was found to contain 0.63 wt.% of ash content, which was not washed or removed. Table 2.2 shows the composition of AAEMs for the biomass samples from ICP analysis. The actual composition of AAEMs in the biomass varies slightly from the targeted concentrations of 0.1, 0.5, 1.0 and 2.0 wt.%, as seen in Table 2.2. The moisture content of the biomass was 6.44 wt.%, and all the results in this study are presented on a dry basis after accounting for this moisture content. Results from component analysis of the biomass are summarized in Table 2.3.

Table 2.1. Proximate and ultimate analyses of biomass used in this study

Proximate Analysis, as received	**Analytical standard**	**Result - Pine**
Ash content, wt. %	ASTM E1755	0.63 ± 0.07
Volatile Matter, wt. %	ASTM E872	77.26 ± 0.32
Moisture content, wt. %	ASTM E871	6.44 ± 0.53
Fixed carbon, wt. %	By balance	15.67 ± 0.48
Heating value, MJ/kg	**ASTM E870**	**18.31 ± 0.21**
Ultimate Analysis	**Analytical instrument**	**Pine**
C, wt. %	Perkin-Elmer, model CHNS/O 2400	45.69 ± 0.29
H, wt. %		6.63 ± 0.08
N, wt. %		0.30 ± 0.09
S, wt. %		0.12 ± 0.01
O, wt. %	By difference	46.97 ± 0.13

The number after ± denotes standard deviation. Ultimate analysis is in dry, ash-free basis

Table 2.2. Actual composition of AAEMs in the biomass (wt. %)[a]

	Ca	Mg	K	Na
Control	0.205% ± 0.018	0.151% ± 0.006	0.113% ± 0.008	0.066% ± 0.012
CA – 0.1%	**0.339% ± 0.020**	0.163% ± 0.012	0.098% ± 0.014	0.059% ± 0.000
CA – 0.5 %	**0.737% ± 0.016**	0.155% ± 0.014	0.102% ± 0.011	0.063% ± 0.002
CA – 1.0 %	**1.293% ± 0.024**	0.149% ± 0.020	0.099% ± 0.018	0.071% ± 0.010
CA – 2.0 %	**2.279% ± 0.046**	0.152% ± 0.014	0.109% ± 0.024	0.078% ± 0.014
K - 0.1 %	0.214% ± 0.013	0.170% ± 0.026	**0.219% ± 0.035**	0.067% ± 0.009
K - 0.5 %	0.219% ± 0.020	0.165% ± 0.016	**0.654% ± 0.059**	0.063% ± 0.006
K - 1.0 %	0.211% ± 0.020	0.168% ± 0.004	**1.107% ± 0.040**	0.077% ± 0.013
K - 2.0 %	0.198% ± 0.017	0.159% ± 0.007	**2.095% ± 0.031**	0.056% ± 0.021
MG - 0.1 %	0.209% ± 0.011	**0.270% ± 0.015**	0.106% ± 0.004	0.079% ± 0.018
MG - 0.5 %	0.196% ± 0.016	**0.682% ± 0.034**	0.101% ± 0.007	0.070% ± 0.011
MG - 1.0 %	0.203% ± 0.015	**1.194% ± 0.039**	0.109% ± 0.000	0.065% ± 0.004
MG - 2.0 %	0.199% ± 0.010	**2.203% ± 0.020**	0.115% ± 0.012	0.061% ± 0.015
NA - 0.1 %	0.182% ± 0.036	0.143% ± 0.032	0.098% ± 0.014	**0.170% ± 0.021**
NA - 0.5 %	0.203% ± 0.014	0.158% ± 0.022	0.102% ± 0.010	**0.543% ± 0.032**
NA - 1.0 %	0.197% ± 0.018	0.147% ± 0.010	0.125% ± 0.021	**1.091% ± 0.018**
NA - 2.0 %	0.204% ± 0.005	0.162% ± 0.000	0.116% ± 0.010	**2.053% ± 0.036**

[a] Number followed by ± sign represents standard deviation.

Table 2.3. Results of component analysis, wt. %, dry basis [a]

Sample	Cellulose %	Hemicellulose %					Lignin %		Extractives %
		Xylan	Galactan	Arabinan	Mannan	Total	AIL	ASL	
Pine	40.93 ± 0.82	7.38 ± 0.13	3.08 ± 0.05	1.52 ± 0.014	10.97 ± 0.09	22.96 ± 0.29	28.82 ± 0.42	1.83 ± 0.07	3.08 ± 0.04

[a] Number followed by ± sign represents standard deviation

2.3.2 Effect of AAEMs on non-catalytic pyrolysis

Pyrolysis products from cellulose and hemicellulose can be broadly classified into 1) anhydrosugars, 2) furan-ring derivatives (alkyl furans, furfural, HMF, 2(5H)-furanone), and 3) low molecular weight compounds (glycolaldehyde, formic acid, acetic acid, acetaldehyde, acetol) along with non-condensable gases (CO, CO_2), water and char. Figure 2.2 and Figure 2.3 show the impact of alkali metals (K, Na) and alkaline earth metals (Msg, Ca) on the fate of several cellulose and hemicellulose derivatives from non-catalytic pyrolysis of biomass. The amount (chromatogram area %) of levoglucosan, the major anhydrosugar produced from biomass pyrolysis, was suppressed severely from 10.77 % in control to 0.63 % and 0.50 % in the presence

of 2.0 wt.% K and Na, respectively while it appears to gradually decrease with increasing concentration of Ca in the biomass. The presence of even 0.1 wt.% of added K and Na was highly detrimental to the fate of levoglucosan formation. Meanwhile, Mg does not seem to have any significant influence.

The decrease in levoglucosan was observed to be accompanied by a corresponding increase in certain low molecular weight compounds (acetaldehyde, acetol, acetic acid, 2-cyclopentenone, 2-hydroxy 3-methyl). In the presence of Na, the area % of acetaldehyde and acetol was observed to be increasing from 0.58 % to 1.18% and 2.3% to 4.13%, respectively. Alkali metals (K and Na) showed a very similar behavior in promoting the formation of these low molecular weight compounds. For example, acetic acid was found to be increasing from 2.8% in control to 4.72% and 4.3% due to the presence of Na and K, respectively. However, it was interesting to note that in the presence of Ca, acetic acid reduced from 2.82% to 0.43%. Meanwhile, several ketones such as 2-cyclopenten-1-one and 2(5H)-furanone were observed to be promoted in the presence of Ca, which correlates well with a previous study from our group where CaO was observed to be effective in suppressing the yield of acetic acid through ketonization reactions [7]. It should be noted that a considerable amount of acetic acid is also produced from lignin depolymerization in addition to the contribution from hemicellulose and it was not possible to distinguish between the two. These results are comparable to previous findings which have reported significantly reduced levoglucosan yield and increased yield of low molecular weight compounds in the presence of alkali and alkaline earth metals [14, 19, 23, 28].

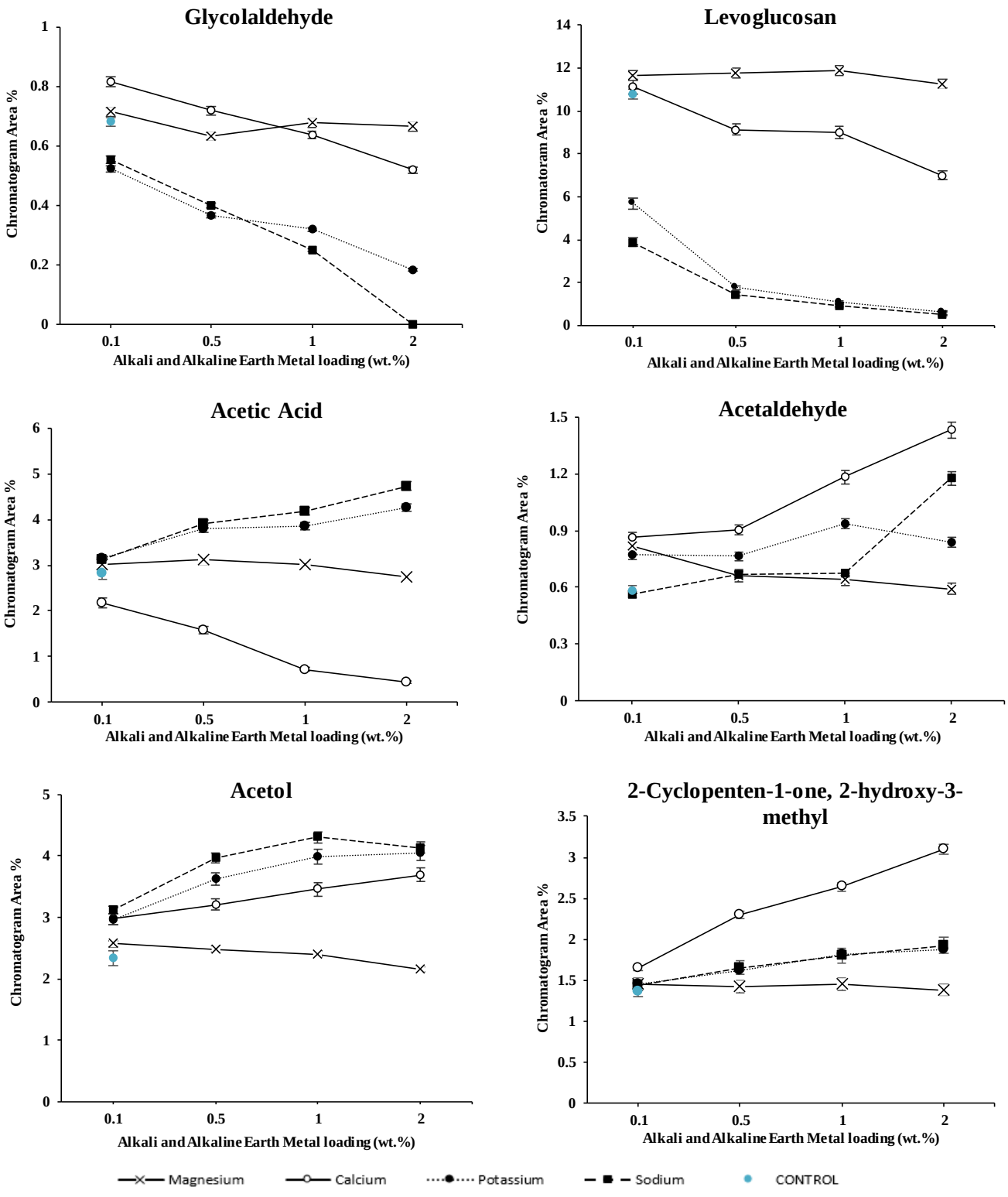

Figure 2.2. Effect of AAEMs on cellulose/hemicellulose derivatives during pyrolysis

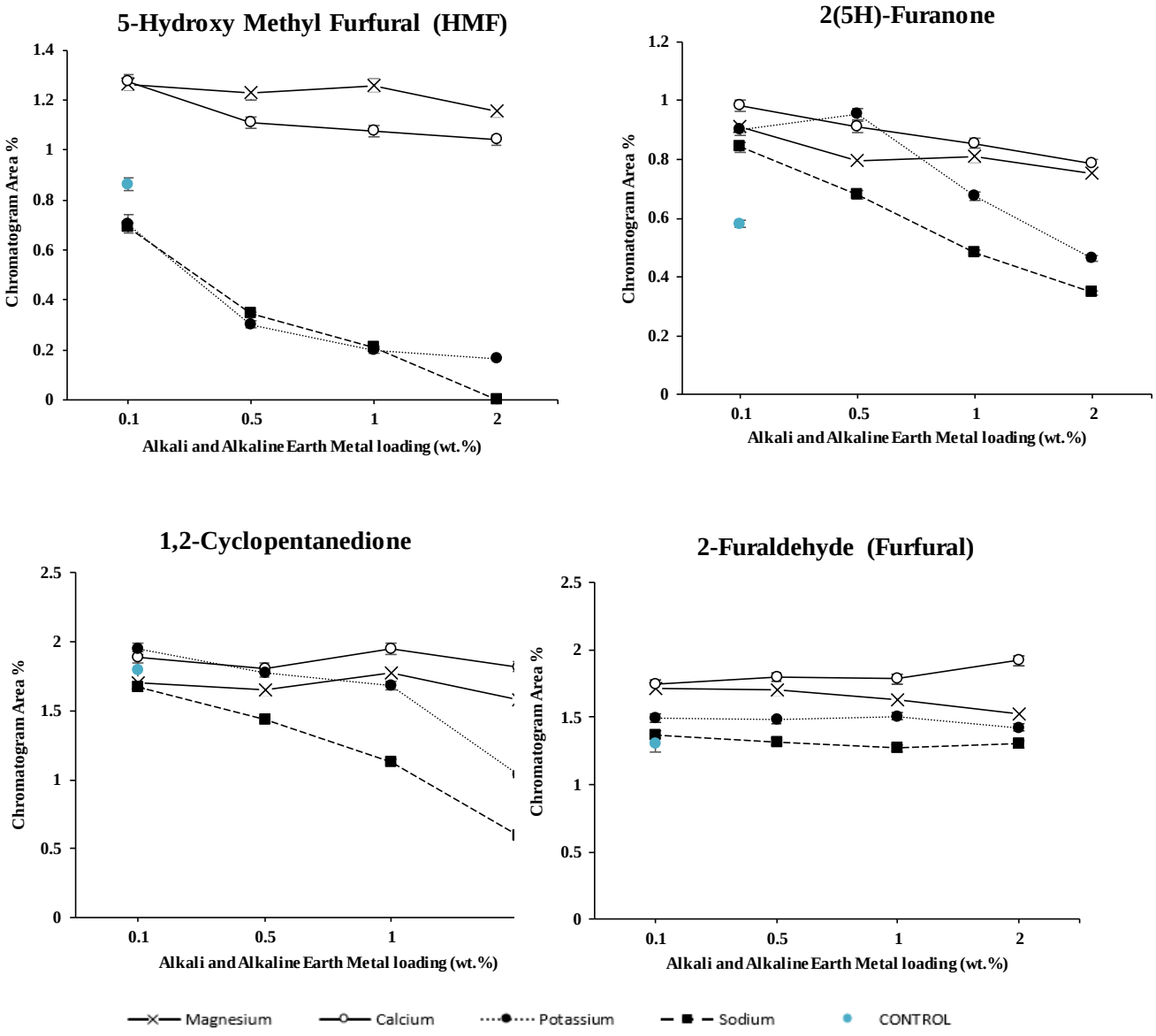

Figure 2.3. Effect of AAEMs on cellulose/hemicellulose derivatives during pyrolysis

Patwardhan et al. [19] studied the influence of AAEMs on the pyrolysis of model compounds for cellulose and observed that the reactions leading to the production of smaller oxygenates such as glycolaldehyde, acetol, formic acid through cleavage of bonds in the pyranose ring was favored in the presence of AAEMs. Yang et al [30] studied the influence of K and Ca

during pyrolysis and predicted that the presence of these metal ions promotes the homolytic scission of several bonds in the pyranose ring resulting in the formation of several low molecular weight compounds. For example, homolytic cleaving at different positions (C1 or C5, C2 or C4 and C3) in the pyranose ring would result in the formation of compounds with corresponding number of carbon atoms: CO_2, glycolaldehyde, acetol, etc. Meanwhile, levoglucosan is formed primarily through the cleavage of glycosidic linkages in cellulose, resulting in a C6 depolymerized fragment. However, the homolytic scission of the C-C bonds in the pyranose ring competes with the cleavage of glycosidic linkages, resulting in a competitive pathway between the formation of low molecular weight compounds and levoglucosan. Our results agree with the mechanisms postulated by Yang et al and Patwardhan et al, since the formation of levoglucosan is severely suppressed along with the increased yield of several low molecular weight compounds in the presence of K, Na and Ca. This suggests that the activation energy for reactions leading to the homolytic scission of various bonds in the pyranose ring is reduced, thereby promoting the formation of these species. However, the only anomaly between our results and the findings of previous studies is the reducing trend of glycolaldehyde with increasing alkali and alkaline earth metal content. It appears that the scission at C2 or C4 position is not favored, which contradicts previous findings using model compounds where the yield of glyceraldehyde also increases along with the other low molecular weight products from cellulose and hemicellulose [19, 28, 31]. The formation of furan-ring derivatives was found to be affected by the type of AAEMs as well as the concentration, as shown in Figure 2.3. The formation of 5-hydromethoxy furfural, 2-furaldehyde and 2(5H)-furanone was promoted by the presence of the lowest concentration of alkaline earth metals (Ca and Mg), whereas higher concentrations did not increase their respective area % thereafter. Alkali metals (K and Na) suppressed the formation of 5-hydroxymethyl furfural

whereas it did not affect the formation of furfural significantly. The activity of alkaline earth metals with respect to the formation of furan-ring derivatives could be due to their role as a dehydration catalyst (MgO CaO), enhancing the formation of these compounds.

While it is clearly established by previous studies and confirmed by our findings that AAEMs influence the distribution of individual chemical species derived from cellulose and hemicellulose, there is not much information available on the effect of these minerals on lignin, which contains upto 40% of the energy content in biomass [32]. Lignin is a complex network of phenylpropanoid units formed through oxidative polymerization of coumaryl, coniferyl and sinapyl alcohols containing aromatic units of phenol, 2-methoxy phenol (guaiacol) and 2,6 dimethoxy phenol (syringol), respectively. Since the degree of methoxylation differs between the various lignin precursors, various types of intermolecular linkages can exist in the polymer, which varies in composition between different types of biomass. However, due to the pre-existing aromatic structure of lignin and its abundant availability, it has good potential as a feedstock for producing aromatic hydrocarbons [33]. During pyrolysis, fragmentation of the polymeric structure of lignin results in the depolymerization of cross-linked coniferyl alcohol, coumaryl alcohol and sinapyl alcohol sub-units (carbon-carbon, aryl ether linkages). As a result, a wide range of aromatic derivatives from each lignin sub-unit are produced along with char (including non-volatile oligomers or polymeric units) and low molecular weight compounds such as CO_2 and acetic acid.

The major lignin-derived compounds formed from the pyrolysis of biomass doped with various AAEMs are shown in Figure 2.4. Alkali metals (K and Na) had a clear impact on the pyrolysis product composition, as the yield of aromatic derivatives from the lignin sub-units increased significantly with increasing concentration of K and Na. The area % of coniferyl alcohol

was found to be initially increasing due to the presence of 0.1 wt.% of K and Na. However at higher concentrations of alkali metals, the formation of lower molecular weight aromatic products from coniferyl alcohol are favored. For example, the amount of guaiacol (phenol, 2-methoxy) increased from 3.12% in the control to 7.43% and 7.18% in the presence of Na and K respectively. Similar increases can be clearly seen in Figure 2.4, where the area % of 4-ethyl 2-methoxy phenol, 2-methoxy 4-vinyl phenol (vinyl guaiacol) and phenol increase linearly with the addition of the alkali metals in the biomass. Alkaline earth metals appear to not have any significant influence on the lignin derived aromatic compounds. As described previously, the amount of acetic acid was observed to be increasing, which correlates well with a greater degree of lignin depolymerization. Overall, our findings suggest that the alkali metals increase the depolymerization of lignin by promoting the cleavage of intermolecular linkages in lignin, similar to its effect on cellulose and hemicellulose. These results are in stark contrast to the findings of Patwardhan et al. [32], who suggested that these alkali and alkaline earth metals did not have a significant difference on the pyrolytic behavior of lignin and that the lignin structure was resilient to the presence of AAEMs. However, their study was performed on lignin obtained after organosolv treatment, which could have been a masking factor due to which the effect of AAEMs on lignin was not observed.

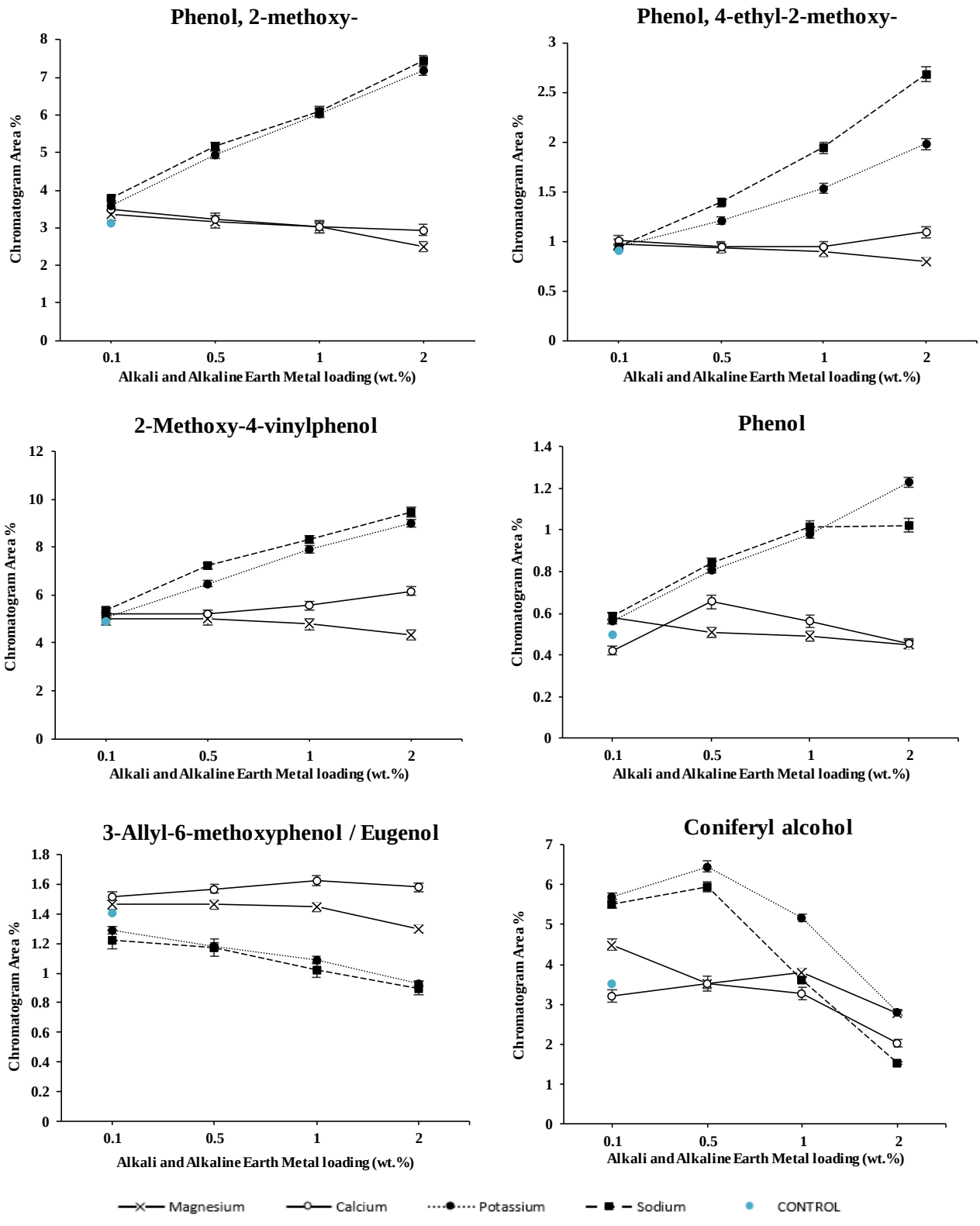

Figure 2.4. Effect of AAEMs on lignin derivatives during pyrolysis

The amount of char and non-condensable gases (CO, CO_2) produced in the presence of AAEMs is shown in Figure 2.5 and Figure 2.6, respectively. Similar to the findings of previous studies, the yield of char and CO_2 increased significantly due to the influence of Ca, K and Na [14, 28]. As explained earlier, since the heterolytic cleavage of glycosidic linkages is suppressed in the presence of Ca, K and Na, scission of linkages in the pyranose ring takes precedence resulting in the formation of low molecular weight compounds, CO_2 and non-volatile oligomers which are converted to carbonaceous residue (char).

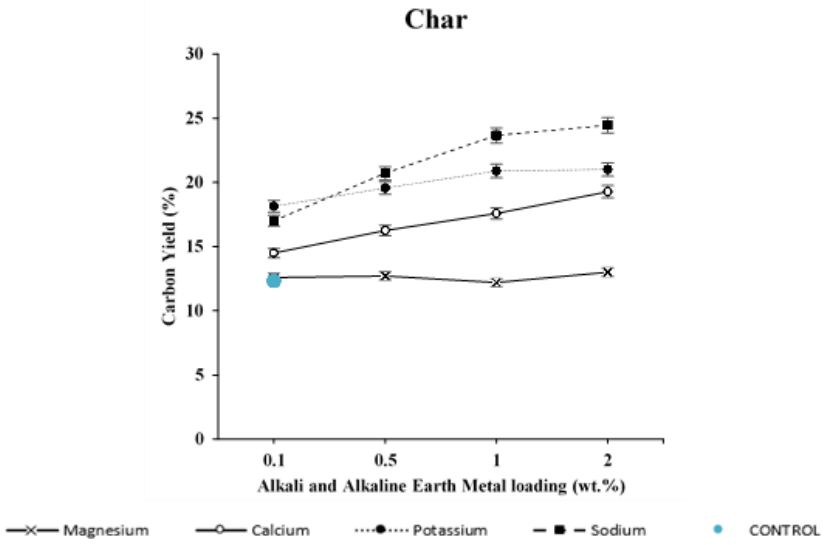

Figure 2.5. Effect of AAEMs on char formation during pyrolysis

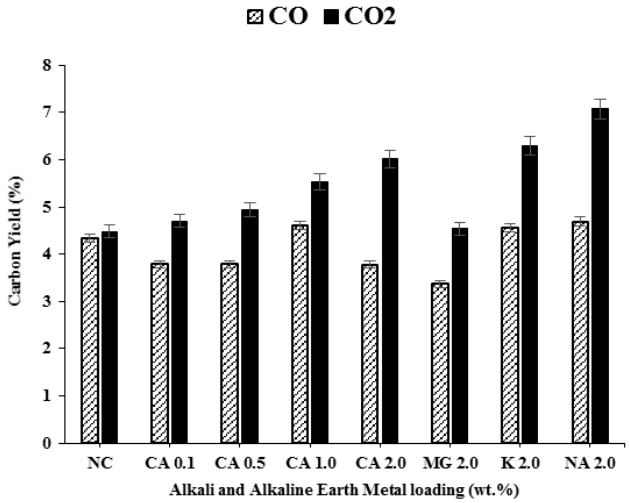

Figure 2.6. Effect of AAEMs on non-condensable gases

2.3.3. Effect of type of AAEM on CFP

Biomass samples impregnated with the same concentration (2.0 wt.%) of Mg, Ca, K and Na were used to understand the influence of the type of AAEM on product distribution and selectivity of desired products from in-situ catalytic pyrolysis experiments. The effect of type of AAEM on the aromatic hydrocarbon yield is shown in Figure 2.7.

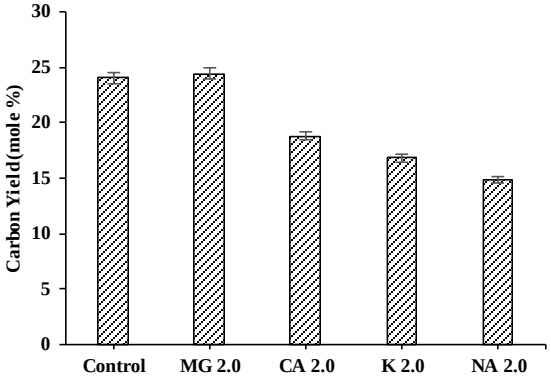

Figure 2.7. Effect of type of AAEMs on aromatic hydrocarbon yields

When compared to the control experiments, the carbon yield of aromatic hydrocarbons decreased significantly due to the influence of Ca, K and Na, while Mg appears to have no effect. The yield of aromatic hydrocarbons decreased in the following the order: Control (24.04%) ~ Mg (24.40%) > Ca (18.77%) > K (16.82%) > Na (14.87%). It is apparent that the trend observed in the yield of aromatic hydrocarbons in CFP correlates well with the decrease in the yield of levoglucosan in the presence of Ca, K and Na in non-catalytic pyrolysis (Figure 2.2). These results correlate well with previously observed CFP studies using model compounds for cellulose doped with AAEMs [14, 28]. Wang et al. showed that the yield of aromatic hydrocarbons from levoglucosan is comparable to the yield from smaller oxygenates such as glycolaldehyde, acetol and formic acid [34], which should theoretically result in a similar yield of aromatic hydrocarbons. However, the amount of pyrolysis vapor (organics) produced is suppressed in the presence AAEMs [28], resulting in a

significant decrease in the yield of aromatic hydrocarbons in the presence of K (16.82%) and Na (14.87%) in CFP. Based on our results from non-catalytic pyrolysis, AAEMs promoted significant increases in the yields of simple phenols and guaiacols. However, the contribution of these lignin-derived aromatic compounds to the aromatic hydrocarbon yield is not clear. Mullen et al. [33] studied the catalytic pyrolysis of different types of lignins and concluded that simple phenols are likely to be a dead-end resulting in deactivation of the acidic active sites on the catalyst and not necessarily a source for producing aromatic hydrocarbons. They postulated that the aromatic linkers and olefins formed from the fragmentation of lignin are a more probable source for producing these hydrocarbons. In order to investigate whether the AAEMs actually have an influence on the catalyst properties and subsequently affect the chemical speciation of the bio-oil, the selectivity of various aromatic hydrocarbons produced has been calculated and reported in Table 2.4. Selectivity of the desired mono-cyclic aromatic hydrocarbons (benzene, toluene, xylene and C9 aromatics) decreased whereas the selectivity of naphthalene and alkyl-substituted naphthalenes increased significantly in the presence of AAEM species. Similar changes in the selectivity of certain products from CFP has been reported previously by Wang et al. [28] and it is probable that this effect is due to the active sites on the catalyst surface being poisoned by the AAEM species, and further studies are required to understand their influence on selectivity of aromatic hydrocarbons. It should also be noted that oxygenated compounds, including phenols/alkyl-substituted phenols, guaiacol, vinyl guaiacol and benzofuran were observed to be increasing in the presence of AAEMs in CFP experiments, as shown in Figure 2.8. The yield of oxygenated compounds in CFP experiments was in the order: K (2.64%) > Na (2.32%) > Ca (1.57%) > Mg (0.38%) > Control (0.23%).

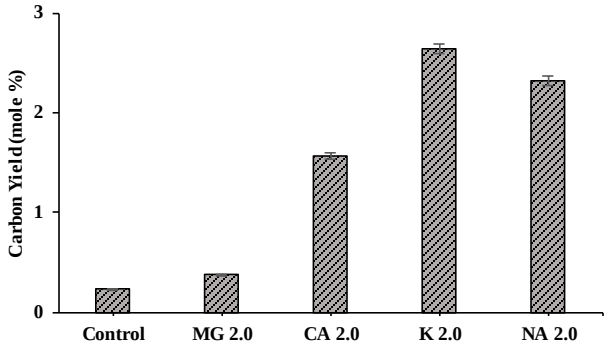

Figure 2.8. Effect of type of AAEMs on oxygenated compounds

Table 2.4. Product distribution from catalytic pyrolysis of pine at 500 ˚C

Component	Overall Carbon Yield (C %)				
	Control	**Mg 2.0**	**Ca 2.0**	**K 2.0**	**Na 2.0**
CO	13.9 ± 0.12	12.88 ± 0.09	12.02 ± 0.11	11.75 ± 0.14	9.87 ± 0.09
CO_2	6.42 ± 0.15	5.97 ± 0.11	8.36 ± 0.33	7.76 ± 0.26	8.0 ± 0.21
Char + Coke	40.2	40.3	45.8	47.3	51.3
Char *	12.32 ± 0.48	13.01 ± 0.19	19.27 ± 0.38	21 ± 0.17	24.46 ± 0.39
Coke **	27.87 ± 0.21	27.28 ± 0.39	26.52 ± 0.10	26.29 ± 0.04	26.83 ± 0.20
Aromatic hydrocarbons	24.04 ± 0.40	24.4 ± 0.24	18.77 ± 0.16	16.82 ± 0.28	14.87 ± 0.14
Olefins (C2-C4)	6.69 ± 0.18	6.6 ± 0.14	5.94 ± 0.06	5.7 ± 0.06	4.54 ± 0.09
Oxygenated Compounds	0.23 ± 0.04	0.38 ± 0.08	1.57 ± 0.13	2.64 ± 0.18	2.32 ± 0.14
Total Carbon Closure	91.48 ± 0.88	90.53 ± 0.93	92.46 ± 0.33	91.97 ± 0.20	90.9 ± 0.84
	Aromatics Selectivity (%)				
Benzene	6.06 ± 0.09	5.99 ± 0.15	5.7 ± 0.10	4.77 ± 0.06	4.5 ± 0.22
Toluene	15.51 ± 0.14	15.3 ± 0.10	14.97 ± 0.08	14.18 ± 0.04	13.22 ± 0.13
Ethyl Benzene	1.08 ± 0.09	1.26 ± 0.09	1.16 ± 0.05	1.2 ± 0.11	0.98 ± 0.07
Xylene	16.89 ± 0.21	16.57 ± 0.31	17.45 ± 0.12	17.3 ± 0.27	17.3 ± 0.11
C9 Aromatics	15.06 ± 0.19	14.7 ± 0.11	14.63 ± 0.16	15.57 ± 0.12	13.98 ± 0.12
C10+ Aromatics	40.18	40.29	41.46	42.99	43.74
Naphthalenes	27.34 ± 0.21	27.51 ± 0.16	29.05 ± 0.15	31.64 ± 0.09	32.11 ± 0.08
Fluorene, Anthracene	12.85 ± 0.15	12.43 ± 0.15	11.13 ± 0.18	9.32 ± 0.16	9.83 ± 0.11

Note: Number after ± sign denotes standard deviation

*Result from non-catalytic experiments performed

**Difference between char+coke from CFP experiment and char yield from non-catalytic

C9 Aromatics include indane, indenes and alkyl benzenes

The total carbonaceous residue (coke + char) produced in CFP experiments in the presence of various AAEMs is shown in Figure 2.9. It is clear that Ca, K and Na catalyze reactions leading to the formation of char, resulting in an increase from 12.32 % (Control) to 24.46% (Na). It should also be noted that the trend observed in the yield of carbonaceous reside and char correlates well

with the drop in aromatic hydrocarbons yield. These results agree well with previous studies on fast pyrolysis, where it has been reported that biomass with high ash content produced increased char yields and non-condensable gases [16, 23, 36]. As mentioned previously, it was not possible to distinguish between thermally-derived char and catalytically-derived coke since the catalyst was mixed with the biomass in CFP experiments. However, it is assumed that the amount of char produced in CFP experiments will be the same as that obtained in non-catalytic pyrolysis. The yield of catalytic coke in Table 2.4 was calculated by subtracting the char yield in non-catalytic pyrolysis from the total carbonaceous residue produced from CFP experiments. Na and K which are considered to be stronger cracking catalysts, should theoretically reduce the amount of coke deposited on the catalyst surface when compared to the control experiments. The decrease in coke formation in the presence of alkali metals has been reported in literature by several studies on fast pyrolysis [14, 20, 23, 28]. Yildiz et al. [14] observed a 66.6 wt.% decrease in coke yield in the presence of ash; Wang et al. [28] reported a decrease from 14.0 wt.% to 10.2% in the presence of calcium. In our study, although the amount of coke produced in the presence of K (26.29%) and Na (26.83%) is statistically significant from the control (27.87%), the effect is not comparable to the results reported in literature. The reason for this anomaly could be the significantly higher yield of phenols produced due to the influence of AAEMs on lignin, which has been known to cause increased coking in the catalyst [35].

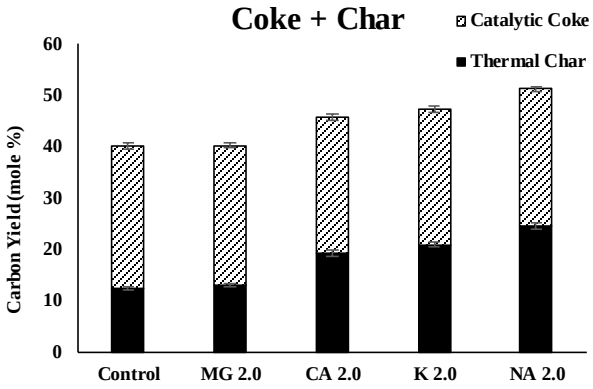

Figure 2.9. Effect of type of AAEMs on carbonaceous residue (coke & char)

The presence of AAEMs influenced the yield of thermally-derived CO and CO_2 as well as the catalytically derived CO and CO_2 shown in Figure 2.10. The yield of thermal CO and CO_2 was highest in the presence of Na, and the effect of different AAEMs followed the order Na > K > Ca > Mg. AAEMs appear to promote cracking reactions in biomass which result in more CO_x gases. However, the yield of catalytically-derived CO is statistically significant, decreasing in the presence of AAEMs, which correlates well with the reduced yield of aromatic hydrocarbons. The yield of aromatic hydrocarbons reduced from 24.03% in the control experiment to 14.87% in the presence of Na. Similarly, the yield of catalytically-derived CO was 9.56% in the control experiments, reducing to 4.18% in the presence of Na. Overall, the presence of these AAEMs in the biomass significantly alters the chemistry in CFP, inhibiting pathways resulting in the production of aromatic hydrocarbons and instead promoting reactions resulting in increased yield of thermally-derived non-condensable gases and char.

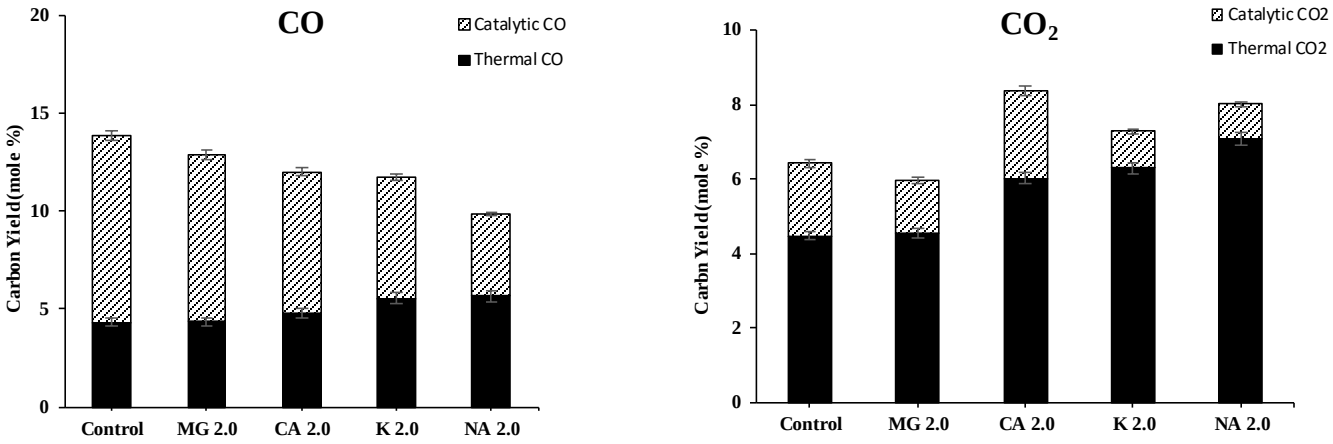

Figure 2.10. Effect of type of AAEMs on non-condensable gases

2.3.4. Effect of AAEM concentration on CFP

Figure 2.11 shows the effect of potassium at various concentrations on the product distribution from CFP. For the sake of brevity, K is used to illustrate the effect of concentration of AAEMs). The lowest concentration of K was sufficient to influence the product distribution significantly, with the carbon yield of aromatic hydrocarbons decreasing from 24.04% (Control) to 19.76% (K 0.1), 18.21% (K 0.5), 17.94% (K 1.0) and 16.82% (K 2.0). As mentioned previously in Section 3.3, the decrease in aromatic hydrocarbons and olefins correlates well with the trend observed in levoglucosan during non-catalytic pyrolysis, where even the lowest concentration of K suppressed the formation of levoglucosan and reduced the abundance of levoglucosan by half, as shown in Figure 2.2. Na being an alkali metal similar to K has a comparable effect in on CFP, while the influence of Ca is much less severe on reducing the levoglucosan and hydrocarbon yields. Similar results of AAEMs from non-catalytic pyrolysis have also been reported elsewhere and agrees well with the trends observed in this study [16, 23, 37-38]. It is also accompanied by a subsequent increase in the yield of thermal char, which was in the order K 2.0 (21.0%) > K 1.0

(20.89%) > K 0.5 (19.56%) > K 0.1 (18.14%) > Control (12.32%). Similar to the effect on levoglucosan, even the lowest concentration of K tested in this study (K 0.1) produced a significant increase on the carbon yield of char and the effect of higher concentrations of K appears to be linear. Similar to the discussion in Section 2.3.3, the effect of concentration of K on catalytic coke is minimal and is far less extensive than the results reported by Wang et al. [28] and Yildiz et al. [14]. The effect of concentration of K on the yield of thermally-derived and catalytically-derived CO_x is shown in Figure 2.11. The carbon yield of thermally-derived CO_2 was increased from 4.48% (Control) to 6.24% (K 0.1) and ultimately to 7.27% (K 2.0), which shows that even the lowest concentration has a significant influence, due to formation of smaller oxygenates from the pyranose ring through enhanced homolytic scission as well as enhanced thermal decomposition of lignin in the presence of K [19].

The selectivity of certain mono-cyclic aromatic hydrocarbons including benzene and toluene decreased while the selectivity for C9 and C10+ aromatics including naphthalenes and alkyl-substituted naphthalenes increased, as summarized in Table 2.5. As mentioned previously, it is not clear whether this effect is due to changes in pyrolysis vapor composition due to AAEMs or due to changes in the properties of the zeolite catalyst due to the presence of AAEMs.

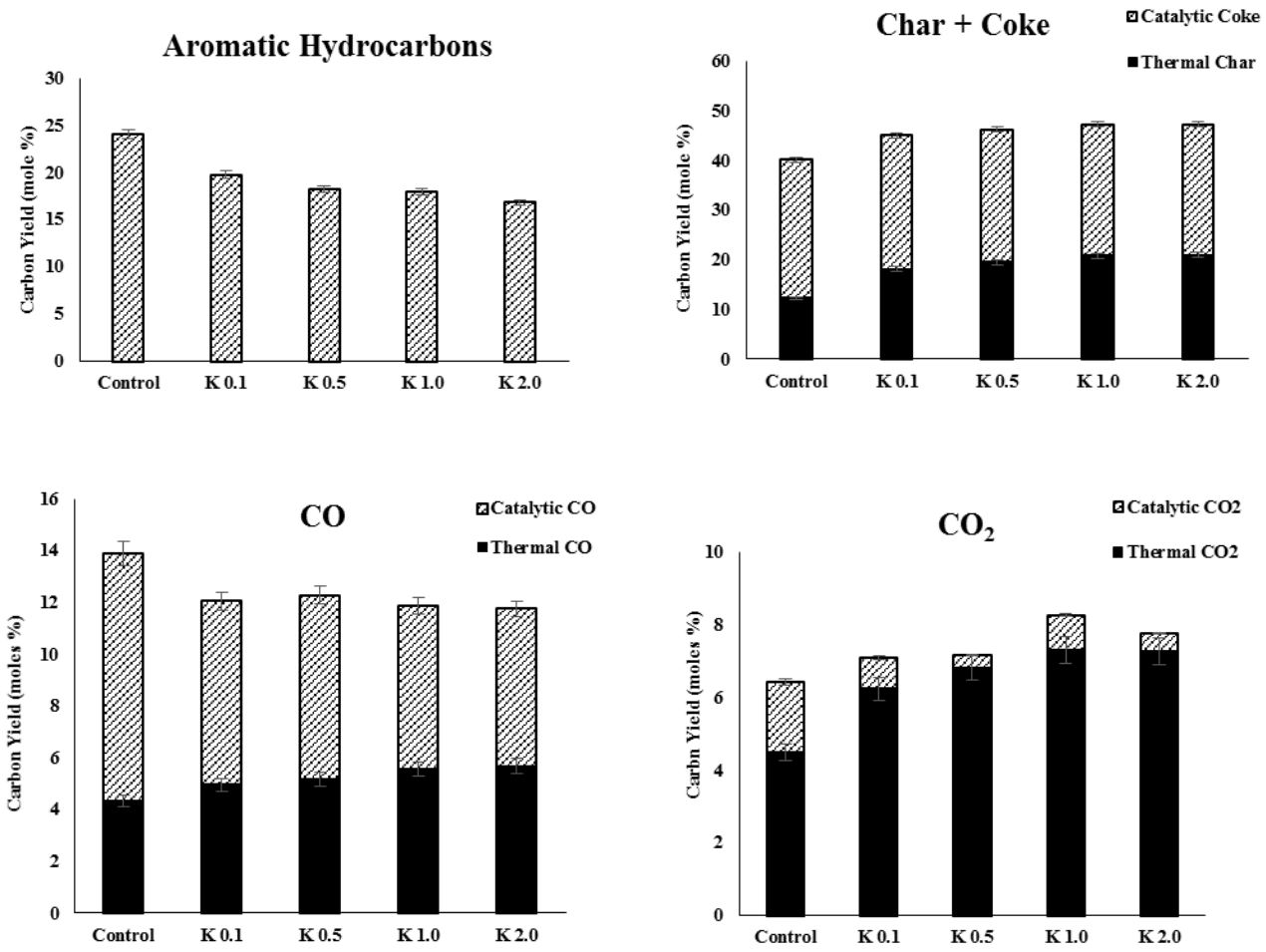

Figure 2.11. Effect of AAEM loading on catalytic pyrolysis of biomass

As such, a study on the influence of individual AAEMs on the catalytic activity of zeolite and the subsequent product selectivity would be essential in order to understand this phenomenon. In addition to changes in selectivity of hydrocarbons, the carbon yield of oxygenated compounds also increased as a function of increasing K concentration. The evolution of lignin-derived guaiacol and vinyl guaiacol was again influenced due to enhanced thermal decomposition of coniferyl alcohol, as shown earlier in Figure 2.4. Overall, the presence of even the lowest concentration of K (0.1) added to the biomass influences the product composition and selectivity significantly, reducing yields of desired aromatic hydrocarbons from CFP as well as increasing the yield of thermally-derived char and non-condensable gases.

Table 2.5. Product distribution from catalytic pyrolysis of pine at 500 ˚C

Component	Overall Carbon Yield (C %)				
	Control	K 0.1	K 0.5	K 1.0	K 2.0
CO	13.9 ± 0.12	12.29 ± 0.07	12.05 ± 0.19	11.89 ± 0.10	11.75 ± 0.14
CO_2	6.42 ± 0.15	7.18 ± 0.11	7.09 ± 0.15	7.45 ± 0.04	7.76 ± 0.26
Char + Coke	40.2	45.13	46.29	47.27	47.3
Char *	12.32 ± 0.48	18.14 ± 0.22	19.56 ± 0.30	20.89 ± 0.53	21 ± 0.17
Coke **	27.87 ± 0.21	26.99 ± 0.18	26.73 ± 0.11	26.38 ± 0.20	26.29 ± 0.04
Aromatic Hydrocarbons	24.04 ± 0.40	19.76 ± 0.30	18.21 ± 0.45	17.94 ± 0.11	16.82 ± 0.28
Olefins (C2-C4)	6.69 ± 0.18	6.14 ± 0.15	5.96 ± 0.07	5.68 ± 0.17	5.7 ± 0.06
Oxygenated Compounds	0.23 ± 0.04	1.48 ± 0.07	1.97 ± 0.10	2.21 ± 0.06	2.64 ± 0.18
Total Carbon Closure	91.48 ± 0.88	91.98 ± 0.41	91.57 ± 0.63	92.44 ± 0.70	91.97 ± 0.20
	Aromatics Selectivity (%)				
Benzene	6.06 ± 0.09	5.05 ± 0.09	5.01 ± 0.04	4.71 ± 0.11	4.77 ± 0.06
Toluene	15.51 ± 0.14	14.69 ± 0.17	14.32 ± 0.13	14.49 ± 0.15	14.18 ± 0.04
Ethyl Benzene	1.08 ± 0.09	1.09 ± 0.04	1.02 ± 0.13	1.03 ± 0.05	1.2 ± 0.11
Xylene	16.89 ± 0.21	17.12 ± 0.11	17.32 ± 0.24	17.19 ± 0.19	17.3 ± 0.27
C9 Aromatics	15.06 ± 0.19	14.95 ± 0.37	15.18 ± 0.11	15.42 ± 0.08	15.57 ± 0.12
C10+ Aromatics	40.18	41.3	41.52	42.28	42.99
Naphthalenes	27.34 ± 0.21	30.69 ± 0.18	30.95 ± 0.32	31.59 ± 0.17	31.64 ± 0.09
Fluorene, Anthracene	12.85 ± 0.15	10.61 ± 0.09	10.57 ± 0.13	9.67 ± 0.11	9.32 ± 0.16

Note: Number after ± sign denotes standard deviation
*Result from non-catalytic experiments performed
**Difference between char+coke from CFP experiment and char yield from non-catalytic
C9 Aromatics include Indane, Indenes and Alkyl Benzenes

2.4. Conclusion

The effect of alkali and alkaline earth metals (AAEMs) on *in-situ* catalytic fast pyrolysis of biomass was studied by impregnating biomass with various concentrations of Mg, Ca, K, Na, and it was shown that the type of AAEM as well as the concentration of these species resulted in undesirable losses in the aromatic hydrocarbon yield. AAEMs were also observed to be influencing the pyrolysis chemistry by enhancing pathways resulting in more thermally-derived non-condensable gases and char, while also affecting the selectivity of desired mono-cyclic aromatic hydrocarbon products from CFP. Results from non-catalytic pyrolysis seem to suggest that the thermal decomposition of lignocellulosic biomass is affected significantly by the presence of AAEMs, which enhanced the breakdown of the polymeric structure of cellulose and lignin

resulting in increased yields of low molecular weight compounds. In order to overcome these drawbacks, rapid removal of char from the pyrolysis reactor is essential since ash concentrations will be much higher in a continuous catalytic fast pyrolysis process.

This chapter has been published and the citation is as follows:

Mahadevan, R., Adhikari, S., Shakya, R., Wang, K., Dayton, D., Lehrich, M., & Taylor, S. E. (2016). **Effect of Alkali and Alkaline Earth Metals on in-Situ Catalytic Fast Pyrolysis of Lignocellulosic Biomass: A Microreactor Study**. Energy & Fuels, 30(4), 3045-3056.

2.5. References

1. Dayton, D.C., et al., *Biomass hydropyrolysis in a pressurized fluidized bed reactor.* Energy & Fuels, 2013. **27**(7): p. 3778-3785.
2. Neupane, S., et al., *Effect of torrefaction on biomass structure and hydrocarbon production from fast pyrolysis.* Green Chemistry, 2015. **17**(4): p. 2406-2417.
3. Carlson, T., et al., *Aromatic Production from Catalytic Fast Pyrolysis of Biomass-Derived Feedstocks.* Topics in Catalysis, 2009. **52**(3): p. 241-252.
4. Bridgwater, A.V., *Review of fast pyrolysis of biomass and product upgrading.* Biomass and Bioenergy, 2012. **38**(0): p. 68-94.
5. Czernik, S. and A.V. Bridgwater, *Overview of Applications of Biomass Fast Pyrolysis Oil.* Energy & Fuels, 2004. **18**(2): p. 590-598.
6. Thangalazhy-Gopakumar, S., et al., *Physiochemical properties of bio-oil produced at various temperatures from pine wood using an auger reactor.* Bioresource Technology, 2010. **101**(21): p. 8389-8395.
7. Mahadevan, R., et al., *Physical and Chemical Properties and Accelerated Aging Test of Bio-oil Produced from in Situ Catalytic Pyrolysis in a Bench-Scale Fluidized-Bed Reactor.* Energy & Fuels, 2015.
8. Peters, J.E., J.R. Carpenter, and D.C. Dayton, *Anisole and Guaiacol Hydrodeoxygenation Reaction Pathways over Selected Catalysts.* Energy & Fuels, 2015. **29**(2): p. 909-916.
9. Mante, O.D., et al., *Catalytic pyrolysis with ZSM-5 based additive as co-catalyst to Y-zeolite in two reactor configurations.* Fuel, 2014. **117, Part A**(0): p. 649-659.
10. Iliopoulou, E.F., et al., *Pilot-scale validation of Co-ZSM-5 catalyst performance in the catalytic upgrading of biomass pyrolysis vapours.* Green Chemistry, 2014. **16**(2): p. 662-674.
11. H. Zhang, J.Z., R.Xiao, *Catalytic Pyrolysis of Willow Wood with Me/ZSM-5 (Me = Mg, K, Fe, Ga, Ni) to Produce Aromatics and Olefins.* BioResources, 2013. **8**(4): p. 5612 - 5621.
12. Guisnet, M. and P. Magnoux, *Deactivation by coking of zeolite catalysts. Prevention of deactivation. Optimal conditions for regeneration.* Catalysis Today, 1997. **36**(4): p. 477-483.
13. Zhang, Y., et al., *Regeneration Kinetics of Spent FCC Catalyst via Coke Gasification in a Micro Fluidized Bed.* Procedia Engineering, 2015. **102**: p. 1758-1765.
14. Yildiz, G., et al., *Effect of biomass ash in catalytic fast pyrolysis of pine wood.* Applied Catalysis B: Environmental, 2015. **168–169**: p. 203-211.

15. Nik-Azar, M., et al., *Mineral matter effects in rapid pyrolysis of beech wood.* Fuel Processing Technology, 1997. **51**(1–2): p. 7-17.
16. Fahmi, R., et al., *The effect of alkali metals on combustion and pyrolysis of Lolium and Festuca grasses, switchgrass and willow.* Fuel, 2007. **86**(10–11): p. 1560-1569.
17. Agblevor, F.A. and S. Besler, *Inorganic Compounds in Biomass Feedstocks. 1. Effect on the Quality of Fast Pyrolysis Oils.* Energy & Fuels, 1996. **10**(2): p. 293-298.
18. Mullen, C.A. and A.A. Boateng, *Accumulation of inorganic impurities on HZSM-5 zeolites during catalytic fast pyrolysis of switchgrass.* Industrial & Engineering Chemistry Research, 2013. **52**(48): p. 17156-17161.
19. Patwardhan, P.R., et al., *Influence of inorganic salts on the primary pyrolysis products of cellulose.* Bioresource Technology, 2010. **101**(12): p. 4646-4655.
20. Shimada, N., H. Kawamoto, and S. Saka, *Different action of alkali/alkaline earth metal chlorides on cellulose pyrolysis.* Journal of Analytical and Applied Pyrolysis, 2008. **81**(1): p. 80-87.
21. Serapiglia, M.J., et al., *Evaluation of the impact of compositional differences in switchgrass genotypes on pyrolysis product yield.* Industrial Crops and Products, 2015. **74**: p. 957-968.
22. Mullen, C.A., Boateng, A.A., *Accumulation of inorganic impurities on HZSM-5 during catalytic fast pyrolysis of switchgrass.* Journal of Industrial and Engineering Chemical Research, 2013. **52**: p. 17156-17161.
23. Aho, A., et al., *Pyrolysis of pine and gasification of pine chars – Influence of organically bound metals.* Bioresource Technology, 2013. **128**: p. 22-29.
24. Stephanidis, S., et al., *Catalytic upgrading of lignocellulosic biomass pyrolysis vapours: Effect of hydrothermal pre-treatment of biomass.* Catalysis Today, 2011. **167**(1): p. 37-45.
25. Mourant, D., et al., *Mallee wood fast pyrolysis: effects of alkali and alkaline earth metallic species on the yield and composition of bio-oil.* Fuel, 2011. **90**(9): p. 2915-2922.
26. Bradbury, A.G.W., Y. Sakai, and F. Shafizadeh, *A kinetic model for pyrolysis of cellulose.* Journal of Applied Polymer Science, 1979. **23**(11): p. 3271-3280.
27. Liden, A., F. Berruti, and D. Scott, *A kinetic model for the production of liquids from the flash pyrolysis of biomass.* Chemical Engineering Communications, 1988. **65**(1): p. 207-221.
28. Wang, K., et al., *The deleterious effect of inorganic salts on hydrocarbon yields from catalytic pyrolysis of lignocellulosic biomass and its mitigation.* Applied Energy, 2015. **148**: p. 115-120.
29. Sluiter, A., et al., *Determination of extractives in biomass.* Laboratory Analytical Procedure (LAP), 2005. **1617**.
30. Yang, C.-y., et al., *TG-FTIR Study on Corn Straw Pyrolysis-influence of Minerals1.* Chemical Research in Chinese Universities, 2006. **22**(4): p. 524-532.
31. Nik-Azar, M., et al., *Mineral matter effects in rapid pyrolysis of beech wood.* Fuel Processing Technology, 1997. **51**(1): p. 7-17.
32. Patwardhan, P.R., R.C. Brown, and B.H. Shanks, *Understanding the Fast Pyrolysis of Lignin.* ChemSusChem, 2011. **4**(11): p. 1629-1636.
33. Mullen, C.A. and A.A. Boateng, *Catalytic pyrolysis-GC/MS of lignin from several sources.* Fuel Processing Technology, 2010. **91**(11): p. 1446-1458.
34. Wang, K., et al., *Catalytic conversion of carbohydrate-derived oxygenates over HZSM-5 in a tandem micro-reactor system.* Green Chemistry, 2015. **17**(1): p. 557-564.
35. Thilakaratne, R., J.-P. Tessonnier, and R.C. Brown, *Conversion of methoxy and hydroxyl functionalities of phenolic monomers over zeolites.* Green Chemistry, 2016.
36. Elliott, D.C., *Water, Alkali and Char in Flash Pyrolysis Oils.* Biomass & Bioenergy, 1994. **7**(1-6): p. 179-185.
37. Eom, I.-Y., et al., *Effect of essential inorganic metals on primary thermal degradation of lignocellulosic biomass.* Bioresource Technology, 2012. **104**: p. 687-694.

38. Mullen, C.A., A.A. Boateng, Dadson R.B and Hashem F.M. *EBiological Minaral Range Effects on Biomass Conversion to Aromatic Hydrocarbons via Catalytic Fast Pyrolysis over HZSM-5.* Energy & Fuels, 2014. **28(11)**: p. 7014-7024.

3. Influence of biomass inorganics on the functionality of HZSM-5 catalyst during *in-situ* catalytic fast pyrolysis

Abstract

Inorganic metal species found in biomass have been known to alter the pathways of thermal breakdown during pyrolysis to produce useful hydrocarbon fuels. However, during *in-situ* catalytic fast pyrolysis (CFP), these species may also volatilize and accumulate on the catalyst, influencing its functionality and the resulting product distribution due to loss of activity. In this study, the contamination of HZSM-5 catalyst by calcium, potassium and sodium was investigated by deactivating the catalyst with various concentrations of these inorganics and the subsequent changes in the properties of the catalyst are reported. The deactivated catalysts were then used in catalytic pyrolysis experiments in a py/GC-MS setup to study the changes in the composition of condensable compounds produced from biomass. BET analysis of the catalysts revealed the progressive reduction in the surface area with increasing concentrations of the inorganics, which could be attributed to pore blocking and diffusion resistance. Chemisorption studies (NH_3-TPD) showed that the Bronsted acid sites on the catalyst had reacted with potassium and sodium, resulting in a clear loss of active sites, whereas the presence of calcium did not appear to cause extensive chemical deactivation. CFP experiments revealed the progressive loss in catalytic activity, evident due the shift in selectivity from producing only aromatic hydrocarbons (BTEX, naphthalenes, PAH's) with the fresh catalyst to oxygenated compounds such as phenols, guaiacols, furans and ketones with increasing contamination by the inorganics. The carbon yield of aromatic hydrocarbons decreased from 22.3 % with the fresh catalyst to 1.4 % and 2.1% when deactivated by K and Na at 2 wt.% respectively and the product composition at 5 wt.% deactivation by these metals showed that the catalyst was completely rendered inactive. However, calcium appears to

only cause physical deactivation since the carbon yield of aromatic hydrocarbons was still 9.8 wt.% at the maximum concentration of calcium on the catalyst. The severe loss in the aromatic hydrocarbon yield due to contamination by potassium and sodium indicates that careful consideration is required in choosing the type of biomass feedstock to be used for CFP.

Keywords: *Biomass Ash, Catalytic Fast Pyrolysis (CFP), Hydrocarbons, In-situ, Deactivation, Bio-oil*

3.1. Introduction

Catalytic Fast Pyrolysis (CFP) has been investigated in recent years as a thermochemical conversion method for producing partially deoxygenated liquid fuel intermediates from biomass. Compared to the quality of oil produced from non-catalytic pyrolysis, the use of heterogeneous catalysts instead of inert heat carriers during *in-situ* CFP results in the removal of oxygen and the production of a liquid product (bio-oil) containing a higher heating value and reduced oxygen content [1, 2]. The catalytic deoxygenation of a wide range of compounds produced from pyrolysis such as ketones, aldehydes, alcohols, carboxylic acids and phenolics reduces the extent of subsequent upgrading required before the bio-oil could be used as a drop-in fuel [3, 4]. The improved thermal stability and lower oxygen content of bio-oil produced from CFP decreases the burden on the economically inefficient hydrotreating step, which utilizes expensive metal catalysts, high temperature and high pressure of hydrogen [5-8]. Solid acid catalysts such as HZSM-5, Y-zeolite, β-zeolite are among the most commonly used materials, which transform the pyrolysis vapor by rejecting oxygen through dehydration ($-H_2O$), decarboxylation (-CO) and decarbonylation ($-CO_2$) reactions, leading to a product composed of aromatic hydrocarbons and olefins.

The zeolite family of catalysts are particularly interesting for CFP, due to the presence of a large number of Bronsted (OH) and Lewis (≡Al) acid sites which are present simultaneously and catalyze a number of cracking reactions with a high selectivity for producing olefins and aromatic hydrocarbons [9, 10]. However, the presence of a large number of acid sites leads to the formation of coke on the surface and in the pores, resulting in a gradual loss in catalytic activity and carbon yield of hydrocarbons. Pyrolysis reactor systems typically counter this problem by employing a regeneration step wherein the coked catalyst is thermally oxidized to remove the carbon deposits in an effort to restore the original activity of the catalyst as well as provide process heat for the pyrolysis zone using the exothermic nature of the oxidation reaction. Among these catalysts, HZSM-5 zeolite has been the most widely studied and considered unique due to its shape selectivity that suppresses the coke formation, while also maximizing the conversion to aromatic hydrocarbons [11].

The catalytic conversion of biomass *via* CFP also faces several challenges due to the inherent complexity of the feedstock, which can vary in its composition (i.e. cellulose, hemicellulose and lignin content), leading to large variations in the yield and distribution of the products, as well as making it difficult to consistently produce a product of uniform quality. Many studies have been performed to investigate and understand the effect of such varying composition of the biomass constituents on non-catalytic pyrolysis [12-20]. The effect of inorganic constituents of the biomass ash, which contains alkali and alkaline earth metals (AAEMs) such as sodium, potassium, calcium and magnesium has also been investigated for non-catalytic pyrolysis [15, 21-30]. The presence of these inorganics in the biomass has been observed to be detrimental due to its influence on the pyrolysis product distribution and yield, promoting the formation of lower

molecular weight cellulose and lignin derivatives while increasing the yield of thermally-derived char and non-condensable gases, as reported in a recent study from our group [31].

Besides causing changes to the pyrolysis mechanism, these metals are mostly retained in the char product after pyrolysis and are usually circulated along with the catalyst to the regeneration reactor. The high temperatures (> 650 ˚C) employed in this zone are sufficient to vaporize the inorganics and these metals have been observed to accumulate on the catalyst by several studies in literature [11, 32-35]. The AAEMs might cause chemical poisoning by reducing the number of acid sites or physical poisoning by blocking the pore mouth, increasing the diffusion resistance and resulting in less accessibility to the active sites of the catalyst. This type of deactivation with AAEMs cannot be reversed without the use of inorganic acids to remove the contaminants and results in permanent deactivation of the catalyst, affecting the economic feasibility of the process. Mullen et al. [36] studied the accumulation of various inorganics on HZSM-5 with a SiO_2/Al_2O_3 ratio of 30 during the *in-situ* CFP of switchgrass and reported the linear accumulation of the total amounts of Ca, Cu, Fe, K, Mg, Na and P on the HZSM-5 surface with increasing exposure of the catalyst to biomass. The accumulation of inorganics on the catalyst was correlated to the drop in catalyst activity for producing deoxygenated product, resulting in decreased yield of aromatic hydrocarbons and the lower carbon to oxygen ratio. Yildiz et al. [32, 37] reported the accumulation up to 3 wt.% of ash from pinewood biomass on the catalyst (HZSM-5) and also observed changes in the distribution and composition of the products from pyrolysis. The conversion of sugars, acids and phenols were suppressed due the presence of higher concentrations of accumulated ash. Paasikallio et al. [35] investigated the *in-situ* CFP of pine sawdust and observed a small increase in the oxygen content of the bio-oil (22.4 to 23.7 wt.%) over the course of a four day pyrolysis run, while the catalyst retained most of its original activity

during the experimental period. Stefanidis et al. [33] studied the hydrothermal deactivation and metal contamination during in-situ CFP of commercial beech wood biomass using HZSM-5 catalyst and reported that the individual rates of accumulation of metals were different, with some metals like potassium accumulating more readily than others. They also reported that hydrothermal deactivation and metal contamination led to a linear loss in catalyst activity during pyrolysis, resulting in the production of bio-oil with higher oxygen contents (from 20 % to 35 wt.%). While the results of these studies suggest the overall correlation between the loss in catalyst activity and the accumulation of inorganics on the catalyst, it is not clear since other factors such as catalyst attrition, loss in surface area during the course of the experiment and decreasing catalyst to biomass ratios were not controlled. Another important consideration for performing this study is the wide variation in the composition of inorganic species in different types of biomass available in various parts of the world. Investigating the individual influence of the inorganic species on the catalyst would help develop a fundamental understanding of their effect on the product distribution and quality from CFP and would eliminate some of the uncertainties associated with utilizing biomass.

In this study, we investigated the effect of individual biomass inorganics on the functionality of HZSM-5 catalyst during *in-situ* CFP. It was performed on the hypothesis that different inorganic minerals (Ca, K, Na) would have varied influence on the functionality of the catalyst, depending on the level of contamination and the type of mineral. ZSM-5 catalysts were impregnated separately with different concentrations (0.5, 1, 2 and 5 wt. %) of Ca, K and Na and characterized to study the impact of doping the metals on the properties of the catalyst. The catalysts deactivated by metal impregnation was subsequently used in *in-situ* CFP experiments in a micro reactor (pyroprobe) coupled with a GC/MS to understand the effect of metal contamination on the product distribution from CFP.

3.2. Materials and methods

3.2.1. Materials

Southern pine wood chips obtained from a local wood chipping plant in Opelika, Alabama were used in this study. After an initial drying period of 72 h to reduce the moisture content of the wood chips, they were processed through a hammer mill (New Holland Grinder Model 358) fitted with a 1.58 mm (1/16 in.) screen. The sawdust obtained from the hammer mill was further sieved and the fraction that was smaller than 200 mesh (74 μm) was used for pyrolysis experiments in this study. The biomass was characterized for analyzing the volatile matter, moisture and ash content according to ASTM standards E871, E872 and E1755, respectively. The standard methods followed for determining the chemical constituents, inorganic content (ICP analysis), proximate and ultimate analyses of the biomass were described elsewhere [31].

The ammonium form of ZSM-5 catalyst (CBV 3024, SiO_2/Al_2O_3 ratio of 30:1) was purchased from Zeolyst International (Conshohocken, PA, USA). The catalyst powder was sieved to remove the coarse particles and the fraction that was smaller than 200 mesh (74 μm) was used in this study. Four concentrations (0.5, 1, 2 and 5 wt. %) of metals were impregnated in the ZSM-5 powder using incipient wetness method. Briefly, appropriate quantities of the nitrates of Ca, K and Na were dissolved in 20 mL DI water according to the required concentration. The solution was stirred with the catalyst for 60 min and subsequently dried at 120 ˚C to evaporate the solvent. The dried catalyst powder was then calcined in air at 550 ˚C for 5 h before use in pyrolysis experiments. The inorganic mineral content of the catalysts was measured after the impregnation by inductively coupled plasma (ICP) using a Thermo Scientific iCAP6300 ICP spectrometer. A known amount of sample for ICP analysis was dissolved in concentrated HNO_3 and then diluted with 100 mL DI water. Calibration standards for Ca, Na and K were also prepared in the same

background (HNO_3) and a four-point calibration curve was developed for each element. The BET surface area of the catalyst was measured using Quantachrome Autosorb-1 automated gas sorption system. About 0.20 – 0.30 g of the catalyst sample was degassed at 300 ˚C under vacuum and then measured at 77.3 K (-195.85 ˚C) using nitrogen as the adsorbate. The strength and abundance of the acid sites on the catalyst were characterized using temperature-programmed desorption of ammonia. The characterization was performed in an Autosorb-iQ (Quantachrome Instruments), where a known amount of sample was degassed at 100 ˚C for 1 h of helium gas flow to remove the trapped water vapor, followed by flowing NH_3 gas (0.1 vol % in Ar) at 25 mL/min for 2 h at 40 ˚C. The saturated catalyst sample was then temperature programmed to 800 ˚C at a rate of 15 ˚C/min. To prepare the biomass/catalyst mixture for *in-situ* CFP experiments, 50 mg of the biomass and 150 mg of the catalyst were mixed using an ultrasonic bath (VWR Scientific, catalog no. 97043-960) to get a mixture having a biomass to catalyst ratio of 1:3. A microbalance with sensitivity of 0.001 mg (Metller Toledo, XP6) was used to measure the sample weight.

3.2.2. Experimental procedure – Pyrolysis GC/MS

Pyrolysis experiments were performed in triplicates using a commercial pyrolyzer (Pyroprobe model 5200, CDS Analytical Inc., Oxford, PA), connected to a gas chromatograph (Agilent Technologies, 7890A). Figure 3.1 shows a schematic diagram of the system used in this study and the heating filament holding a sample tube containing the analyte. For each experiment, approximately 2 mg of the catalyst/biomass mixture was packed between quartz wool in the sample tube (1.9 mm I.D, 25 mm long) and placed in the pyrolysis chamber. The catalytic pyrolysis experiments were carried out at a filament temperature of 550 ˚C at a heating rate of 2000 ˚C/s and the filament temperature was held at 550 ˚C for 90 s. The interface temperature was maintained at

300 ˚C and was purged with helium gas flowing at a rate of 20 mL/min. The products from pyrolysis were absorbed by a trap maintained at 40 ˚C and these products were desorbed by heating the trap to 300 ˚C and transferred to the GC column through a transfer line and injector maintained at 300 ˚C and 250 ˚C respectively.

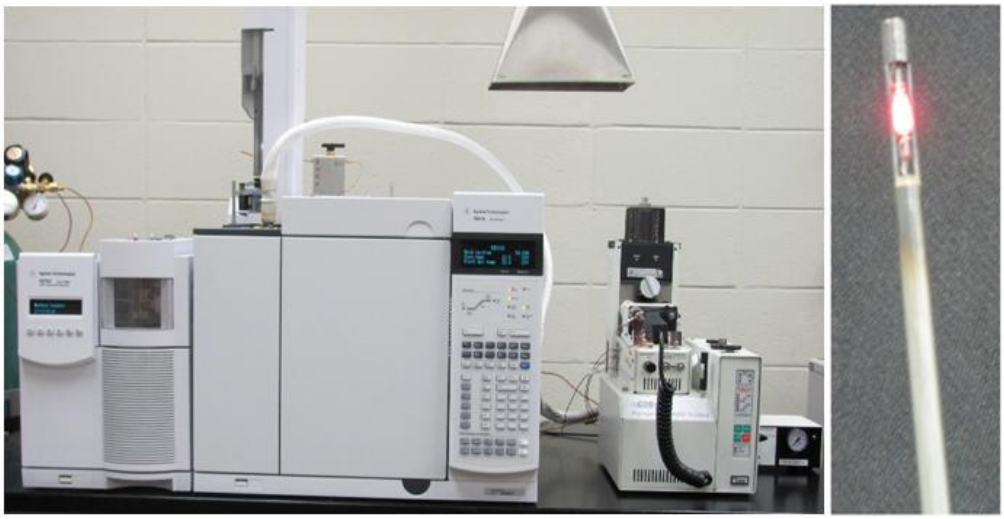

Figure 3.1. Pyrolysis-GC/MS experimental setup used in this study (left) and a resistively heated platinum filament holding a sample tube (right)

The condensable pyrolysis products were separated in the gas chromatograph using a Agilent DB 1701 capillary column (60 m × 0.250 mm and 0.250 µm film thickness). A split ratio of 1:100 was used for sample injection into the column and the GC oven was programmed to start at 40 ˚C (hold time - 3 min), after which it was ramped at 5 ˚C/min up to the final temperature of 270 ˚C (hold time – 6 min). The column was connected to a mass spectrometer (Agilent Technologies, 5975MS) for compound identification using the National Institute of Standard and Technology (NIST) mass spectral library and quantified by using calibration standards. Some of the major aromatic hydrocarbons identified were quantified using pure compounds purchased from Sigma-Aldrich

(St. Louis, Missouri). Three different concentrations of the standards were prepared to obtain calibration factors for quantification.

Two factors of interest at various levels – 1) Type of inorganic metal added to the catalyst (Ca, K, Na); 2) Amount of inorganic metal added to biomass (5000, 10000, 20000, 50000 ppm or 0.5, 1.0, 2.0, 5.0 wt.%) were the focus of this study. The samples are labelled with their name followed by its metal loading in the catalyst. For example, CA 0.5 refers to calcium 0.5 wt.% loading in the catalyst. Results labelled as 'control' are from experiments performed using catalyst without any added inorganics. Statistical analysis of the results was performed (ANOVA, Tukey's HSD) at 95% confidence interval using JMP software (SAS Institute, Cary, North Carolina). The product distribution from CFP experiments is reported in terms of carbon yield, which is the ratio of carbon in a specific product or group to the carbon contained in the feedstock. Selectivity of a particular aromatic hydrocarbon is defined as the ratio of moles of carbon in that product to the total moles of carbon in all aromatic hydrocarbons produced.

3.3. Results and Discussion

3.3.1. Biomass Characterization

The biomass used in this study (southern pine) was characterized to measure the ash content, moisture content, heating value (HHV) and elemental composition, summarized in Table 3.1. The natural ash content of the biomass (0.63 wt.%) was not washed or removed and ICP analysis revealed that it was composed of 0.2 % calcium, 0.15 % magnesium, 0.11 % potassium and 0.06% sodium [31]. The composition of the biomass used was also determined in terms of the cellulose, hemicellulose and lignin contents, shown in Table 3.2.

Table 3.1. Proximate and ultimate analyses of biomass used in this study [a]

Proximate Analysis, as received	Analytical standard	Result - Pine
Ash content, wt. %	ASTM E1755	0.63 ± 0.07
Volatile Matter, wt. %	ASTM E872	77.26 ± 0.32
Moisture content, wt. %	ASTM E871	6.44 ± 0.53
Fixed carbon, wt. %	By balance	15.67 ± 0.48
Heating value, MJ/kg	**ASTM E870**	**18.31 ± 0.21**
Ultimate Analysis	**Analytical instrument**	**Pine**
C, wt. %	Perkin-Elmer, model CHNS/O 2400	45.69 ± 0.29
H, wt. %		6.63 ± 0.08
N, wt. %		0.30 ± 0.09
S, wt. %		0.12 ± 0.01
O, wt. %	By difference	46.97 ± 0.13

[a] The number after ± denotes standard deviation. Ultimate analysis is in dry, ash-free basis

Table 3.2. Results of component analysis, wt. %, dry basis [a]

Sample	Cellulose %	Hemicellulose %					Lignin %		Extractives %
		Xylan	Galactan	Arabinan	Mannan	Total	AIL	ASL	
Pine	40.93 ± 0.82	7.38 ± 0.13	3.08 ± 0.05	1.52 ± 0.014	10.97 ± 0.09	22.96 ± 0.29	28.82 ± 0.42	1.83 ± 0.07	3.08 ± 0.04

[a] Number followed by ± sign represents standard deviation

3.3.2. Effect of biomass inorganics on the properties of HZSM-5

HZSM-5 catalysts were deactivated with each metal (Ca, K and Na) at different levels (0.5, 1, 2 and 5 wt. %) and the deactivated catalysts were subsequently analyzed to quantify the accuracy of metal impregnation. Two sets of samples were prepared for all the catalysts and the ICP analysis was performed by analyzing six successive injections of each sample. The results from ICP analysis of the deactivated catalysts are summarized in Figure 3.2. It is clear that the observed metal loading on the catalysts was always lower that the targeted metal loading at all concentrations. However, the observed loading of potassium was close to the targeted value (0.47,

0.93, 1.92 and 4.85 wt.%), whereas the sodium levels were consistently lower (0.42, 0.88, 1.74 and 4.7 wt. %).

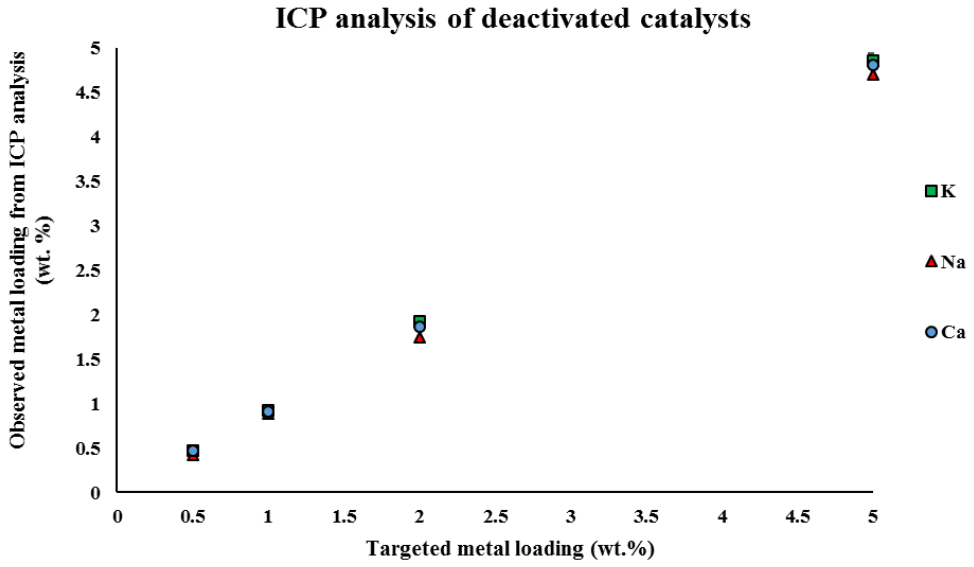

Figure 3.2. Observed concentration of biomass inorganics on the HZSM-5 catalyst

The change in surface area of the HZSM-5 catalysts deactivated by the inorganic metals is shown in Figure 3.3 and it can be seen that the surface area decreases linearly with increase in the concentration of inorganics impregnated in the catalyst. Physical deactivation reduces accessibility to the active sites in the catalyst by increasing diffusion resistance due to blocking of the pore mouth. The fresh catalyst had a surface area of 289.1 m^2/g, which reduced to 89.3 m^2/g when 5 wt.% of potassium was impregnated in the catalyst. However, the surface area of the catalyst with 5 wt.% calcium impregnated was significantly higher at 132.4 m^2/g. The difference between the surface area of the catalysts deactivated by the same loadings of various metals could be due to their individual rate of diffusion into the pores of the zeolite structure. Stefanidis et al. [33] studying the hydrothermal deactivation and metal contamination of HZSM-5 catalysts also reported a similar decrease in the surface area when they doped increasing amounts of inorganics

(up to 90000 ppm of K, Ca, Mg and Na collectively). Similarly, Paasikallio et al. [35] reported decrease in catalyst surface area from 212 m^2/g to 118 m^2/g after a 96 h CFP experiment with HZSM-5 catalyst. However, a major part of that loss in surface area was during the heat up phase and less pronounced during the course of the experiment.

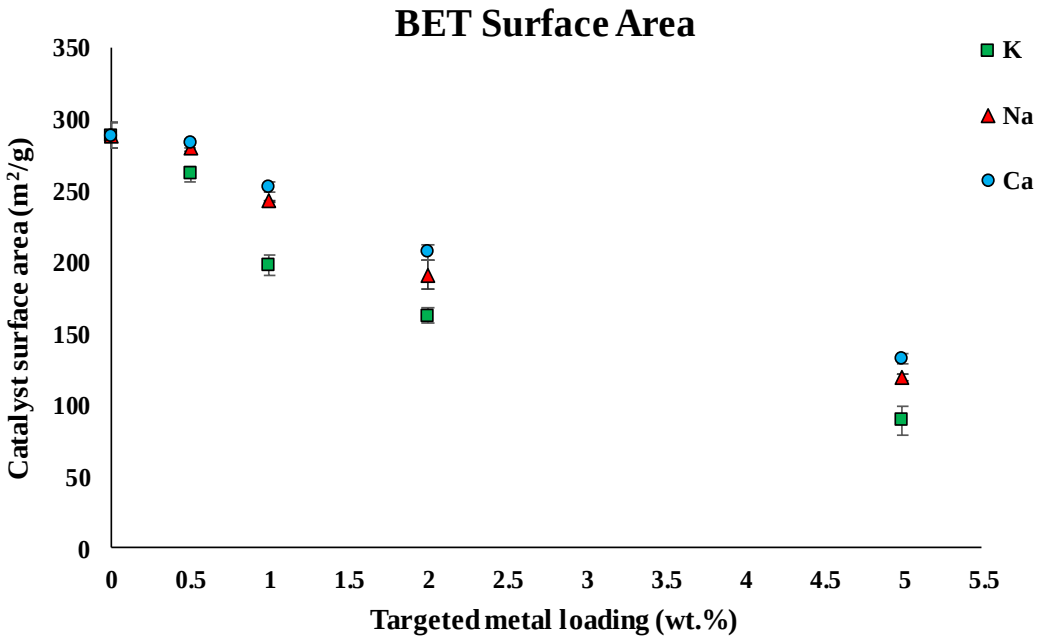

Figure 3.3. BET surface area of HZSM-5 catalyst impregnated with biomass inorganics

As mentioned earlier, inorganics added to the catalyst could cause physical as well as chemical poisoning. In physical poisoning, the active sites with proton functionality in the catalyst have less accessibility, whereas in chemical poisoning those sites are rendered inactive. Chemisorption studies using NH_3 as a probe molecule were performed to distinguish between physical and chemical deactivation. The NH_3-TPD profiles from different catalysts are shown in Figure 3.4, where the TPD curve for the fresh catalyst can be seen to exhibit two distinct desorption peaks at different temperatures: a lower temperature peak between 200 ˚C and 300 ˚C, and a higher temperature peak between 400 ˚C and 500 ˚C. The two peaks could be attributed to the presence

of the weaker acid sites and the stronger acid sites in the HZSM-5 catalyst respectively. From the NH_3-desorption profiles, it can be clearly seen that the amount of strong acid sites is severely reduced by the presence of potassium and sodium, whereas calcium only reduces the amount of strong acid sites marginally, indicating that it does not cause significant chemical poisoning. In the case of potassium and sodium, a significant decrease in the peak corresponding to the weak acid sites could also be observed. Zheng et al. [38] observed the deactivation of V_2O_5-WO_3-TiO_2 SCR catalyst in a biomass combustion study and proposed that potassium could poison the Bronsted acid site by proton-exchange and render them inactive for NH_3 adsorption, which is consistent with the TPD profile observed here. Li et al. [39] studying the application of HZSM-5 catalyst for propane dehydrogenation also observed a similar decrease in the strong acid sites as a result of alkali metal impregnation on the catalyst. Paasikallio et al [35] as well as Stefanidis et al. [33] also observed a negative correlation between increase in the accumulation of inorganics and the acidity of the catalyst.

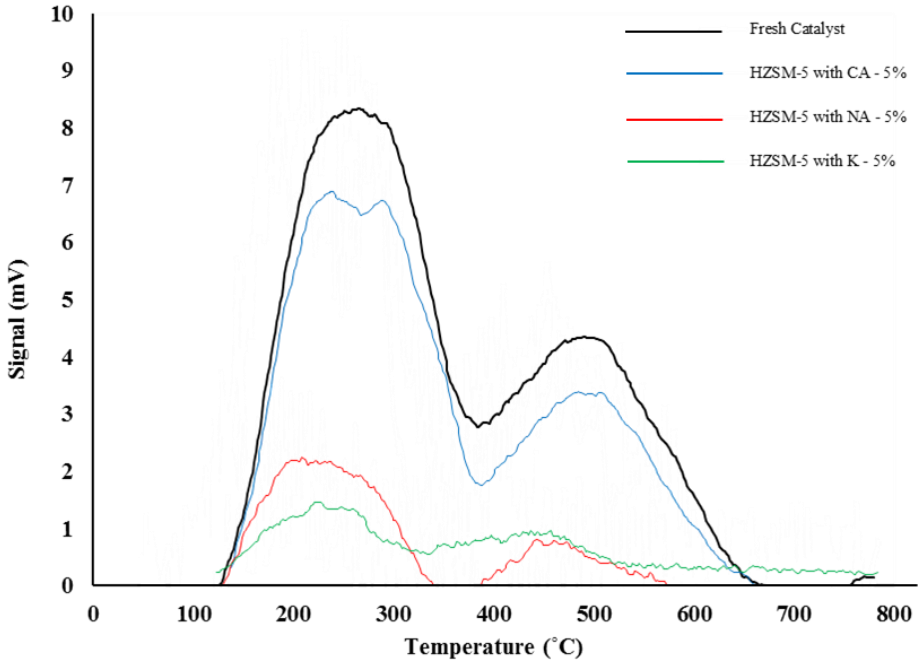

Figure 3.4. NH3-Temperature Programmed Desorption profiles from the HZSM-5 catalysts deactivated with inorganic species

3.3.3. Effect of biomass inorganics on in-situ CFP

The fresh catalyst (control) and the catalysts deactivated by various levels of inorganic species were used as *in-situ* catalysts mixed with biomass in CFP experiments in a py/GC-MS setup. Major compounds identified from all the experiments were quantified using calibration standards and classified divided into five groups, listed in Table 3.3. For the sake of the discussion here, phenols, guaiacols, furans and ketones are further classified under the group of oxygenated compounds to compare with the aromatic hydrocarbons group. Trendlines that best fit the data have been shown to describe the trends observed in the results from the pyrolysis product composition.

Table 3.3. List of compounds quantified from in-situ CFP experiments

Aromatic Hydrocarbons	Phenols	Guaiacols	Furans
Benzene	Phenol	Phenol, 2-methoxy	Furan, 2-methyl
Toluene	Phenol, 2-methyl	Phenol, 2-methoxy-4-methyl	Furan, 2,5 dimethyl
Xylene	Phenol, 4-methyl	Phenol, 4-ethyl 2-methoxy	Furfural
Ethyl benzene	Phenol, 2,4-dimethyl	Eugenol	2(5H)-Furanone
Benzene, 1-ethyl-2-methyl-	Phenol, 3,5 dimethyl	Phenol, 2-methoxy 4-vinyl	Furan, 2-ethyl-5-methyl
Trimethyl Benzene	Phenol, 3-ethyl	Vanillin	2-Furancarboxaldehyde, 5-methyl
Naphthalene	Phenol, 4-ethyl	**Ketones**	
Naphthalene, 1-methyl		2-Cyclopenten-1-one,2-methyl	
Naphthalene, 2,6 dimethyl		2-Cyclopenten-1-one,3-methyl	
Naphthalene, 2-methyl		2-Cyclopenten-1- 2,3dimethyl	
Phenanthrene			
Fluorene			
Anthracene			

The total carbon yield of all the major compounds observed and quantified from the CFP experiments are presented in Figure 3.5. It is clear that the presence of all the inorganic species results in a loss in carbon yield, which reduced significantly from 22.5 % in the control experiments using the fresh catalyst to about 10.7 % and 10.8% when the catalyst was deactivated by 5 wt.%

of potassium and sodium. The rate of decrease also appears to be dramatic, reducing significantly with the presence of the 0.5 wt.% and 1.0 wt.% of potassium and sodium. Meanwhile, the presence of calcium at 0.5 wt.% appears to benefit the carbon yield initially, showing a small increase when compared to the fresh catalyst. However, increase in the concentration of calcium beyond that causes a linear decrease in the total carbon yield. Progressive worsening of the carbon yield of condensable compounds could be related to the shift in product distribution due to the presence of the inorganics on the catalyst, which are known to promote the formation of solid residues (char and coke) as well as non-condensable gases by influencing the decomposition of cellulose, hemicellulose and lignin during pyrolysis [5, 22, 40]. However, it was not possible to confirm this known effect due to limitations of using a py-GC/MS setup, which made it difficult to extract and measure the yield and carbon content of the solid residues consistently.

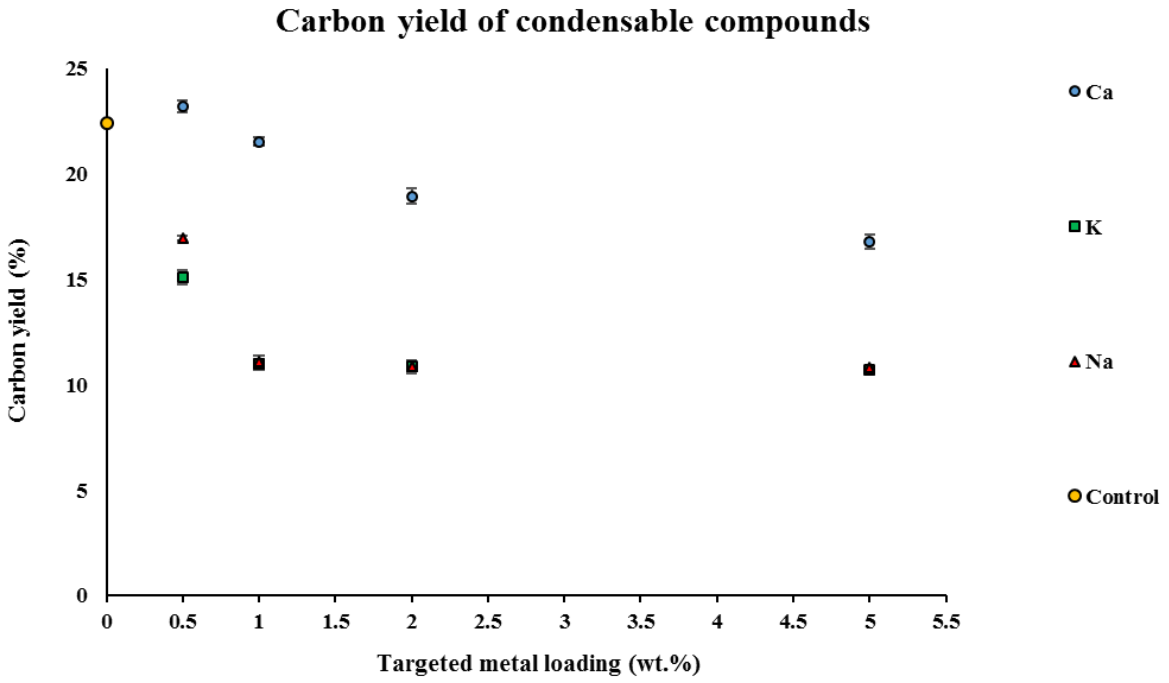

Figure 3.5. Total carbon yield from in-situ CFP experiments with HZSM-5 catalysts deactivated by inorganics

The [illegible] the oxygen content of t[illegible]ounds from

cellulose, hemicellulose and lignin such as phenols, guaiacols, furans, ketones, acids and sugars such as levoglucosan. The Bronsted acid (H^+) sites on the catalyst, where H^+ binds to the negatively charged AlO_4^- unit, acts as the active sites where the cracking reactions and decarboxylation, decarbonylation and dehydration reactions occur, resulting in the formation of the aforementioned hydrocarbons. In this study, the fresh catalyst (control) produced a carbon yield of 22.4 % aromatic hydrocarbons, as shown in Figure 3.6. Deactivation by calcium accumulation on the catalyst produced a linear decrease in the yield of aromatic hydrocarbons, reducing to 9.8 % at the maximum loading of calcium added to the catalyst. Meanwhile, contamination by sodium and potassium appears to rapidly deactivate the catalyst, with 1 wt.% of these alkali metals reducing the yield of aromatic hydrocarbons by more than 75 % (from 22.4 % to 4.9 % and 5.5% respectively). At the maximum loading of sodium and potassium, the production of aromatic hydrocarbons is completely suppressed and the condensable compounds identified in the GC-MS appear to resemble the product composition from non-catalytic pyrolysis of biomass.

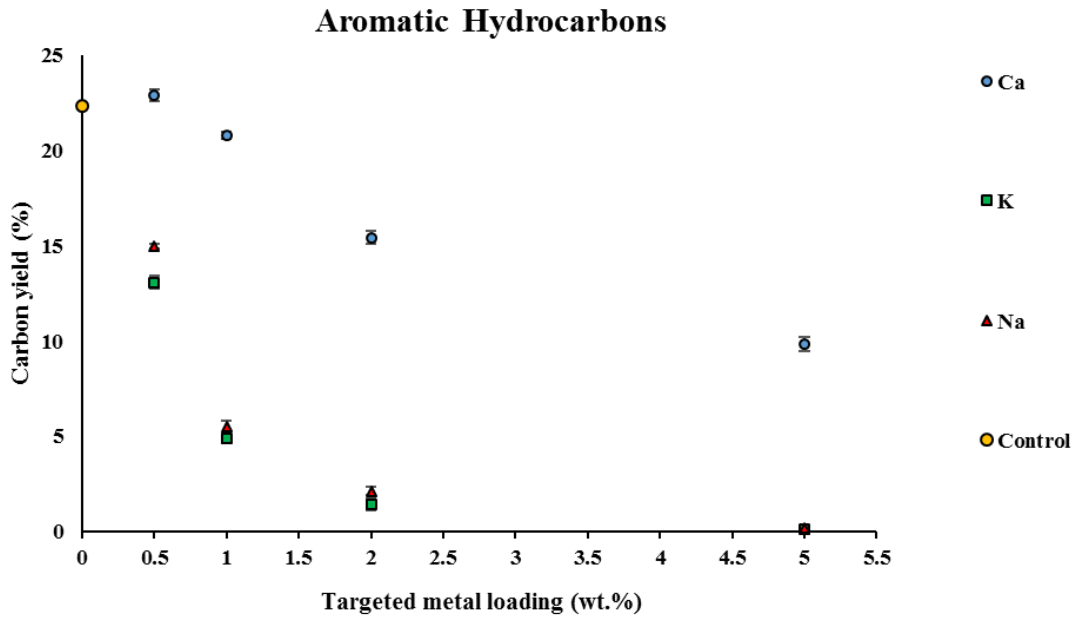

Figure 3.6. Aromatic hydrocarbons yield from in-situ CFP experiments with HZSM-5 catalysts deactivated by inorganics

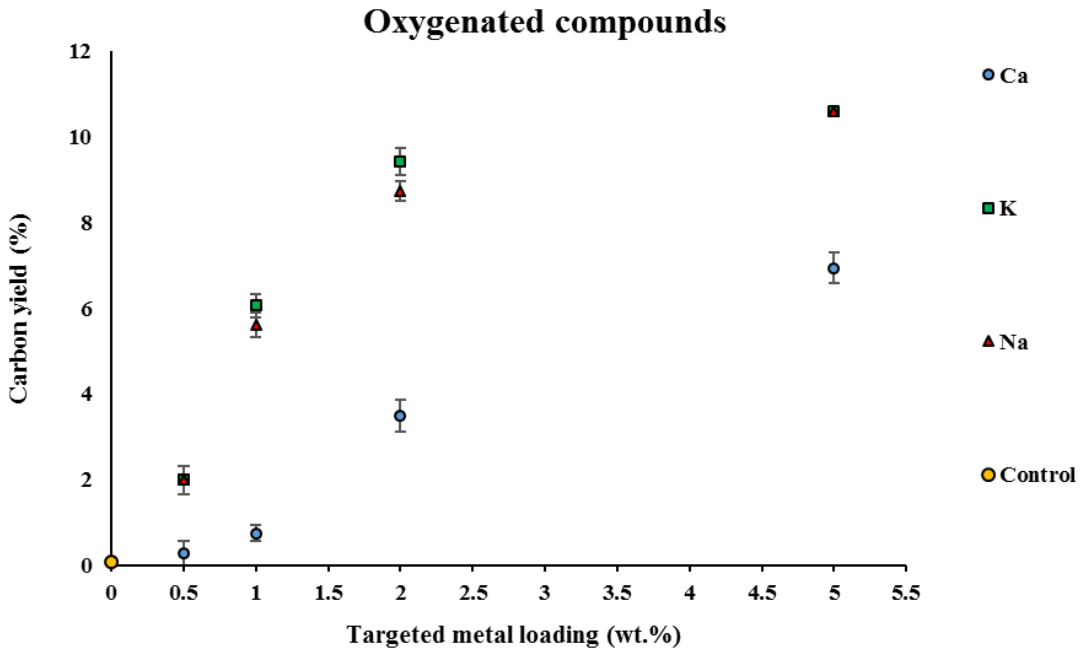

Figure 3.7. Oxygenated compounds yield from in-situ CFP experiments with HZSM-5 catalysts deactivated by inorganics

The exponential rate at which this deactivation occurs is further confirmed by the evolution of oxygenated compounds with increasing levels of deactivation by inorganics. The yield of oxygenated compounds is expected to be inversely proportional to the activity of the catalyst, correlated well by the data from Figure 3.7. Several studies on *in-situ* CFP have also reported decreasing deoxygenation efficiency of the HZSM-5 catalyst with increasing exposure to biomass ash [32, 33, 36, 40]. In this study, CFP experiments with the fresh ZSM-5 catalyst resulted in complete deoxygenation of the pyrolysis vapor, resulting in all the products composed of monocyclic and poly aromatic hydrocarbons. Increasing concentrations of inorganics can be clearly seen to be shifting the product composition towards the formation of oxygenated compounds, with linear increase observed again with calcium and exponential increase in the case of potassium and sodium. At a concentration of 5 wt.%, the catalysts deactivated by potassium and sodium yielded 10.6 % of oxygenated compounds, with negligible amounts (<0.5 %) of aromatic hydrocarbons. It has to be noted that the loss in the carbon yield of aromatic hydrocarbons is not directly compensated by the evolution of these oxygenated compounds and the loss in carbon yield could be a result of a change in product distribution towards the formation of coke and non-condensable gases. These results correlate well with the observations made from surface area and acidity characterizations of the catalysts. The changes due to deactivation by calcium appeared to primarily cause physical poisoning by limiting access to the active sites on the catalyst. The exponential rate at which the product composition changes due to sodium and potassium clearly

shows the combined influence of physical poisoning as well as the inorganics affecting the active sites by removing the proton functionality of the catalyst.

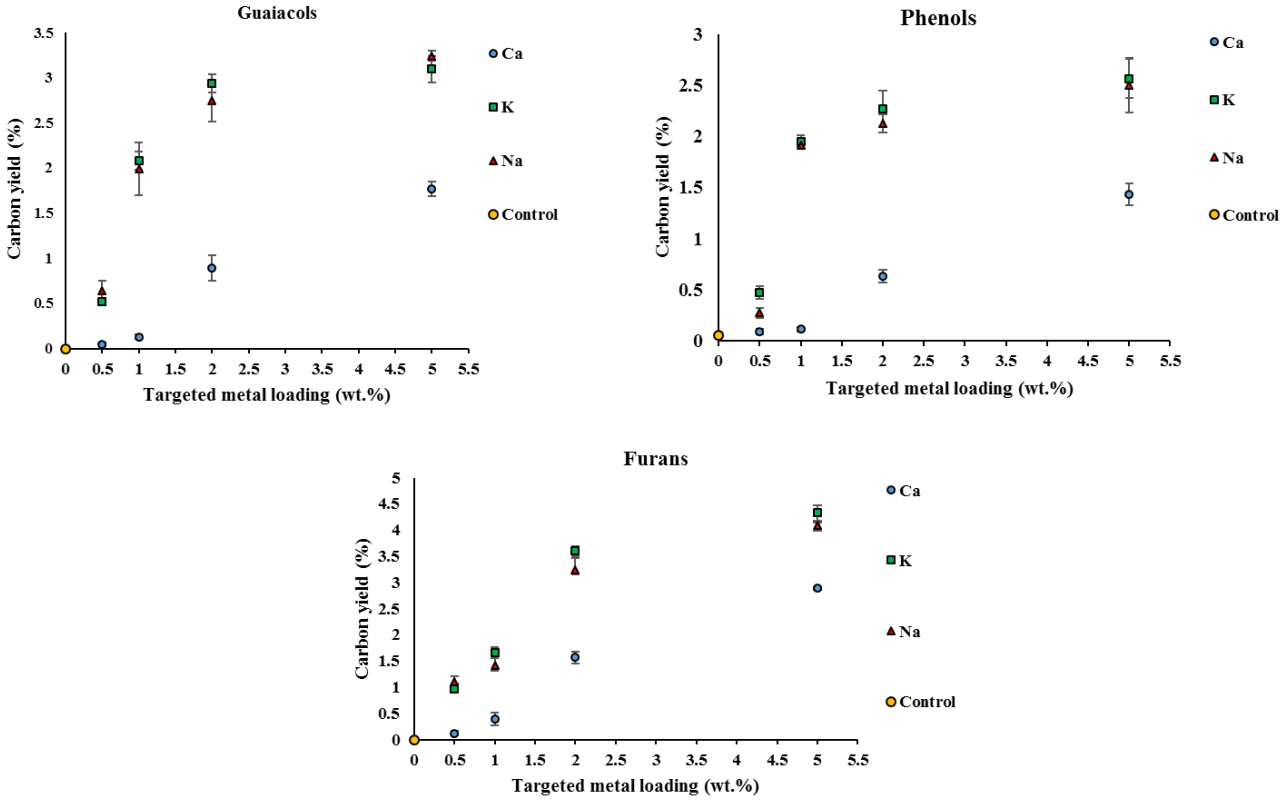

Figure 3.8. Yield of guaiacols, phenols and furans from in-situ CFP experiments with HZSM-5 catalysts deactivated by inorganics

The major oxygenated compounds observed (guaiacols, phenols, furans) showed a clear increasing trend (Figure 3.8) as the concentration of inorganics on the catalyst increased. Furans formed from the decomposition of sugars in biomass have been known to be a precursor for the formation of aromatic hydrocarbons over zeolite catalysts. With increasing levels of deactivation by the inorganics, it is not surprising to observe that the yield of major compounds such as alkyl furans, furfural, 2(5H)-furanone and 2-furancarboxaldehyde, 5-methyl increased. The difference in the yield of furans between potassium-deactivated HZSM-5 (4.33 %) and calcium deactivated-HZSM-5 (2.8 %) could be another indicator that the calcium deactivated catalyst still retains some

of the activity whereas the potassium-deactivated catalyst is completely inert. Similar changes in the yields of guaiacols and phenols were also observed, which increased with increasing presence of the inorganics. However, the evolution of these compounds could also be a result of the catalytic activity of potassium and sodium on lignin, which were shown in a previous study from our group to enhance the depolymerization of lignin during pyrolysis and produce increased yield of monomeric units such as phenols, alkyl phenols and guaiacols [31]. The consequences of deactivation of CFP catalysts due to inorganics observed in this study clearly demonstrates the need to consider the choice of biomass, pyrolysis reactor design and the robustness of the catalyst to prolonged exposure to inorganics found in biomass. Reactor designs that minimize the exposure of the catalyst to char and the inorganics, such as ex-situ upgrading could potentially be the solution to avoid rapid catalyst deactivation.

3.4. Conclusion

The accumulation of biomass inorganics and the resulting deactivation of the catalyst used in CFP is a critical issue that affects the commercial viability of the process. The effect of calcium, potassium and sodium on the deactivation of HZSM-5 was studied and the inorganic species were found to affect its functionality by physical and chemical poisoning of the catalyst. All the inorganic species reduced accessibility to the active sites, but sodium and potassium also chemically deactivated the catalyst by ion-exchange with the acid site (H^+) and reducing the strength of acid sites. The influence of deactivation by these metals on CFP was investigated in a py/GC-MS setup, which clearly indicated the strong negative influence on the performance of the catalyst. Accumulation of sodium and potassium in very low concentrations (0.5 wt.%) was found to be sufficient to cause exponential loss in catalyst activity, whereas higher concentrations

rendered the catalyst inert, losing its ability to deoxygenate pyrolysis vapor and produce aromatic hydrocarbons.

3.5. References

1. Carlson, T., et al., *Aromatic Production from Catalytic Fast Pyrolysis of Biomass-Derived Feedstocks.* Topics in Catalysis, 2009. **52**(3): p. 241-252.
2. Dayton, D.C., et al., *Design and operation of a pilot-scale catalytic biomass pyrolysis unit.* Green Chemistry, 2015. **17**(9): p. 4680-4689.
3. Peters, J.E., J.R. Carpenter, and D.C. Dayton, *Anisole and Guaiacol Hydrodeoxygenation Reaction Pathways over Selected Catalysts.* Energy & Fuels, 2015. **29**(2): p. 909-916.
4. Mante, O.D., et al., *Catalytic pyrolysis with ZSM-5 based additive as co-catalyst to Y-zeolite in two reactor configurations.* Fuel, 2014. **117, Part A**(0): p. 649-659.
5. Mullen, C.A., et al., *Biological Mineral Range Effects on Biomass Conversion to Aromatic Hydrocarbons via Catalytic Fast Pyrolysis over HZSM-5.* Energy & Fuels, 2014. **28**(11): p. 7014-7024.
6. Lødeng, R., et al., *Chapter 11 - Catalytic Hydrotreatment of Bio-Oils for High-Quality Fuel Production*, in *The Role of Catalysis for the Sustainable Production of Bio-fuels and Bio-chemicals*, K.S. Triantafyllidis, A.A. Lappas, and M. Stöcker, Editors. 2013, Elsevier: Amsterdam. p. 351-396.
7. Baker, E.G. and D.C. Elliott, *Catalytic hydrotreating of biomass-derived oils.* Pyrolysis Oils from Biomass, 1988. **376**: p. 353.
8. Mahadevan, R., et al., *Physical and Chemical Properties and Accelerated Aging Test of Bio-oil Produced from in Situ Catalytic Pyrolysis in a Bench-Scale Fluidized-Bed Reactor.* Energy & Fuels, 2015.
9. Mihalcik, D.J., C.A. Mullen, and A.A. Boateng, *Screening acidic zeolites for catalytic fast pyrolysis of biomass and its components.* Journal of Analytical and Applied Pyrolysis, 2011. **92**(1): p. 224-232.
10. L.Shirazi, E.J., M.R. Ghasemi, *The effect of Si/Al ratio of ZSM-5 zeolite on its morphology, acidity and crystal size.* Cryst. Res. Technol, 2008. **43**(12): p. 1300-1306.
11. Iliopoulou, E.F., et al., *Pilot-scale validation of Co-ZSM-5 catalyst performance in the catalytic upgrading of biomass pyrolysis vapours.* Green Chemistry, 2014. **16**(2): p. 662-674.
12. Mahadevan, R., et al., *Fast Pyrolysis of Biomass: Effect of Blending Southern Pine and Switchgrass.* Transactions of the Asabe, 2016. **59**(1): p. 5-10.
13. Serapiglia, M.J., et al., *Evaluation of the impact of compositional differences in switchgrass genotypes on pyrolysis product yield.* Industrial Crops and Products, 2015. **74**: p. 957-968.
14. Pasangulapati, V., et al., *Effects of cellulose, hemicellulose and lignin on thermochemical conversion characteristics of the selected biomass.* Bioresource Technology, 2012. **114**(0): p. 663-669.
15. Wang, S., et al., *Comparison of the pyrolysis behavior of lignins from different tree species.* Biotechnology Advances, 2009. **27**(5): p. 562-567.
16. Garcia-Perez, M., et al., *Fast Pyrolysis of Oil Mallee Woody Biomass: Effect of Temperature on the Yield and Quality of Pyrolysis Products.* Industrial & Engineering Chemistry Research, 2008. **47**(6): p. 1846-1854.

17. Yang, H., et al., *In-Depth Investigation of Biomass Pyrolysis Based on Three Major Components: Hemicellulose, Cellulose and Lignin.* Energy & Fuels, 2005. **20**(1): p. 388-393.
18. Boateng, A.A., et al., *Bench-Scale Fluidized-Bed Pyrolysis of Switchgrass for Bio-Oil Production†.* Industrial & Engineering Chemistry Research, 2007. **46**(7): p. 1891-1897.
19. Thangalazhy-Gopakumar, S., et al., *Physiochemical properties of bio-oil produced at various temperatures from pine wood using an auger reactor.* Bioresource Technology, 2010. **101**(21): p. 8389-8395.
20. Bridgwater, A.V., *Review of fast pyrolysis of biomass and product upgrading.* Biomass and Bioenergy, 2012. **38**(0): p. 68-94.
21. Eom, I.-Y., et al., *Effect of essential inorganic metals on primary thermal degradation of lignocellulosic biomass.* Bioresource Technology, 2012. **104**: p. 687-694.
22. Patwardhan, P.R., et al., *Influence of inorganic salts on the primary pyrolysis products of cellulose.* Bioresource Technology, 2010. **101**(12): p. 4646-4655.
23. Agblevor, F.A. and S. Besler, *Inorganic Compounds in Biomass Feedstocks. 1. Effect on the Quality of Fast Pyrolysis Oils.* Energy & Fuels, 1996. **10**(2): p. 293-298.
24. Aho, A., et al., *Pyrolysis of pine and gasification of pine chars – Influence of organically bound metals.* Bioresource Technology, 2013. **128**: p. 22-29.
25. Patwardhan, P.R., R.C. Brown, and B.H. Shanks, *Understanding the Fast Pyrolysis of Lignin.* ChemSusChem, 2011. **4**(11): p. 1629-1636.
26. El-Nashaar, H., et al., *Genotypic variability in mineral composition of switchgrass.* Bioresource technology, 2009. **100**(5): p. 1809-1814.
27. Monti, A., N. Di Virgilio, and G. Venturi, *Mineral composition and ash content of six major energy crops.* Biomass and Bioenergy, 2008. **32**(3): p. 216-223.
28. Park, H.J., Y.-K. Park, and J.S. Kim, *Influence of reaction conditions and the char separation system on the production of bio-oil from radiata pine sawdust by fast pyrolysis.* Fuel Processing Technology, 2008. **89**(8): p. 797-802.
29. Fahmi, R., et al., *The effect of alkali metals on combustion and pyrolysis of Lolium and Festuca grasses, switchgrass and willow.* Fuel, 2007. **86**(10–11): p. 1560-1569.
30. Yang, C.-y., et al., *TG-FTIR Study on Corn Straw Pyrolysis-influence of Minerals1.* Chemical Research in Chinese Universities, 2006. **22**(4): p. 524-532.
31. Mahadevan, R., et al., *Effect of Alkali and Alkaline Earth Metals on in-Situ Catalytic Fast Pyrolysis of Lignocellulosic Biomass: A Microreactor Study.* Energy & Fuels, 2016. **30**(4): p. 3045-3056.
32. Yildiz, G., et al., *Effect of biomass ash in catalytic fast pyrolysis of pine wood.* Applied Catalysis B: Environmental, 2015. **168–169**: p. 203-211.
33. Stefanidis, S.D., et al., *Catalyst hydrothermal deactivation and metal contamination during the in situ catalytic pyrolysis of biomass.* Catalysis Science & Technology, 2016. **6**(8): p. 2807-2819.
34. Mullen, C.A. and A.A. Boateng, *Accumulation of inorganic impurities on HZSM-5 zeolites during catalytic fast pyrolysis of switchgrass.* Industrial & Engineering Chemistry Research, 2013. **52**(48): p. 17156-17161.
35. Paasikallio, V., et al., *Product quality and catalyst deactivation in a four day catalytic fast pyrolysis production run.* Green Chemistry, 2014. **16**(7): p. 3549-3559.
36. Mullen, C.A., Boateng, A.A., *Accumulation of inorganic impurities on HZSM-5 during catalytic fast pyrolysis of switchgrass.* Journal of Industrial and Engineering Chemical Research, 2013. **52**: p. 17156-17161.
37. Yildiz, G., et al., *Catalytic Fast Pyrolysis of Pine Wood: Effect of Successive Catalyst Regeneration.* Energy & Fuels, 2014. **28**(7): p. 4560-4572.

38. Zheng, Y., A.D. Jensen, and J.E. Johnsson, *Deactivation of V2O5-WO3-TiO2 SCR catalyst at a biomass-fired combined heat and power plant.* Applied Catalysis B: Environmental, 2005. **60**(3–4): p. 253-264.
39. Huang Li, Z.S., Zhou Yuming, Zhang Yiwei, Xu Jun, Wang Li, *Influence of the Alkali Treatment of HZSM-5 Zeolite on Catalytic Performance of PtSn-Based Catalyst for Propane Dehydrogenation.* China Petroleum Processing & Petrochemical Technology 2013. **15**(2): p. 11-18.
40. Wang, K., et al., *The deleterious effect of inorganic salts on hydrocarbon yields from catalytic pyrolysis of lignocellulosic biomass and its mitigation.* Applied Energy, 2015. **148**: p. 115-120.

4. Effect of torrefaction temperature on lignin macromolecule and product distribution from fast pyrolysis

Abstract

Torrefaction is a low-temperature process considered as an effective pretreatment technique to improve the grindability of biomass as well as enhance the production of aromatic hydrocarbons from Catalytic Fast Pyrolysis (CFP). This study was performed to understand the effect of torrefaction temperature on structural changes in the lignin macromolecule and its subsequent influence on *in-situ* CFP process. Lignin extracted from southern pine and switchgrass (*via* organosolv treatment) was torrefied at four different temperatures (150, 175, 200 and 225 ˚C) in a tubular reactor. Between the two biomass types studied, lignin from pine appeared to have greater thermal stability during torrefaction when compared with switchgrass lignin. The structural changes in lignin as a result of torrefaction were followed by using FTIR spectroscopy, solid state CP/MAS ^{13}C NMR, ^{31}P NMR spectroscopy and it was found that higher torrefaction temperature (200 and 225 ˚C) caused polycondensation and de-methoxylation of the aromatic units of lignin. Gel permeation chromatography analysis revealed that polycondensation during torrefaction resulted in an increase in the molecular weight and polydispersity of lignin. The torrefied lignin was subsequently used in CFP experiments using H^+ZSM-5 catalyst in a micro-reactor (Py-GC/MS) to understand the effect of torrefaction on the product distribution from pyrolysis. It was observed that although the selectivity of benzene-toluene-xylene compounds from CFP of pine improved from 58.3% (torrefaction temp at 150 ˚C) to 69.0% (torrefaction temp at 225 ˚C), the severity of torrefaction resulted in a loss of overall aromatic hydrocarbon yield from 11.6% to 4.9% under same conditions. Torrefaction at higher temperatures also increased the yield of carbonaceous residues from 63.9% to 72.8%. Overall, torrefying lignin caused structural

transformations in both type of lignins (switchgrass and pine), which is ultimately detrimental to achieving a higher aromatic hydrocarbon yield from CFP.

Keywords: *Biomass, Catalytic Fast Pyrolysis (CFP), Torrefaction, Lignin*

4.1. Introduction

Biomass has been considered to be a sustainable carbon source for producing chemicals and liquid intermediates through fast pyrolysis, which could be upgraded to renewable fuels and other valuable products [1-13]. It consists of three major components cellulose, hemicellulose and lignin, whose composition varies from one species to another. Cellulose is a linear polymer composed of 1,4 beta-D linked anhydroglucose subunits, whereas hemicellulose is a branched, amorphous polysaccharide made of five carbon sugar compounds. Lignin is the third constituent, which occurs between the cells and cell walls. In general, it can be defined as an amorphous aromatic polymer of phenyl propane units which has small amounts of extractives and inorganic materials. It is a complex and high molecular weight polymer formed by the dehydrogenation of hydroxyl cinnamyl alcohols such as coniferyl and sinapyl alcohols. The degree of methoxylation differs between the various lignin precursors and various types of intermolecular linkages (β-O-4, α-O-4, 5-5, β-5, and β-β) can occur, which varies in composition between different types of biomass. The decomposition of lignin results in the formation of compounds such as guaiacol, vanillin, syringol, anisole and other phenolic compounds. Due to such complexity in the structure of biomass, the thermal breakdown of these constituents (cellulose, hemicellulose and lignin) during pyrolysis results in the formation of a complex mixture of condensable compounds along with non-condensable gases and char.

This liquid intermediate from pyrolysis (bio-oil) suffers from certain undesirable properties such as (1) high oxygen content (~30-40%) making the product immiscible with conventional fuels; (2) presence of organic acids, causing corrosion and instability during storage; (3) low heating value (~19 MJ/kg) when compared to fossil-based fuels; (4) alkali and alkaline earth metals (Na, K, Ca and Mg) in biomass, which alters pyrolysis chemistry. A number of studies in the past decade have focused on improving these properties by deoxygenating the bio-oil from pyrolysis through catalytic upgrading and hydrodeoxygenation [9, 14-19]. Promising catalysts including zeolites are being actively studied for *in-situ* catalytic fast pyrolysis (CFP) to upgrade the pyrolysis vapors and produce a highly deoxygenated liquid product. However recently, mild thermal pretreatment (torrefaction) has been suggested as an effective process to improve the properties of biomass before it is used as a feedstock for pyrolysis. Some of the advantages of torrefaction, such as (1) improved grindability of biomass; (2) lower O/C ratio; (3) improved biomass hydrophobicity; make it a promising technique to improve the economics of biomass-to-energy conversion.

During torrefaction, biomass is generally heated at moderate temperatures (200 – 300 ˚C) in an inert environment, which results in reduced oxygen content in the torrefied biomass mainly due to extensive decomposition of hemicellulose in this temperature range. Hemicellulose decomposition products such as acetic acid, furfural, water, CO and CO_2 are released from biomass during this process [20]. Meanwhile, the structure of cellulose remains relatively intact during this process since higher temperatures (>300 ˚C) are required for complete decomposition. Recent studies on torrefaction of biomass have shown that torrefaction is an effective pre-treatment which improves the yield and selectivity of aromatic hydrocarbons from CFP of torrefied biomass [21-26]. Recent publications by Neupane et al. [21] and Srinivasan et al. [25] discussed the effect of torrefaction parameters such as residence time and temperature on the structural changes in biomass and its

subsequent influence on the product distribution from catalytic pyrolysis of biomass. Neupane et al. observed higher carbon yield of aromatic hydrocarbons from CFP of torrefied biomass and proposed that this could be a result of de-etherification and de-methoxylation of lignin during torrefaction. However, since very limited studies have focused on the torrefaction and CFP of individual components of biomass, this hypothesis could not be confirmed. Further, the structural changes in lignin as a function of torrefaction at various temperatures is also not clear. Thus, the objective of this study was to understand the effect of torrefaction temperature on the structural changes in lignin and its influence on the product distribution from pyrolysis. Torrefaction of lignin extracted from southern pine and switchgrass through organosolv treatment was performed in a tubular reactor. Subsequently, the non-catalytic and *in-situ* CFP of torrefied lignin were performed in a micro-pyrolyzer.

4.2. Materials and methods

4.2.1. Biomass Preparation

The southern pine used in this study was obtained from a local wood chipping plant in Opelika, Alabama and switchgrass was obtained from E.V. Smith Research Center, Macon County, Alabama. Biomass was first air dried for 72 h and a hammer mill (New Holland Grinder Model 358) fitted with a 1.58 mm (1/16 in.) sized screen was used to grind the samples. Subsequently, it was fractionated using a sieve shaker and particles in the desired size range (400 µm to 840 µm) were used for organosolv lignin extraction.

4.2.2. Organosolv Extraction

A known amount (350 g) of the biomass (dry weight) was soaked for 24 h in 65% ethanol and 1.0% (w/w) sulfuric acid (based on biomass) in a solid to liquid ratio of 1:7. The mixture containing biomass and liquor was loaded in a 4.0 L Parr reactor and pretreated at 170 °C for 1 h with a stirring rate of 60 rpm. After pretreatment, the reactor was cooled in a water bath and the resulting slurry was separated into a solid fraction and a liquid fraction by filtration. The solid fraction was washed with warm ethanol three times to remove the extractable lignin and stored at -20°C. To prepare ethanol organosolv lignin (EOL) from biomass, 3-fold volume of water was added to organosolv spent liquor (the liquid fraction) after pretreatment. Organosolv lignin was precipitated and collected by vacuum filtration on Whatman No. 1 filter paper, washed with warm water to remove the water-soluble compounds and then dried. Since the pyrolysis was to be performed in a micro-pyrolyzer, the lignin had to be sieved further using a 200 mesh (74 μm) and the fraction that passed was used for characterization, torrefaction and pyrolysis experiments in this study.

4.2.3. Lignin Torrefaction and Characterization

Lignin from pine and switchgrass was torrefied at four temperatures (150, 175, 200, 225 ˚C) for 15 min in a tubular reactor (18 in. long, 1 in. outer diameter) placed in a programmed furnace (Thermo Scientific model TF55035A-1). 5 g of organosolv lignin was used for torrefaction at each condition, and the volatiles released from lignin during torrefaction were swept away by nitrogen gas flow at 1 l/min. Treatment time was said to begin when the furnace reached the desired set point. At the end of the treatment time, the torrefied samples were pulled from the furnace and immediately placed in desiccators to prevent further treatment and combustion. The samples (shown in Supplementary Information Figure S1) were weighed before and after torrefaction to

calculate the mass loss as a result of torrefaction using a microbalance (Mettler Toledo, model XP6). Moisture and ash contents were determined for the lignin samples according to ASTM E872 and E1755 standards, respectively. Ultimate analysis to measure the carbon, hydrogen, nitrogen, oxygen and sulfur contents was performed for raw and torrefied lignin using a CHNS elemental analyzer (Thermo Scientific, model Flash 2000). Component analysis to measure extractives, cellulose, hemicellulose and lignin contents was performed according to Laboratory Analytical Procedure (LAP) developed by National Renewable Energy Laboratory [27]. Thermogravimetric (TG) analysis to calculate the weight loss as a function of temperature of raw and torrefied lignin was performed (TA Instruments, 2050 TGA) with a heating rate of 10 ˚C/min and helium flow rate of 20 ml/min. FTIR analysis to study the structure of raw and torrefied lignin was done using a Perkin Elmer Spectrum model 400 (Perkin Elmer Co., Waltham, MA). Each spectrum was recorded after 32 scans from 4000 to 650 cm^{-1}, by applying a vertical load on the sample at room temperature. Solid-state CP/MAS ^{13}C NMR analysis was performed on a Bruker Avance III 400 MHz spectrometer, according to the methods previously described by Neupane et al [21].

The lignin samples for Gel Permeation Chromatography (GPC) analysis were manually milled in a jar for 5-10 min. The molecular weight of lignin was analyzed by GPC after lignin acetylation. The derivatization of lignin was conducted on a basis of 10 mg lignin in 1 mL of 1:1 pyridine/acetic anhydride in the dark at room temperature for 24 h, 200 RPM. The solvent/reagents were removed by co-evaporation at 45ºC with ethanol, several times, using a rotatory evaporator until dry. The resulting acetylated lignin was dissolved in tetrahydrofuran (THF) and the solution was filtered through 0.45 μm membrane filter before GPC analysis. The hydroxyl groups in lignins were quantitated by ^{31}P NMR after lignin phosphitylation. In detail, the lignin samples were vacuum dried at 45 ˚C overnight before phosphitylation and 25.0 mg of lignin was accurately weighted

into a 4-mL tube. 0.5 mL of a prepared stock solution of pyridine/deuterated chloroform (1.6/1, v/v) including 1 mg/mL $Cr_{(acac)3}$ and 4 mg/mL internal standard (endo N-hydroxy-5-norbene-2,3-dicarboxylic acid imide) was added to dissolve lignin. The phosphitylation was performed by adding 50 µL of the phosphitylating reagent TMDP (2-chloro-4,4,5,5-tetramethyl-1,3,2-dioxaphospholane). Quantitative ^{31}P NMR spectra were acquired on a Bruker Advance 400 MHz spectrometer equipped with a BBO probe with 64-scans and a total runtime of 28 min. All chemical shifts reported are relative to the product of TMDP with water, which has been observed to give a sharp signal in pyridine/$CDCl_3$ at 132.2 ppm.

4.2.4. Catalyst

A commercially available HZSM-5 catalyst (CBV 2314 with a SiO_2/Al_2O_3 ratio of 23:1, Zeolyst, USA) was used in the *in-situ* CFP experiments. The catalyst was sieved using a 200 mesh and the fraction that passed through the sieve (<74 µm) was used in this study. It was then calcined for 5 hours at 550 ˚C in a muffle furnace to convert the catalyst to the acid form prior to use. The lignin/catalyst mixture for *in-situ* CFP experiments was prepared by mixing 50 mg of the lignin and 200 mg of the catalyst using an ultrasonic bath (VWR Scientific, catalog no. 97043-960) to get a mixture having a lignin to catalyst ratio of 1:4. A microbalance with sensitivity of 0.001 mg (Mettler Toledo, XP6) was used to measure the sample weight.

4.2.5. Experimental procedure

Pyrolysis experiments were carried out on a Tandem micro-reactor system (Frontier Laboratories, Rx-3050 TR), which was connected to a gas chromatograph (Agilent Technologies, 7890A). Figure 4.1 shows a schematic diagram of the system used in this study containing two quartz pyrolysis tube reactors (4.7 mm ID, 114 mm length) arranged in series.

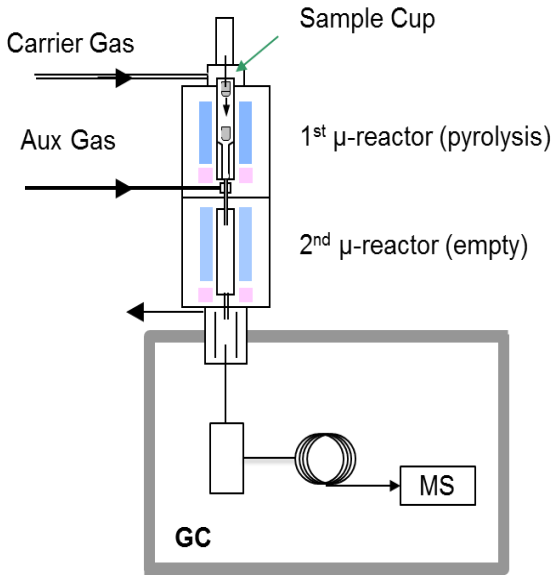

Figure 4.1. Schematic of tandem micro-reactor used in this study

The reactors were equipped with independent temperature control between 40-900 ˚C and an independent temperature controlled interface between the two reactors to prevent condensation of pyrolysis products. Samples were placed in deactivated stainless steel sample cups and loaded into the reactor. Helium gas flow for 45 seconds purged the reaction environment and the sample cup was then dropped into the pyrolysis reactor (drop time of 15-20 milliseconds [28]). The products of pyrolysis from the first reactor were swept into a GC-MS using helium gas flow for analyzing the product composition. In the non-catalytic experiments, 0.5 mg of the lignin was pyrolyzed in the first reactor, and the second reactor was empty. For *in-situ* CFP experiments in this study,

approximately 2.5 mg of the lignin/catalyst mixture (lignin:catalyst – 1:4) was pyrolyzed in the first reactor and the second reactor was empty. The second reactor was also maintained at the same temperature as the interface at 350 ˚C in order to prevent condensation of pyrolysis vapor. A gas chromatograph (Agilent Technologies, 7890A) equipped with an Agilent DB 1701 capillary column (60 m × 0.250 mm and 0.250 µm film thickness) was used to separate and analyze condensable compounds from pyrolysis. A split ratio of 1:100 was used for sample injection into the column and the GC inlet was maintained at 250 ˚C. The GC oven was programmed to start at 40 ˚C and hold for 3 min, after which it was ramped at 5 ˚C/min up to the final temperature of 270 ˚C. The final temperature was held for 6 min and the overall time of the oven program was 55 min. The column was connected to a mass spectrometer (Agilent Technologies, 5975C) for compound identification and quantification by using calibration standards. Some of the major products identified (non-catalytic pyrolysis products from lignin / aromatic hydrocarbons from *in-situ* CFP) were quantified using pure compounds purchased from Sigma-Aldrich (St. Louis, Missouri). Calibration factors for quantification were prepared by using three different concentrations of the standards. A Porous Layer Open Tubular (PLOT) column (Agilent Technologies, GS-GasPro) was used to analyze the composition of non-condensable gas (NCG) products (CO, CO_2, CH_4, C_2H_4, C_2H_6, C_3H_6, C_3H_8 and C_4H_8) and a standard gas mixture of these NCG was used to calibrate the yield of non-condensable gases. The weight of the sample cup before and after the experiment was measured in order to calculate the char yield. However, it was not possible to distinguish between pyrolysis char and catalytic coke in the *in-situ* CFP experiments which were performed with the catalyst mixed along with the lignin in the sample cup.

Each experiment was performed in duplicate in order to obtain a standard deviation for the results and verify the reproducibility of the data. Three factors of interest at various levels – 1) type of

biomass used (pine, switchgrass); 2) torrefaction temperature (150, 175, 200, 225 ˚C); and 3) with and without catalyst – were the focus of this study. The nomenclature of the samples in this study is shown in Table 4.1. Results labelled as CFP are from experiments using HZSM-5 as the *in-situ* catalyst. JMP software (SAS Institute, Cary, North Carolina) was used to perform statistical analysis of the results such as ANOVA, Tukey's HSD at a 95% confidence interval. However due to the accuracy of the results from using the micro-pyrolyzer, the standard deviation of the results was less than 5% and is not shown. The ratio of carbon in a specific product or group to the carbon contained in the feedstock is the total carbon yield of that product or group and is used to report the results from CFP experiments. Selectivity of a particular aromatic hydrocarbon is defined as the ratio of moles of carbon in that product to the total moles of carbon in all aromatic hydrocarbons produced. The overall carbon balance for most of the experiments was close to or above 90 % with the remaining fraction including large molecular weight compounds not identified by the GC.

Table 4.1. Nomenclature used for samples torrefied at different temperatures

Nomenclature	Torrefaction Temperature (˚C)	Description
RLP	Control	Raw (Non-torrefied) Lignin Pine
TP 150	150	Torrefied Lignin Pine - 150 °C
TP 175	175	Torrefied Lignin Pine - 175 °C
TP 200	200	Torrefied Lignin Pine - 200 °C
TP 225	225	Torrefied Lignin Pine - 225 °C
RLS	Control	Raw (Non-torrefied) Lignin Switchgrass
TS 150	150	Torrefied Lignin Switchgrass - 150 °C
TS 175	175	Torrefied Lignin Switchgrass - 175 °C
TS 200	200	Torrefied Lignin Switchgrass - 200 °C
TS 225	225	Torrefied Lignin Switchgrass - 225 °C

4.3. Results and Discussion

4.3.1. Lignin characterization and mass yield after torrefaction

Raw lignin obtained from organosolv treatment of pine was measured to have moisture and ash contents of 2.6 ± 0.15 (wt.% on wet basis) and 0.65 ± 0.09 (wt.% on dry basis), while lignin from switchgrass had moisture and ash contents of 1.8 ± 0.22 (wt.%) and 1.2 ± 0.18 (wt.%), respectively. Torrefaction produced a small increase in the carbon content of lignin along with a corresponding decrease in the oxygen content as shown in Table 4.2, possibly due to the removal of moisture and volatile oxygenates during torrefaction. Although lignin generally does not decompose completely below 300 ˚C, mass yield results from Table 4.3 shows that at a torrefaction temperature of 225 ˚C, the mass loss for lignin was greater than 10% with both pine and switchgrass. The chemical composition of the organosolv lignin is shown in Table 4.4, which shows that some residual sugars were present in the lignin even after multiple steps of purification.

Table 4.2. Ultimate analysis of raw and torrefied samples *

Sample	Carbon (wt.%)	Hydrogen (wt.%)	Oxygen (wt.%)
RLP	65.52 ^{A}	5.63 ^{A}	28.60 ^{A}
TP 150	65.90 ^{A}	5.44 ^{B}	28.42 ^{A}
TP 175	66.29 ^{B}	5.41 ^{B}	28.07 ^{B}
TP 200	67.34 ^{C}	5.41 ^{B}	27.03 ^{C}
TP 225	67.78 ^{C}	5.33 ^{C}	26.68 ^{C}
RLS	64.88 ^{A}	5.69 ^{A}	28.79 ^{A}
TS 150	65.17 ^{B}	5.62 ^{B}	28.58 ^{A}
TS 175	65.77 ^{C}	5.68 ^{A}	27.95 ^{B}
TS 200	65.83 ^{C}	5.63 ^{B}	27.92 ^{B}
TS 225	66.59 ^{D}	5.57 ^{A}	27.23 ^{C}

*Results in dry, ash-free basis. Values connected by same letter are not statistically different.

Table 4.3. Mass yield of torrefied samples *

Sample	Mass yield (wt.%)
TP 150	97.90
TP 175	94.34
TP 200	92.41
TP 225	89.33
TS 150	95.19
TS 175	92.78
TS 200	89.11
TS 225	87.16

*Dry, ash-free basis. Single run only.

Table 4.4. Chemical composition of organosolv lignins used for torrefaction *

Chemical Composition, wt.%	RLP	RLS
Glucan	1.5	0.8
Xylan	1.9	2.3
Mannan	0.0	0.5
Arabinan	0.6	0.0
Galactan	0.5	0.2
Klason lignin	93.6	94.3
Ash (%)	0.65	1.2

*Dry, ash-free basis. Single run only.

TG and differential TG (DTG) curves obtained for the raw and torrefied lignins are shown in Figure 4.2 and Figure 4.3, which clearly show that the thermal degradation of lignin occurs over a wide temperature range (100 ˚C – 600˚C). From the DTG curves for pine and switchgrass lignins, the initial/onset temperature of devolatalization (T_i, corresponding to 5 % weight loss) can be observed to be increasing with increase in torrefaction temperature. As torrefaction severity increased, the initial peak in the DTG curve (between 120 ˚C – 250˚C) decreased, which could be attributed to the fact that extensive depolymerization and side-chain splitting of lignin could have already taken place during torrefaction at higher temperatures [22]. The characteristic parameters from these curves listed in Table 4.5 also show that the maximum weight loss rate (DTG_{max}) was

significantly higher for lignin from switchgrass when compared to lignin from pine. It should also be noted that torrefaction of lignins at higher temperatures led to an increase in the amount of residues, which increased from 44.47 wt.% to 50.11 wt.% for pine and a similar increase for switchgrass lignin. While these TG/DTG curves give us useful information, they cannot be used as a standalone analytical technique to predict the effect of torrefaction on pyrolysis behavior, since the heating rate employed in this analysis cannot be compared to the heating rates during fast pyrolysis.

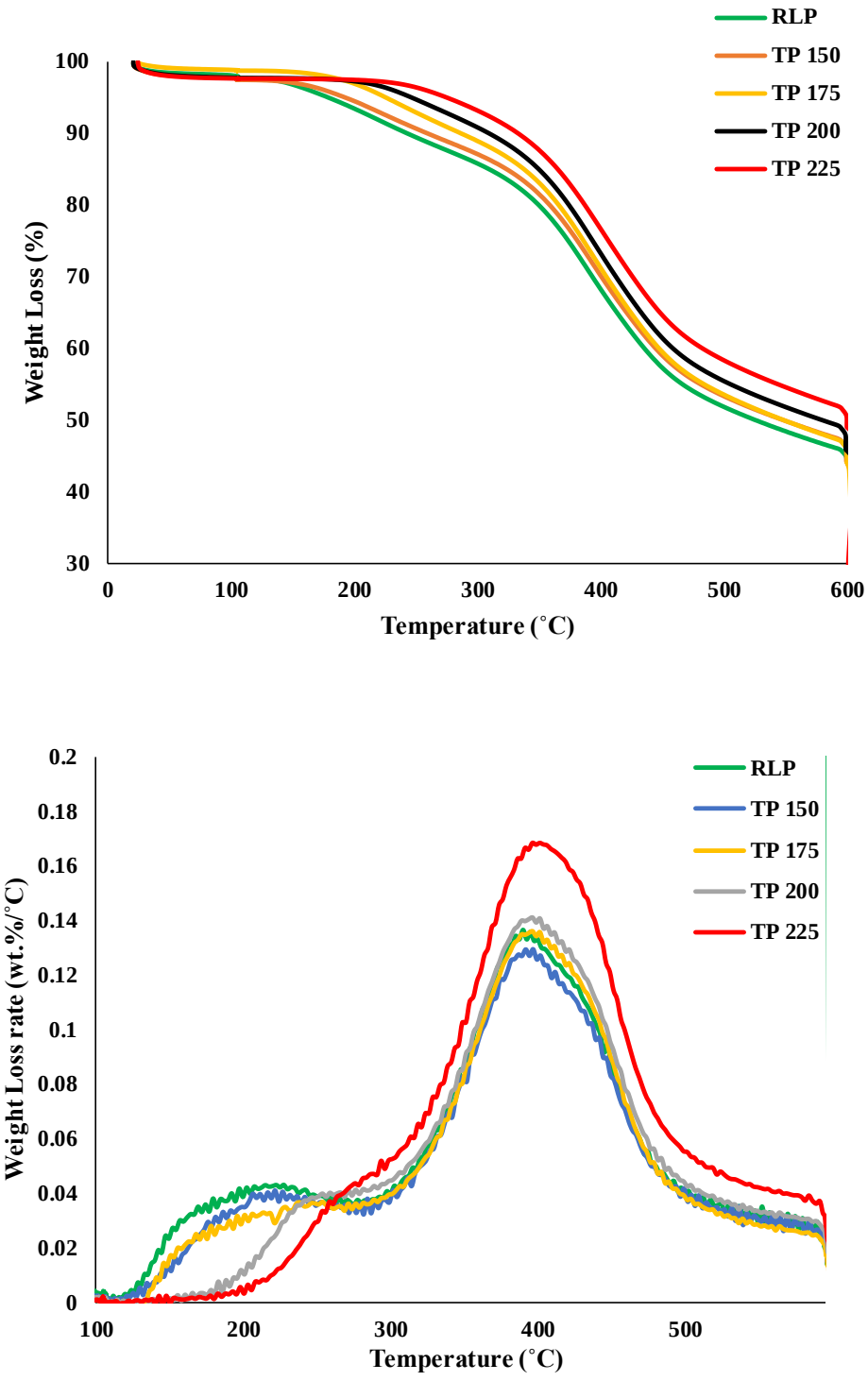

Figure 4.2. TG/DTG curves of lignin from pine torrefied at different temperatures

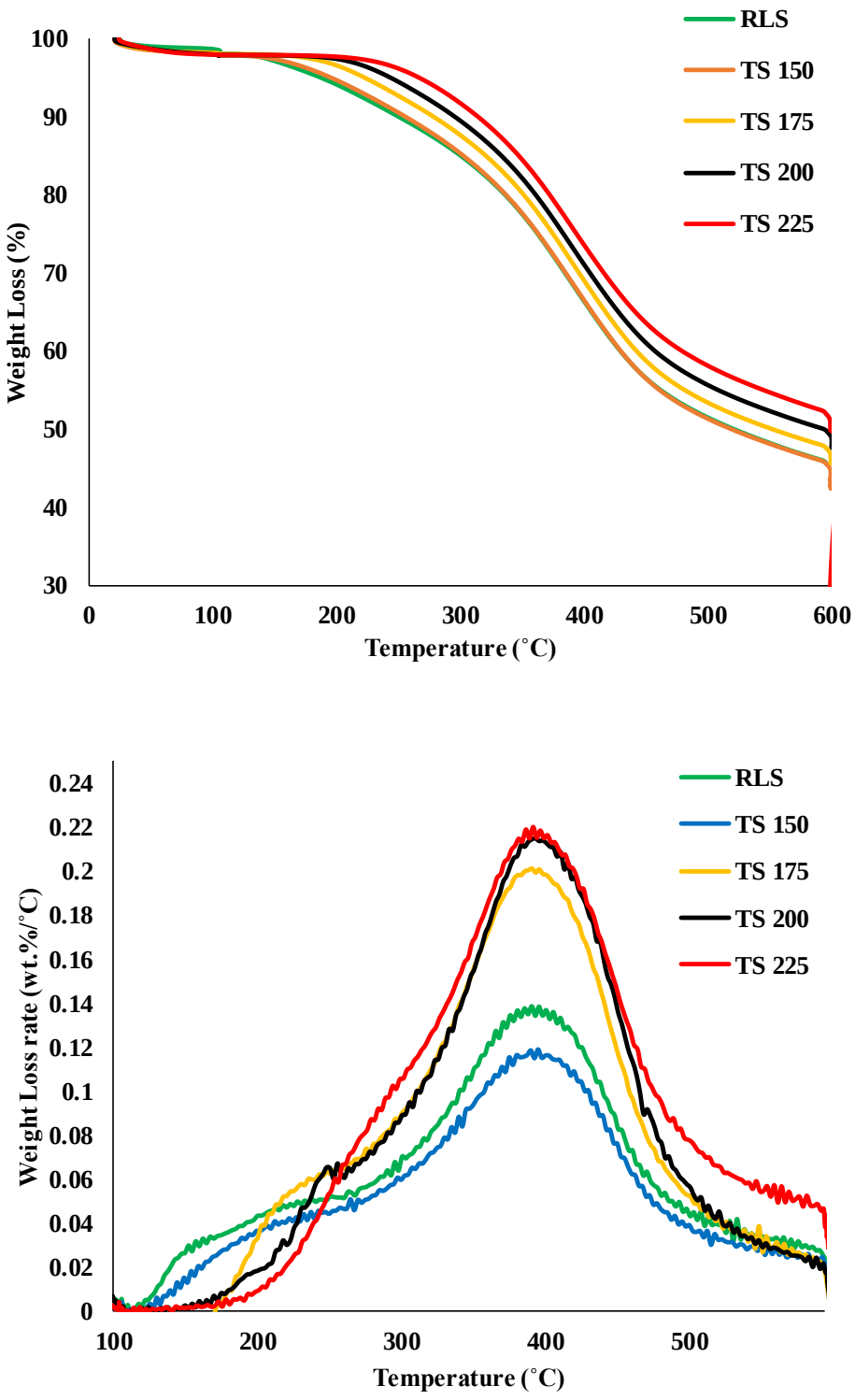

Figure 4.3. TG/DTG curves of lignin from switchgrass torrefied at different temperatures

Table 4.5. Characteristic parameters from TG/DTG analysis of raw and torrefied lignins

Feedstock	T_i (°C)	DTG_{max} (wt.%/min)	Residue* (wt.%)
RLP	182	0.134	44.47
TP 150	193	0.130	45.78
TP 175	227	0.137	45.38
TP 200	248	0.140	47.55
TP 225	276	0.167	50.11
RLS	189	0.138	44.71
TS 150	197	0.120	44.52
TS 175	223	0.200	46.57
TS 200	242	0.214	48.63
TS 225	269	0.220	50.86

*Note: The residue (wt.%) is the amount of sample observed at the final temperature of 600 °C

4.3.3. Structural characterization of torrefied lignins

Structural transformations in lignin during torrefaction were characterized by FTIR, ^{13}C CP/MAS NMR and ^{31}P NMR spectroscopy. Further, GPC analysis was performed to observe the change in the molecular weight of the lignins as a result of torrefaction. The FTIR spectra of raw and torrefied lignins from pine and switchgrass are shown in Figure 4.4 and Figure 4.5. The band assignments shown in Table 4.6 were based on literature data on FTIR analysis of lignins from softwood and herbaceous plants [29]. All the lignin samples showed a broad band at 3420 cm^{-1} (OH stretch) and peaks at 2927 cm^{-1} and 2856 cm^{-1} corresponding to C-H stretching of methyl/methoxyl groups. With increase in torrefaction temperature, there is an increase in the intensity of signals at 1601 cm^{-1} and 1209 cm^{-1} (C-C, C-O and C=O stretch), which could be indicative of aliphatic side chain splitting and polycondensation reactions of lignin [22, 30]. Meanwhile, a sharp decrease in the intensity of signals at 1712 cm^{-1} and 1511 cm^{-1} (aromatic skeletal vibrations in lignin), 1459 and 1426 cm^{-1} (methoxy group ($O-CH_3$) of the lignin structure), 1263 cm^{-1} (guaiacyl ring and C-O stretch in lignin) are possible indicators for the demethoxylation, cleavage of β-O-4 linkages in

lignin during torrefaction. Further, it can also be seen that bands listed in Table 4.6 corresponding to guaiacyl and syringyl units in switchgrass appear to also decrease as a result of torrefaction.

Table 4.6. FTIR analysis of lignin – assignment of main bands between 1800 and 900 cm-*1*

Wave number (cm^{-1})	Band origin
3420	O-H stretch
2927	C-H stretch in CH_3 or CH_2 groups
2856	C-H vibration of methyl group of methoxyl
1712	Aromatic skeletal vibration in lignin, C=O stretch (unconjugated)
1665	Aromatic skeletal vibration in lignin, C=O stretch (conjugated)
1601	Aromatic skeletal vibration in lignin, C=O stretch
1511	Aromatic skeletal vibration in lignin
1459,1426	Asymmetry in −CH3 and −CH2− and the methoxy group (O−CH3) of the lignin structure
1370	Aliphatic C-H stretch in CH_3, phenolic OH
1263	Guaiacyl ring and C-O stretch in lignin
1209	C-C, C-O and C=O stretch
1116-1127	Syringyl ring breathing
1032	Aromatic C-H plane deformation (G+S), C-O deformation in primary alcohols, C=O stretch (unconjugated)

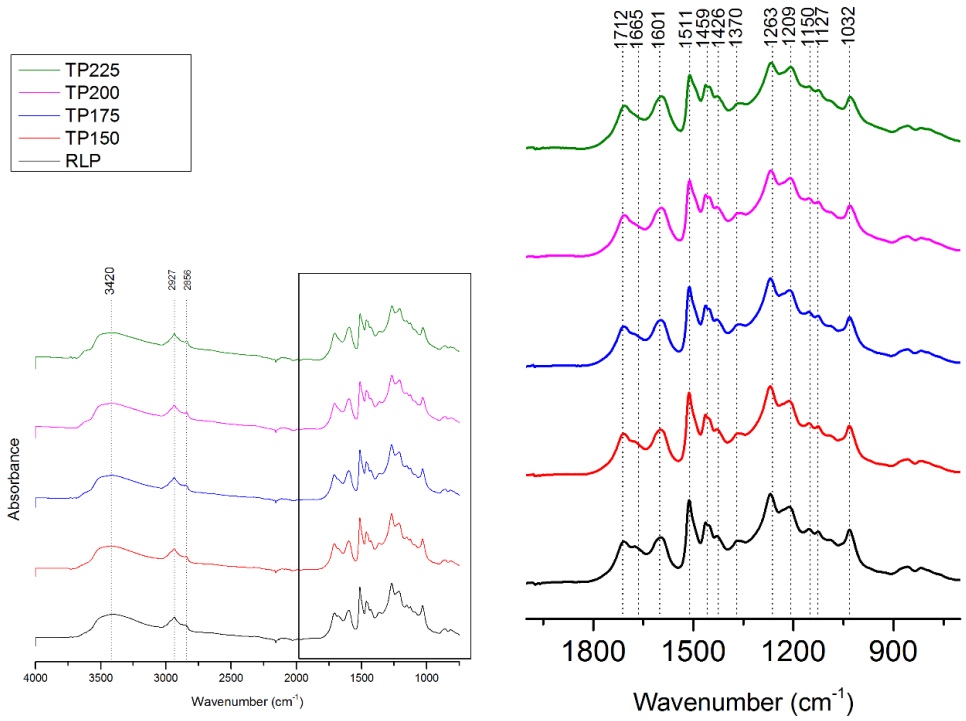

Figure 4.4. FTIR spectra of lignin from pine torrefied at different temperatures

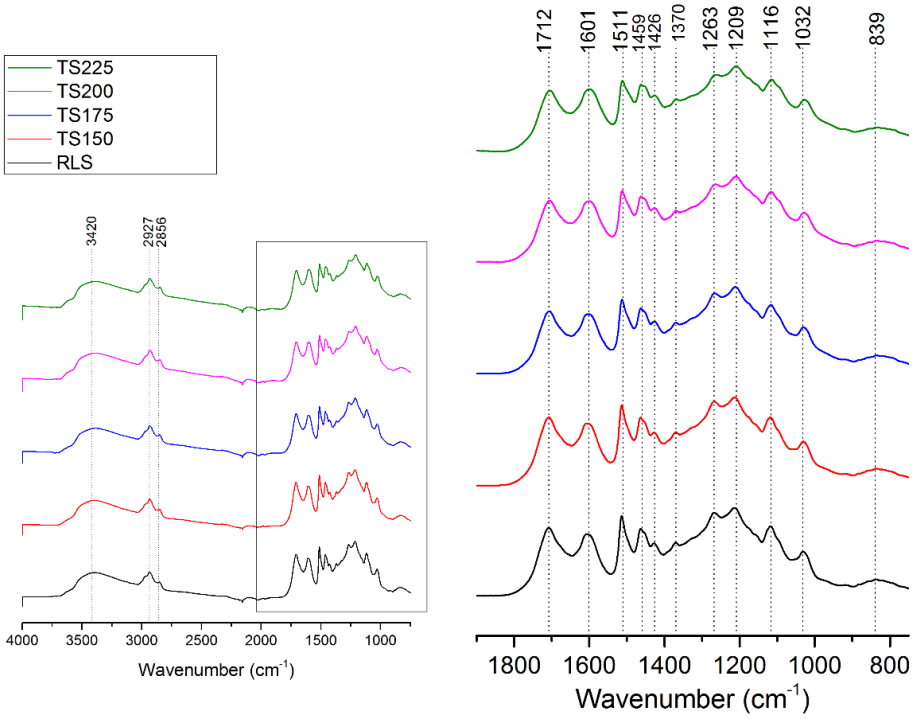

Figure 4.5. FTIR spectra of lignin from switchgrass torrefied at different temperatures

The ^{13}C CP/MAS NMR spectra of raw lignin, lignin torrefied at 175 ˚C and 225 ˚C is shown in Figure 4.6, with chemical shift (ppm) plotted against the normalized intensity of the signals. The signal with peak between 140-160 ppm is assigned to the presence of oxygenated aromatic carbons, 120-140 for aromatic C=C structures and the signal between 50-60 ppm is assigned to the methoxyl group in lignin. From Figure 4.6, the intensity of the signal at 50-60 ppm can be observed to decrease in the samples torrefied at 225 ˚C, when compared with the raw lignin, which indicates the demethoxylation of lignin during torrefaction. This result correlates well with the product distribution from non-catalytic pyrolysis of these samples discussed in section 3.3, as well as with previous studies on biomass torrefaction by Neupane et al. [21] and Zheng et al [22, 23] where the intensity of methoxyl carbons was reported to decrease as a result of torrefaction. Ben et al. [31] and Zheng et al. reported an increase in the intensity of aromatic C=C structures as a result of torrefaction, which was proposed as an indicator of polycondensation reactions occuring in lignin. However in this study, no clear trend can be observed from the signal at 120-140 ppm which is assigned to aromatic C=C structures.

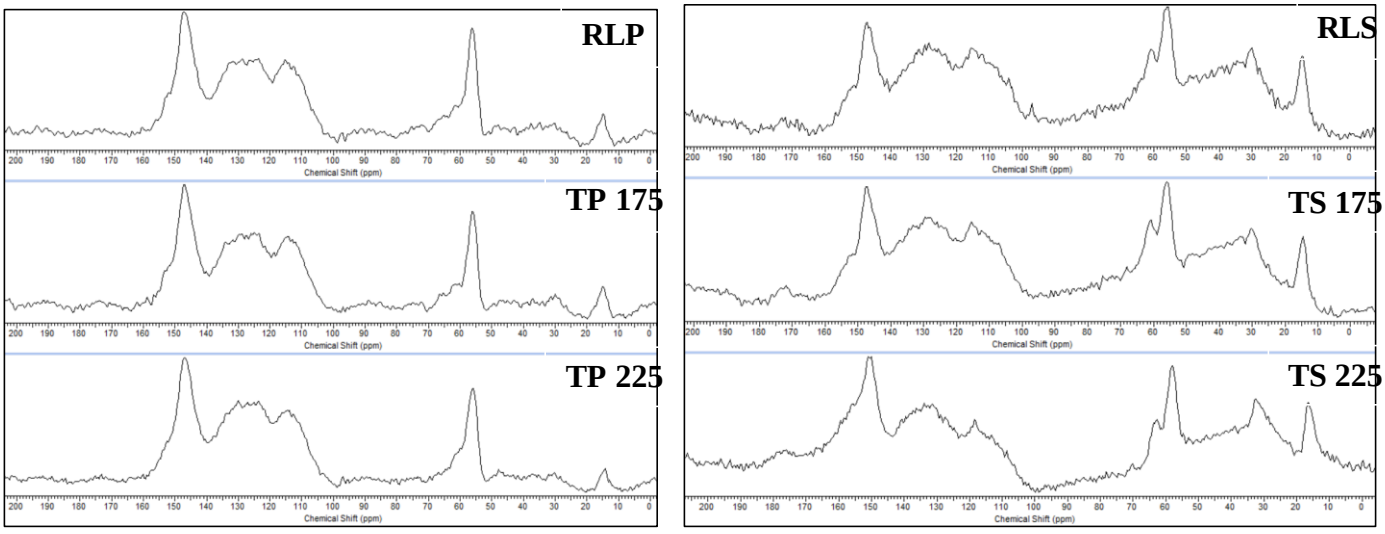

Figure 4.6. ^{13}C CP/MAS NMR spectra of lignins from pine and switchgrass

The results from ^{31}P NMR analysis of the raw and torrefied lignins are summarized in Figure 4.7. The ^{31}P NMR data shows a clear decrease in the aliphatic OH groups content, which decreases at even mild torrefaction temperatures and severely at the highest torrefaction temperature (225 ˚C). The guaiacyl OH

group content also clearly decreases in both pine and switchgrass lignins as a result of a greater degree of demethoxylation reactions at higher torrefaction temperatures. The decrease in the OH group also correlates with the lower oxygen content of the torrefied lignin samples discussed earlier in the elemental composition in section 3.1.

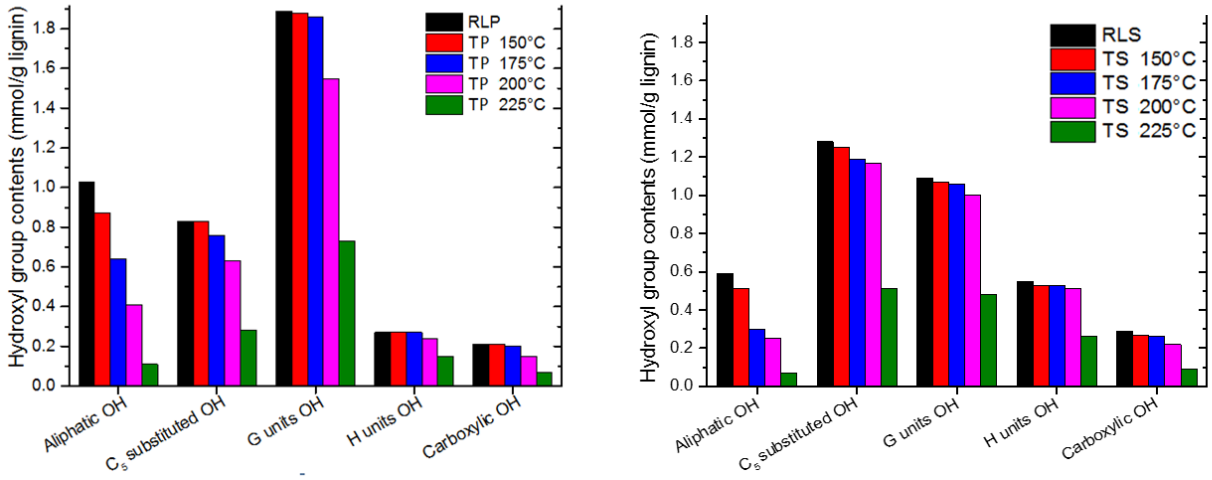

Figure 4.7. Hydroxyl group contents from 31P NMR analysis of lignin from pine and switchgrass torrefied at different temperatures

The average molecular weights (M_n, M_w) and polydispersity index (PDI) obtained for the lignin samples are summarized in Figure 4.8. The polydispersity index is calculated by dividing the weight average molecular weight with the number average molecular weight. Although the ^{13}C NMR data was inconclusive with regards to the occurrence of polycondensation reactions, the number average molecular weight and weight average molecular weights of the lignin samples from GPC analysis could be seen to increase initially with increase in torrefaction temperature, for instance, TLS at 200ºC and TLP at 175ºC. This indicates the possible formation of condensed aromatic polymers, linked with C-O and C-C bonds. However, it is interesting to note that at the highest torrefaction temperature, 225 ˚C, the molecular weights as well as the polydispersity index

decreases significantly as the treatment temperature causes further decomposition of these bonds between the condensed polymers.

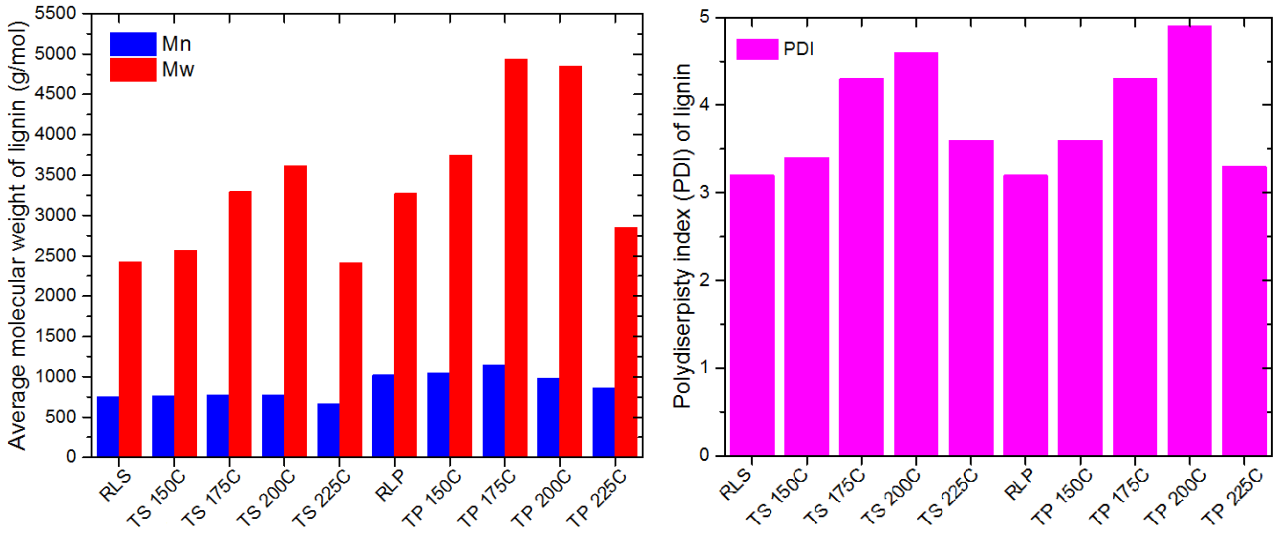

Figure 4.8. Average molecular weights (Mn, Mw) and polydispersity index

4.3.3. Effect of torrefaction temperature on non-catalytic pyrolysis of lignin

The major products identified and quantified from the non-catalytic and catalytic pyrolysis of lignin were grouped into four major groups – aromatic hydrocarbons, phenols, guaiacols and syringols. The complete list of compounds is listed in Supplementary Information Table S2, where naphthalenes and other polyaromatic hydrocarbons are also included in the aromatic hydrocarbons group. The product distribution from the pyrolysis of lignins from pine and switchgrass is shown in Figure 4.9, whereas detailed product yields including the yields of all the compounds quantified are presented in Table 4.7. In terms of carbon yield, higher torrefaction temperatures appear to cause a significant reduction in the total yield of guaiacols from both pine and switchgrass, whereas the yield of phenols shows an increasing trend with increase in torrefaction temperature. For instance, the yield of guaiacols from raw lignin of pine was 29.8 %, which reduced to 10.7 % for the sample torrefied at 225 ˚C. Lignin from switchgrass showed a similar trend, albeit to a lesser

extent since the yield of guaiacols was lower when compared to pine. Similar results were discussed previously by Adhikari et al. [32], as well as by Yang et al. [33] investigating the effects of torrefaction on lignin and switchgrass, respectively.

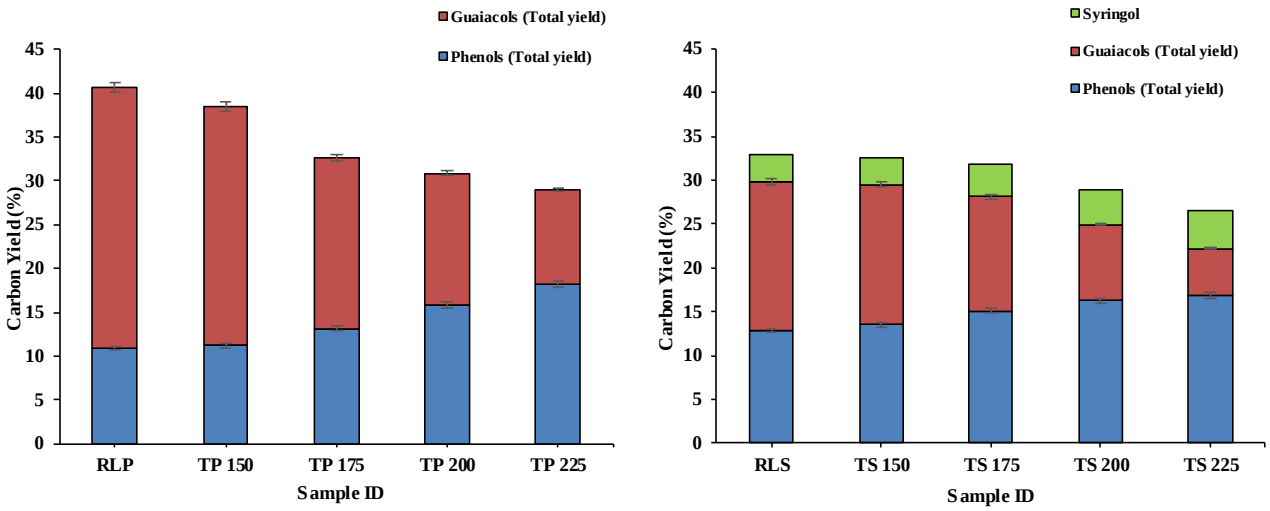

Figure 4.9. Product distribution from pyrolysis of lignin from pine and switchgrass torrefied at different temperatures

Further, Neupane et al. [21] proposed that torrefaction could enhance demethoxylation and the cleavage of aryl ether linkages in lignin, resulting in the observed decrease in the yield of guaiacols. The results from non-catalytic pyrolysis as well as the structural characterization of torrefied lignins discussed previously seem to support this hypothesis. However, demethoxylation of lignin does not seem to lead to the formation of only phenolic compounds, since the total yield of condensable organic compounds shown in Figure 4.9, as well as the overall carbon closure data from Table 4.7 clearly worsen during the pyrolysis of torrefied lignin samples. The total carbon closure (or balance) reduced from 82.2 % (RLP) to 76.9 % (TP 225) as a result of torrefying pine, while torrefying switchgrass resulted in overall carbon closure to reduce in a similar fashion. Torrefaction of lignin at higher temperatures also appears to produce an increase in the amount of carbonaceous residues (char) from non-catalytic pyrolysis.

Table 4.7. Product distribution from non-catalytic pyrolysis of raw and torrefied lignins at 500 ˚C

Component	Overall Carbon Yield (C%)									
	RLP	**TP 150**	**TP 175**	**TP 200**	**TP 225**	**RLS**	**SP 150**	**SP 175**	**SP 200**	**SP 225**
Condensable compounds	40.71	38.45	32.64	30.91	28.95	34.02	33.75	32.73	29.6	26.94
Char	31.2	32.9	33.3	34.5	35.9	32.1	32.9	33.3	34.2	35.8
Non-condensable gases	10.3	10.9	11.3	12.5	12.1	11.9	11.7	12.2	12.9	13.3
Total Carbon Closure	82.21	82.25	77.24	77.91	76.95	78.02	78.35	78.23	76.7	76.04
Phenols	**Overall Carbon Yield (C%)**									
Phenol	2.62	3.41	3.28	4.23	4.91	3.12	3.29	4.31	4.12	4.83
Phenol, 2-methyl	1.21	1.19	1.42	1.3	1.44	1.12	1.13	1.2	1.29	1.43
Phenol, 4-methyl	1.1	1.21	2.49	2.81	3.03	2.65	2.71	2.99	3.32	4.15
Phenol, 2,4-dimethyl	0.55	0	0	0	0	1.03	1.19	1.18	1.26	1.4
Phenol, 2,4,6 trimethyl	0	0	0	0	0	0.75	0.69	0.63	0.4	0
Phenol, 3,5 dimethyl	1.62	1.81	1.83	2.22	2.51	0	0	0	0	0
Phenol, 3-ethyl	0.51	0	0	0	0	0	0	0	0	0
Phenol, 4-ethyl	0.72	0.9	1.52	2.1	2.89	1.94	2.38	2.51	3.01	3.22
Catechol	1.19	1.21	1.16	1.24	1.11	1.15	1.18	1.23	1.5	1.32
Phenol, 4-vinyl	0.81	1.27	1.42	1.89	2.3	0	0	0.19	0.49	0.51
Catechol, 4-methyl	0.51	0.2	0	0	0	1.1	0.95	0.9	0.85	0
Total Phenolic Yield	10.84	11.2	13.12	15.79	18.19	12.86	13.52	15.14	16.24	16.86
Guaiacols	**Overall Carbon Yield (C%)**									
Phenol, 2-methoxy	6.49	5.82	3.11	2.49	1.93	4.63	4.45	3.69	2.5	1.46
Phenol, 2-methoxy-4-methyl	10.79	10.93	7.32	4.67	2.11	6.55	6.13	5.14	3.1	1.2
Phenol, 4-ethyl 2-methoxy	2.52	2.91	2.88	2.95	2.92	1.58	1.63	1.67	1.55	1.56
Eugenol	1.11	0.59	0	0	0	0	0	0	0	0
Iso-eugenol	0.97	0	0	0	0	0	0	0	0	0
Phenol, 2-methoxy 4-vinyl	4.93	4.12	3.59	2.66	1.71	4.15	3.78	2.52	1.6	1.15
Vanillin	3.061	2.88	2.62	2.35	2.09	1.07	1.13	0.98	0.6	0.41
Total Guaiacols Yield	29.84	27.25	19.52	15.12	10.76	17.98	17.12	14	9.35	5.78
Syringols	**Overall Carbon Yield (C%)**									
Phenol, 2,6 dimethoxy	N/A	N/A	N/A	N/A	N/A	3.18	3.11	3.59	4.01	4.3

N/A: Not available

Further, an interesting observation could be made from the yield of syringol (Phenol, 2,6 dimethoxy) in Table 4.7. While the demethoxylation of G-derivatives from pine (a softwood containing p-hydroxyphenyl and guaiacyl units) appears to be clearly taking place, the yield of syringol from switchgrass lignin (with two methoxy groups) actually increased from 3.18 % (RLS) to 4.3 % (TS 225). These results suggest that the degradation behavior of G- and S- units in lignin

could be considerably different during torrefaction and pyrolysis. This difference could be a direct result of the inherent difference in the structure of the two types of lignins. While switchgrass contains both syringyl as well as guaiacyl units in the lignin macromolecule, pine being a softwood contains mostly guaiacyl, p-hydroxyphenyl units and no syringyl units. It has been shown by previous studies that the ether bonds linking syringyl units are easier to split than those between guaiacyl units, which would directly explain the increased production of syringol from switchgrass lignin [34, 35]. Further, the G-units of lignin undergo condensation and coupling reactions very easily, which results in the formation of stable high molecular weight compounds or char. Since several high molecular weight compounds from lignin pyrolysis as well as GC-undetectable compounds were not quantified and accounted for in our carbon balance, it would explain the reason behind the deteriorating carbon closure and increasing carbonaceous residues with increasing torrefaction severity. Finally, it should be noted that while some studies in the past have reported the increased formation of aromatic hydrocarbons from non-catalytic pyrolysis of torrefied biomass / lignin [25, 32], none of the hydrocarbons were detected at any level from the pyrolysis of lignin samples torrefied at any temperature in this study.

4.3.4. Effect of torrefaction temperature on CFP of lignin

The product distributions from the CFP of raw and torrefied lignins from pine and switchgrass are shown in Figure 4.10 and Figure 4.11, respectively. The group aromatic hydrocarbons contains major compounds that were identified and quantified – benzene, toluene, xylene, ethyl benzene, indane, indene, 2-methyl indene, naphthalene, 1-methyl naphthalene, 2-methyl naphthalene, 2,6 dimethyl naphthalene, phenanthrene, fluorene and anthracene. Although several contemporary studies that investigated the CFP of lignin or biomass at catalyst:biomass

ratios similar to this study have reported the formation of small amounts of oxygenated compounds (< 3%) such as phenols or guaiacols, those compounds were not identified in this study which could be a result of uniform sample preparation (catalyst:biomass mixture) [22, 25, 32].

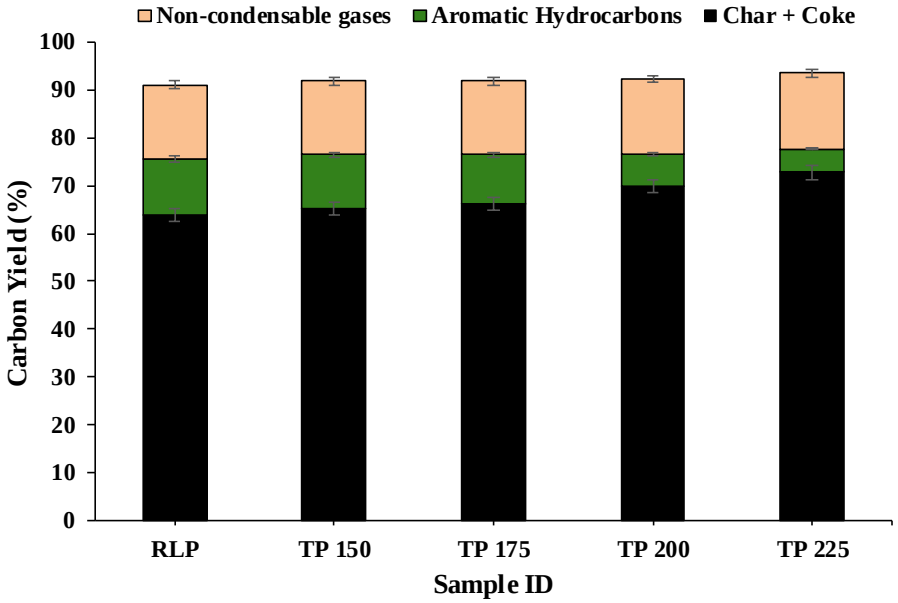

Figure 4.10. Product distribution from CFP of raw and torrefied lignins from pine at 500 ˚C

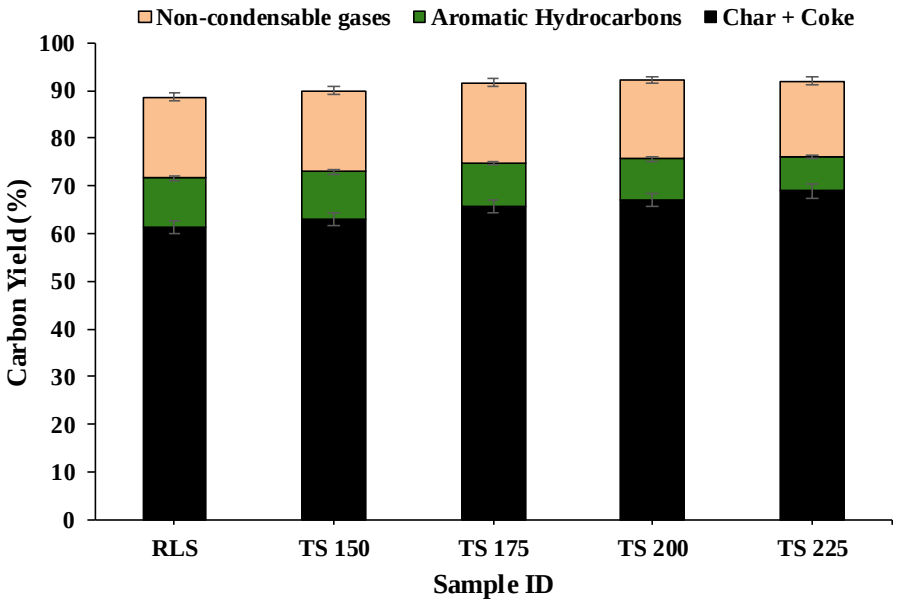

Figure 4.11. Product distribution from CFP of raw and torrefied lignins from switchgrass at 500 ˚C

As shown in Figure 10, the yield of aromatic hydrocarbons from raw lignin of pine was 11.6 %, which decreased to 4.9 % at the maximum torrefaction temperature of 225 ˚C. The decrease in the yield of aromatic hydrocarbons was accompanied by a corresponding increase in the yield of carbonaceous residues (coke + char), which increased from 63.9 % to 72.8 %. A similar trend can also be observed clearly in the product distribution from CFP of torrefied switchgrass lignin from Figure 11. Zheng et al. proposed that the increase in carbonaceous residues from CFP could be related to the increasing polycondensation of lignin samples torrefied at higher temperatures [22]. Further, several studies including the work on CFP of various types of lignins by Mullen et al. [19] and the CFP conversion of model compounds for lignin (phenol, anisole) by Thilakaratne et al. [36] have suggested that simple phenols are more likely to lead to the formation of coke rather than to an increased yield of aromatic hydrocarbons. These results shed more light on the product distribution from CFP of torrefied lignins from pine and switchgrass since the higher yield of phenols at higher temperatures of torrefaction has clearly caused the increased formation of coke. Finally, the selectivity of BTX compounds shown in Table 4.8 could be seen to improve with an increase in torrefaction temperature, from 49.7 % from RLP to 61.5 % from TP 225. A very similar increase can also be seen in the selectivity of BTX compounds produced from CFP of torrefied lignins from switchgrass, which is primarily due to the loss in yield of some poly aromatic hydrocarbons such as naphthalenes, fluorene and anthracene with increase in torrefaction temperature. These polyaromatics are primarily formed from the reaction of olefins with the phenyl radical and hence the decrease in their yields as a result of torrefaction is expected. However, looking into any change in selectivity has very little practical significance when the carbon yield of the desired product (aromatic hydrocarbons) is reduced significantly as a result of torrefaction.

Table 4.8. Product distribution from CFP of raw and torrefied lignins at 500 ˚C

Component	Overall Carbon Yield (C %)									
	RLP	TP 150	TP 175	TP 200	TP 225	RLS	SP 150	SP 175	SP 200	SP 225
CO	5.9	5.57	5.78	5.01	4.87	6.9	6.68	6.49	5.88	5.19
CO_2	5.48	5.77	6.14	7.68	8.97	6.71	6.81	7.38	7.92	8.27
Char + Coke	63.9	65.1	66.3	69.9	72.8	61.3	63.1	65.7	67.1	68.9
Char *	31.2	32.9	33.3	34.5	35.9	32.1	31.9	32.2	32.4	32.8
Coke **	32.7	32.2	33	35.4	36.9	29.2	31.2	33.5	34.7	36.1
Aromatic hydrocarbons	11.6	11.3	10.1	6.8	4.9	10.4	9.9	9.1	8.6	7.1
Olefins (C2-C4)	4.17	4.12	3.45	2.86	1.93	3.96	3.02	2.89	2.7	2.53
Non-condensable gases	15.55	15.46	15.37	15.55	15.77	17.57	16.51	16.76	16.5	15.99
Oxygenated Compounds	0	0	0	0	0	0	0	0	0	0
Total Carbon Closure	91.05	91.86	91.77	92.25	93.47	89.27	89.51	91.56	92.2	91.99
	Aromatics Selectivity (%)									
Benzene	13.9	14.1	14.8	15.6	16.1	11.3	11.9	12.6	16.32	15.8
Toluene	16.89	17.92	18.66	19.59	20.47	20.2	20.9	22.19	21.86	23.52
Xylene	18.9	19.4	22.9	23.8	24.9	17.8	17.4	18.2	18.7	20.1
BTX Selectivity	49.69	51.42	56.36	58.99	61.47	49.3	50.2	52.99	56.88	59.42
Ethyl Benzene	0.99	0.94	0.23	0	0	0	0	0	0	0
C9 Aromatics	13.01	12.9	12.01	11.15	9.7	14.1	14.86	14.01	13.5	12.92
C10+ Aromatics	36.31	34.74	31.4	29.86	28.83	36.6	34.94	33	29.62	27.66
Naphthalenes	26.78	25.61	23.29	22.14	21.39	29.4	27.6	26.1	23.9	22.12
Fluorene, Anthracene	9.53	9.13	8.11	7.72	7.44	7.2	7.34	6.9	5.72	5.54

Note: Std. deviation was negligible and is not shown since the error was within 5% for all the results
*Result from non-catalytic experiments performed
**Difference between char+coke from CFP experiment and char yield from non-catalytic
C9 Aromatics include indane, indenes and alkyl benzenes

4.4. Conclusion

Organosolv lignin extracted from pine and switchgrass was subjected to torrefaction at various temperatures (150 ˚C, 175 ˚C, 200 ˚C and 225 ˚C) in order understand the effect of torrefaction on structural changes in the lignin macromolecule. FTIR and NMR spectroscopy of torrefied lignins shed light on the enhanced cleavage of aryl ether linkages in lignin and the demethoxylation/polycondensation of guaiacyl lignin. Non-catalytic pyrolysis of the torrefied lignins confirmed the results from previous studies on biomass torrefaction, resulting in a significant shift in the pyrolysis product distribution towards producing more phenols and

carbonaceous residues. The behavior of guaiacyl and syringyl lignin units during torrefaction was also shown to be significantly different. However, *in-situ* CFP experiments showed that torrefaction negatively impacts lignin resulting in a significant loss in the yield of aromatic hydrocarbons (11.6% to 4.9% in pine; 10.4% to 7.1% in switchgrass).

4.5. References

1. Bridgwater, A.V., *Review of fast pyrolysis of biomass and product upgrading.* Biomass and Bioenergy, 2012. **38**(0): p. 68-94.
2. Effendi, A., H. Gerhauser, and A.V. Bridgwater, *Production of renewable phenolic resins by thermochemical conversion of biomass: A review.* Renewable and Sustainable Energy Reviews, 2008. **12**(8): p. 2092-2116.
3. Shakya, R., et al., *Effect of temperature and Na2CO3 catalyst on hydrothermal liquefaction of algae.* Algal Research, 2015. **12**: p. 80-90.
4. Carlson, T., et al., *Aromatic Production from Catalytic Fast Pyrolysis of Biomass-Derived Feedstocks.* Topics in Catalysis, 2009. **52**(3): p. 241-252.
5. Huber, G.W., S. Iborra, and A. Corma, *Synthesis of transportation fuels from biomass: chemistry, catalysts, and engineering.* Chem Rev, 2006. **106**(9): p. 4044-98.
6. Ayalur Chattanathan, S., S. Adhikari, and N. Abdoulmoumine, *A review on current status of hydrogen production from bio-oil.* Renewable and Sustainable Energy Reviews, 2012. **16**(5): p. 2366-2372.
7. Dickerson, T. and J. Soria, *Catalytic Fast Pyrolysis: A Review.* Energies, 2013. **6**(1): p. 514-538.
8. Mahadevan, R., et al., *Physical and Chemical Properties and Accelerated Aging Test of Bio-oil Produced from in Situ Catalytic Pyrolysis in a Bench-Scale Fluidized-Bed Reactor.* Energy & Fuels, 2015.
9. Peters, J.E., J.R. Carpenter, and D.C. Dayton, *Anisole and Guaiacol Hydrodeoxygenation Reaction Pathways over Selected Catalysts.* Energy & Fuels, 2015. **29**(2): p. 909-916.
10. Bahng, M.-K., et al., *Current technologies for analysis of biomass thermochemical processing: A review.* Analytica Chimica Acta, 2009. **651**(2): p. 117-138.
11. Chheda, J.N., G.W. Huber, and J.A. Dumesic, *Liquid-Phase Catalytic Processing of Biomass-Derived Oxygenated Hydrocarbons to Fuels and Chemicals.* Angewandte Chemie International Edition, 2007. **46**(38): p. 7164-7183.
12. Mohan, D., C.U. Pittman, and P.H. Steele, *Pyrolysis of Wood/Biomass for Bio-oil: A Critical Review.* Energy & Fuels, 2006. **20**(3): p. 848-889.
13. Yaman, S., *Pyrolysis of biomass to produce fuels and chemical feedstocks.* Energy Conversion and Management, 2004. **45**(5): p. 651-671.
14. de Miguel Mercader, F., et al., *Hydrodeoxygenation of pyrolysis oil fractions: process understanding and quality assessment through co-processing in refinery units.* Energy & Environmental Science, 2011. **4**(3): p. 985-997.
15. Choudhary, T. and C. Phillips, *Renewable fuels via catalytic hydrodeoxygenation.* Applied Catalysis A: General, 2011. **397**(1): p. 1-12.
16. Kwon, K.C., et al., *Catalytic deoxygenation of liquid biomass for hydrocarbon fuels.* Renewable Energy, 2011. **36**(3): p. 907-915.

17. Furimsky, E., *Catalytic hydrodeoxygenation.* Applied Catalysis A: General, 2000. **199**(2): p. 147-190.
18. Mullen, C.A. and A.A. Boateng, *Accumulation of inorganic impurities on HZSM-5 zeolites during catalytic fast pyrolysis of switchgrass.* Industrial & Engineering Chemistry Research, 2013. **52**(48): p. 17156-17161.
19. Mullen, C.A. and A.A. Boateng, *Catalytic pyrolysis-GC/MS of lignin from several sources.* Fuel Processing Technology, 2010. **91**(11): p. 1446-1458.
20. Prins, M.J., K.J. Ptasinski, and F.J. Janssen, *Torrefaction of wood: Part 1. Weight loss kinetics.* Journal of Analytical and Applied Pyrolysis, 2006. **77**(1): p. 28-34.
21. Neupane, S., et al., *Effect of torrefaction on biomass structure and hydrocarbon production from fast pyrolysis.* Green Chemistry, 2015. **17**(4): p. 2406-2417.
22. Zheng, A., et al., *Impact of Torrefaction on the Chemical Structure and Catalytic Fast Pyrolysis Behavior of Hemicellulose, Lignin, and Cellulose.* Energy & Fuels, 2015. **29**(12): p. 8027-8034.
23. Zheng, A., et al., *Catalytic Fast Pyrolysis of Biomass Pretreated by Torrefaction with Varying Severity.* Energy & Fuels, 2014. **28**(9): p. 5804-5811.
24. Boateng, A. and C. Mullen, *Fast pyrolysis of biomass thermally pretreated by torrefaction.* Journal of Analytical and Applied Pyrolysis, 2013. **100**: p. 95-102.
25. Srinivasan, V., et al., *Catalytic Pyrolysis of Torrefied Biomass for Hydrocarbons Production.* Energy & Fuels, 2012. **26**(12): p. 7347-7353.
26. Basu, P., *Chapter 3 - Pyrolysis and Torrefaction*, in *Biomass Gasification and Pyrolysis*, P. Basu, Editor. 2010, Academic Press: Boston. p. 65-96.
27. Sluiter, A., et al., *Determination of extractives in biomass.* Laboratory Analytical Procedure (LAP), 2005. **1617**.
28. Patwardhan, P.R., et al., *Influence of inorganic salts on the primary pyrolysis products of cellulose.* Bioresource Technology, 2010. **101**(12): p. 4646-4655.
29. Hu, G., et al., *Structural Characterization of Switchgrass Lignin after Ethanol Organosolv Pretreatment.* Energy & Fuels, 2012. **26**(1): p. 740-745.
30. Windeisen, E., C. Strobel, and G. Wegener, *Chemical changes during the production of thermo-treated beech wood.* Wood Science and Technology, 2007. **41**(6): p. 523-536.
31. Ben, H. and A.J. Ragauskas, *Torrefaction of Loblolly pine.* Green Chemistry, 2012. **14**(1): p. 72-76.
32. Adhikari, S., V. Srinivasan, and O. Fasina, *Catalytic Pyrolysis of Raw and Thermally Treated Lignin Using Different Acidic Zeolites.* Energy & Fuels, 2014. **28**(7): p. 4532-4538.
33. Yang, Z., et al., *Effects of torrefaction and densification on switchgrass pyrolysis products.* Bioresource technology, 2014. **174**: p. 266-273.
34. Jakab, E., O. Faix, and F. Till, *Thermal decomposition of milled wood lignins studied by thermogravimetry/mass spectrometry.* Journal of Analytical and Applied Pyrolysis, 1997. **40**: p. 171-186.
35. Harkin, J., *Recent developments in lignin chemistry.* Heidelberg:Springer Berlin, 1966: p. 58-101.
36. Thilakaratne, R., J.-P. Tessonnier, and R.C. Brown, *Conversion of methoxy and hydroxyl functionalities of phenolic monomers over zeolites.* Green Chemistry, 2016.

5. Summary and Future Directions

5.1. Summary

The influence of natural variability in the physical and chemical properties of different biomass resources on catalytic fast pyrolysis due to the presence of varying amounts of alkali and alkaline earth metals and lignin has been discussed successfully in this dissertation. The overall goal of this study was divided into three specific objectives and in the first objective, alkali and alkaline earth metals (AAEMs) were impregnated on biomass at different concentrations (0.1, 0.5, 1.0 and 2.0 wt.%). The metal-impregnated biomass was used in non-catalytic and catalytic pyrolysis experiments to understand the influence of the type and concentration of individual AAEMs on the thermal breakdown of biomass and on the CFP product distribution. Results showed that the type of AAEM as well as the concentration were producing significant changes to the yield of major condensable products from cellulose and lignin pyrolysis, leading to the formation of low molecular weight compounds. AAEMs were found to change the chemistry of biomass pyrolysis by promoting reactions leading to the formation of undesirable co-products (char and non-condensable gases) while suppressing the desired reaction pathways leading to the formation of aromatic hydrocarbons from CFP.

In the second objective, the influence of accumulation of AAEMs after pyrolysis on the CFP catalyst and the resulting loss in activity due to the deactivation was discussed. ZSM-5 catalyst was deactivated by different levels (0.5, 1.0, 2.0 and 5.0 wt.%) of Ca, K and Na and the resulting changes in the properties of the catalyst are reported through BET surface area and NH_3-TPD measurements. The biomass inorganics were found to cause physical and chemical poisoning of the catalyst. Calcium was observed to cause physical deactivation by restricting access to the

active sites of the catalyst, whereas sodium and potassium chemically deactivated the catalyst by reducing the acidity of the catalyst. CFP experiments utilizing the catalysts deactivated at different levels of AAEMs showed the strong negative influence on the performance of the catalyst, which showed exponential losses in activity at very low concentrations (0.5 wt.%) of sodium and potassium. Higher levels of deactivation were observed to render the catalyst inert, limiting its function to a heat carrier and losing its activity to promote deoxygenation of pyrolysis vapor. Based on these two studies, it is recommended that careful consideration is placed on choosing the type of biomass used in CFP, especially with regards to the composition of various metal species in the biomass. Reactor designs that limit the exposure of the catalyst to the AAEMs are also recommended to avoid the potential economic drawbacks due to rapid catalyst deactivation.

In the third objective, the changes observed in the structure of lignin during torrefaction and its influence on the product distribution from CFP were elucidated. Organosolv lignin extracted from pine and switchgrass was torrefied at different temperatures (150 ˚C, 175 ˚C, 200 ˚C and 225 ˚C) to study the effect of torrefaction on structural changes in the lignin macromolecule. Spectroscopic analysis of torrefied lignins revealed the enhanced cleavage of aryl ether linkages in lignin and the demethoxylation/polycondensation of guaiacyl lignin. Findings from previous studies regarding the shift in product selectivity from guaiacols to phenols due to torrefaction were confirmed from non-catalytic pyrolysis experiments. The behavior of guaiacyl and syringyl lignin units during torrefaction was also shown to be significantly different. However, *in-situ* CFP experiments showed that torrefaction negatively impacts lignin resulting in a significant loss in the yield of aromatic hydrocarbons (11.6% to 4.9% in pine; 10.4% to 7.1% in switchgrass).

5.2. Limitations of this dissertation and future directions

This research has shed light over the influence of biomass variability and its effect on CFP for the production of renewable transportation fuels. The effect of biomass ash on the thermal decomposition of biomass as well as its influence on the functionality of ZSM-5 catalyst during CFP has been revealed. Changes in the structure of lignin during torrefaction and the resulting yields from CFP of torrefied lignins has also been discussed in this study. However, there are several limitations, mainly due to the choice of reactor, experimental conditions and methods (such as organosolv extraction, methods followed in impregnating AAEMs on biomass and catalyst), which creates the scope for future research in the following areas:

- **Develop mild pretreatments of biomass which selectively removes K and Na**

  Among the constituents of biomass ash, sodium and potassium have been proven from the results of this study to be damaging towards biomass pyrolysis as well as causing slagging, fouling and corrosion in the reactors. However, complete removal of these minerals through severe pretreatment techniques such as acid washing has been shown to degrade the quality of biomass. There is a need to investigate and research techniques by which these harmful minerals could be selectively removed through mild pre-treatment techniques, without causing significant structural damage to cellulose, hemicellulose and lignin in biomass.

- **Identify and develop catalysts that are resistant to deactivation by AAEMs**

While zeolite-based catalysts that depend on the Bronsted and Lewis acid sites for their activity have been observed from this study to be deactivated rapidly by AAEMs, this investigation could be extended to understand the performance of several basic oxides that are commonly used as catalysts in CFP, such as CaO, MgO, ZnO among other metal oxide catalysts. Such a study would help us identify and develop catalysts that are resistant to deactivation by AAEMs.

- **Study the efficiency of different char-catalyst separation techniques**

  Rapid removal of char from the pyrolysis and regeneration zone is essential to limit the contact between char and catalyst particles, thereby reducing the rate of accumulation of various biomass inorganics on the catalyst. A study on identifying and analyzing mechanisms to efficiently separate the char and the catalyst before the catalyst is regenerated would be critical to improving the lifetime of the catalyst and the economic feasibility of biomass conversion to hydrocarbons.

- **Quantify the impact on carbon conversion and energy efficiency due to AAEMs**

  From this study, we were able to understand the fundamental chemistry behind the role of AAEMs in CFP of biomass. However, since this study was performed in a micro-reactor, the results cannot be directly translated to the impact on a large scale production facility. To understand that, biomasses with high ash content, specifically of sodium and potassium need to be processed in a bench-scale or pilot-scale reactor system to understand their impact on carbon conversion to the desired products as well as the energy efficiency in converting biomass to liquid biofuels. That data can be compared to the results from

processing low ash content feedstocks such as pine, so that biomass resources could be graded for their quality based on their ash composition and expected product yields.

- **Torrefaction of lignins extracted through mild pre-treatment processes**

  In Chapter 4, the use of organosolv pretreatment had weakened the ether bonds linking various lignin units existing in biomass, which could have been a reason why the lignin decomposed at lower temperatures resulting in polycondensation reactions. Extracting lignins through milder techniques such as alkali pre-treatment or utilizing milled wood lignins could be a better alternative to study the effect of torrefaction, since the lignins will not have significant damages to its structure from the extraction process. Further, other biomasses such as hardwoods like hybrid poplar could be studied for lignin torrefaction, since most of the existing literature is on softwoods and herbaceous grasses like switchgrass.

6. Supplementary Information:

Chapter 2

Table S1. Detailed product distributions from *in-situ* catalytic pyrolysis of biomass doped with various amounts of Mg (Number after ± sign denotes standard deviation. Connecting letters from Tukey HSD test comparison (JMP) provided, where results not connected by same alphabet are statistically different at α=0.05)

Component	Overall Carbon Yield (C %)				
	Control	Mg 0.1	Mg 0.5	Mg 1.0	Mg 2.0
CO	13.9 ± 0.12 ^{A}	13.57 ± 0.19 ^{B}	13.28 ± 0.21 ^{BC}	13.01 ± 0.06 ^{C}	12.88 ± 0.09 ^{C}
CO_2	6.42 ± 0.15 ^{A}	6.27 ± 0.06 ^{A}	6.13 ± 0.17 ^{AB}	6 ± 0.08 ^{B}	5.97 ± 0.11 ^{B}
Char + Coke	40.2	40.35	40.24	39.81	40.3
*Char **	12.32 ± 0.48 ^{A}	12.59 ± 0.30 ^{A}	12.71 ± 0.21 ^{AB}	12.2 ± 0.37 ^{A}	13.01 ± 0.19 ^{B}
*Coke ***	27.87 ± 0.21 ^{A}	27.76 ± 0.17 ^{A}	27.53 ± 0.32 ^{A}	27.61 ± 0.28 ^{A}	27.28 ± 0.39 ^{A}
Aromatic hydrocarbons	24.04 ± 0.40 ^{A}	24.09 ± 0.32 ^{A}	24.18 ± 0.21 ^{A}	24.31 ± 0.16 ^{A}	24.4 ± 0.24 ^{A}
Olefins (C2-C4)	6.69 ± 0.18 ^{A}	6.72 ± 0.12 ^{A}	6.65 ± 0.05 ^{A}	6.6 ± 0.08 ^{A}	6.6 ± 0.14 ^{A}
Oxygenated Compounds	0.23 ± 0.04 ^{A}	0.31 ± 0.04 ^{AB}	0.36 ± 0.06 ^{B}	0.34 ± 0.04 ^{B}	0.38 ± 0.08 ^{B}
Total Carbon Closure	91.48 ± 0.88 ^{A}	91.31 ± 0.71 ^{A}	90.84 ± 0.63 ^{A}	90.07 ± 0.68 ^{A}	90.53 ± 0.93 ^{A}
	Aromatics Selectivity (%)				
`Benzene	6.06 ± 0.09 ^{A}	6.08 ± 0.11 ^{A}	6.04 ± 0.19 ^{A}	6.05 ± 0.08 ^{A}	5.99 ± 0.15 ^{A}
Toluene	15.51 ± 0.14 ^{A}	15.47 ± 0.09 ^{A}	15.49 ± 0.17 ^{A}	15.41 ± 0.21 ^{A}	15.3 ± 0.10 ^{A}
Ethyl Benzene	1.08 ± 0.09 ^{A}	1.14 ± 0.08 ^{A}	1.23 ± 0.04 ^{A}	1.17 ± 0.10 ^{A}	1.26 ± 0.09 ^{A}
Xylene	16.89 ± 0.21 ^{A}	16.83 ± 0.10 ^{A}	16.66 ± 0.17 ^{A}	16.59 ± 0.29 ^{A}	16.57 ± 0.31 ^{A}
C9 Aromatics	15.06 ± 0.19 ^{A}	15.14 ± 0.05 ^{A}	15.01 ± 0.06 ^{A}	14.89 ± 0.03 ^{B}	14.7 ± 0.11 ^{C}
C10+ Aromatics	40.18	40.1	39.87	40.04	40.29
Naphthalenes	27.34 ± 0.21 ^{A}	27.39 ± 0.13 ^{A}	27.38 ± 0.18 ^{A}	27.51 ± 0.19 ^{A}	27.51 ± 0.16 ^{A}
Fluorene, Anthracene	12.85 ± 0.15 ^{A}	12.71 ± 0.09 ^{AB}	12.49 ± 0.12 ^{B}	12.53 ± 0.09 ^{B}	12.43 ± 0.15 ^{B}

Table S2. Detailed product distributions from *in-situ* catalytic pyrolysis of biomass doped with various amounts of Ca (Number after ± sign denotes standard deviation. Connecting letters from Tukey HSD test comparison (JMP) provided, where results not connected by same alphabet are statistically different at α=0.05)

Component	Overall Carbon Yield (C %)				
	Control	Ca 0.1	Ca 0.5	Ca 1.0	Ca 2.0
CO	13.9 ± 0.12 ^{A}	13.17 ± 0.15 ^{A}	12.66 ± 0.23 ^{AB}	12.35 ± 0.18 ^{B}	12.02 ± 0.11 ^{C}
CO_2	6.42 ± 0.15 ^{A}	7.13 ± 0.13 ^{B}	7.49 ± 0.08 ^{C}	7.85 ± 0.20 ^{D}	8.36 ± 0.33 ^{D}
Char + Coke	40.2	42.1	43.48	44.57	45.8
*Char **	12.32 ± 0.48 ^{A}	14.49 ± 0.40 ^{B}	16.25 ± 0.53 ^{C}	17.58 ± 0.55 ^{D}	19.27 ± 0.38 ^{E}
*Coke ***	27.87 ± 0.21 ^{A}	27.61 ± 0.20 ^{A}	27.23 ± 0.13 ^{B}	26.99 ± 0.38 ^{BC}	26.52 ± 0.10 ^{C}
Aromatic hydrocarbons	24.04 ± 0.40 ^{A}	21.76 ± 0.31 ^{A}	20.01 ± 0.26 ^{C}	19.72 ± 0.18 ^{C}	18.77 ± 0.16 ^{D}
Olefins (C2-C4)	6.69 ± 0.18 ^{A}	6.33 ± 0.21 ^{AB}	6.19 ± 0.08 ^{B}	6.01 ± 0.15 ^{BC}	5.94 ± 0.06 ^{C}
Oxygenated Compounds	0.23 ± 0.04 ^{A}	0.88 ± 0.07 ^{B}	0.96 ± 0.11 ^{BC}	1.13 ± 0.09 ^{C}	1.57 ± 0.13 ^{D}
Total Carbon Closure	91.48 ± 0.88 ^{AB}	91.37 ± 0.42 ^{A}	90.79 ± 0.91 ^{A}	91.63 ± 0.40 ^{A}	92.46 ± 0.33 ^{B}
	Aromatics Selectivity (%)				
Benzene	6.06 ± 0.09 ^{A}	5.98 ± 0.06 ^{A}	6.02 ± 0.10 ^{A}	5.76 ± 0.06 ^{B}	5.7 ± 0.10 ^{B}
Toluene	15.51 ± 0.14 ^{A}	15.21 ± 0.18 ^{AB}	15.17 ± 0.25 ^{AB}	15.05 ± 0.07 ^{B}	14.97 ± 0.08 ^{B}
Ethyl Benzene	1.08 ± 0.09 ^{A}	1.14 ± 0.09 ^{A}	1.09 ± 0.05 ^{A}	1.15 ± 0.08 ^{A}	1.16 ± 0.05 ^{A}
Xylene	16.89 ± 0.21 ^{A}	16.93 ± 0.20 ^{A}	17.08 ± 0.09 ^{AB}	17.21 ± 0.05 ^{B}	17.45 ± 0.12 ^{C}
C9 Aromatics	15.06 ± 0.19 ^{A}	14.97 ± 0.12 ^{A}	14.82 ± 0.13 ^{AB}	14.77 ± 0.19 ^{AB}	14.63 ± 0.16 ^{B}
C10+ Aromatics	40.18	40.13	40.42	40.6	41.46
Naphthalenes	27.34 ± 0.21 ^{A}	27.82 ± 0.18 ^{B}	28.51 ± 0.20 ^{C}	28.84 ± 0.14 ^{CD}	29.05 ± 0.15 ^{D}
Fluorene, Anthracene	12.85 ± 0.15 ^{A}	12.31 ± 0.24 ^{B}	11.91 ± 0.12 ^{B}	11.76 ± 0.26 ^{B}	11.13 ± 0.18 ^{C}

Table S3. Detailed product distributions from *in-situ* catalytic pyrolysis of biomass doped with various amounts of K (Number after ± sign denotes standard deviation. Connecting letters from Tukey HSD test comparison (JMP) provided, where results not connected by same alphabet are statistically different at α=0.05)

Component	Overall Carbon Yield (C %)				
	Control	K 0.1	K 0.5	K 1.0	K 2.0
CO	13.9 ± 0.12 ^{A}	12.29 ± 0.07 ^{B}	12.05 ± 0.19 ^{BC}	11.89 ± 0.10 ^{C}	11.75 ± 0.14 ^{C}
CO_2	6.42 ± 0.15 ^{A}	7.18 ± 0.11 ^{B}	7.09 ± 0.15 ^{B}	7.45 ± 0.04 ^{C}	7.76 ± 0.26 ^{C}
Char + Coke	40.2	45.13	46.29	47.27	47.3
*Char **	12.32 ± 0.48 ^{A}	18.14 ± 0.22 ^{B}	19.56 ± 0.30 ^{C}	20.89 ± 0.53 ^{D}	21 ± 0.17 ^{D}
*Coke ***	27.87 ± 0.21 ^{A}	26.99 ± 0.18 ^{B}	26.73 ± 0.11 ^{B}	26.38 ± 0.20 ^{D}	26.29 ± 0.04 ^{D}
Aromatic hydrocarbons	24.04 ± 0.40 ^{A}	19.76 ± 0.30 ^{B}	18.21 ± 0.45 ^{C}	17.94 ± 0.11 ^{C}	16.82 ± 0.28 ^{D}
Olefins (C2-C4)	6.69 ± 0.18 ^{A}	6.14 ± 0.15 ^{B}	5.96 ± 0.07 ^{B}	5.68 ± 0.17 ^{C}	5.7 ± 0.06 ^{C}
Oxygenated Compounds	0.23 ± 0.04 ^{A}	1.48 ± 0.07 ^{B}	1.97 ± 0.10 ^{C}	2.21 ± 0.06 ^{D}	2.64 ± 0.18 ^{E}
Total Carbon Closure	91.48 ± 0.88 ^{A}	91.98 ± 0.41 ^{A}	91.57 ± 0.63 ^{A}	92.44 ± 0.70 ^{A}	91.97 ± 0.20 ^{A}
	Aromatics Selectivity (%)				
Benzene	6.06 ± 0.09 ^{A}	5.05 ± 0.09 ^{B}	5.01 ± 0.04 ^{B}	4.71 ± 0.11 ^{C}	4.77 ± 0.06 ^{C}
Toluene	15.51 ± 0.14 ^{A}	14.69 ± 0.17 ^{B}	14.32 ± 0.13 ^{C}	14.49 ± 0.15 ^{BC}	14.18 ± 0.04 ^{C}
Ethyl Benzene	1.08 ± 0.09 ^{A}	1.09 ± 0.04 ^{A}	1.02 ± 0.13 ^{A}	1.03 ± 0.05 ^{A}	1.2 ± 0.11 ^{A}
Xylene	16.89 ± 0.21 ^{A}	17.12 ± 0.11 ^{A}	17.32 ± 0.24 ^{A}	17.19 ± 0.19 ^{A}	17.3 ± 0.27 ^{A}
C9 Aromatics	15.06 ± 0.19 ^{A}	14.95 ± 0.37 ^{A}	15.18 ± 0.11 ^{A}	15.42 ± 0.08 ^{B}	15.57 ± 0.12 ^{B}
C10+ Aromatics	40.18	41.3	41.52	42.28	42.99
Naphthalenes	27.34 ± 0.21 ^{A}	30.69 ± 0.18 ^{B}	30.95 ± 0.32 ^{B}	31.59 ± 0.17 ^{C}	31.64 ± 0.09 ^{C}
Fluorene, Anthracene	12.85 ± 0.15 ^{A}	10.61 ± 0.09 ^{B}	10.57 ± 0.13 ^{B}	9.67 ± 0.11 ^{C}	9.32 ± 0.16 ^{D}

Table S4. Detailed product distributions from *in-situ* catalytic pyrolysis of biomass doped with various amounts of Na (Number after ± sign denotes standard deviation. Connecting letters from Tukey HSD test comparison (JMP) provided, where results not connected by same alphabet are statistically different at α=0.05)

Component	Overall Carbon Yield (C %)				
	Control	Na 0.1	Na 0.5	Na 1.0	Na 2.0
CO	13.9 ± 0.12 ^{A}	11.89 ± 0.29 ^{B}	11.01 ± 0.11 ^{C}	10.55 ± 0.24 ^{D}	9.87 ± 0.09 ^{E}
CO_2	6.42 ± 0.15 ^{A}	7.11 ± 0.17 ^{B}	7.28 ± 0.08 ^{B}	7.56 ± 0.11 ^{C}	8.0 ± 0.21 ^{D}
Char + Coke	40.2	44.67	48.01	50.75	51.3
*Char **	12.32 ± 0.48 ^{A}	17.01 ± 0.61 ^{B}	20.71 ± 0.33 ^{C}	23.66 ± 0.31 ^{D}	24.46 ± 0.39 ^{D}
*Coke ***	27.87 ± 0.21 ^{A}	27.66 ± 0.29 ^{AB}	27.3 ± 0.18 ^{B}	27.09 ± 0.27 ^{BC}	26.83 ± 0.20 ^{C}
Aromatic hydrocarbons	24.04 ± 0.40 ^{A}	19.43 ± 0.26 ^{B}	18.01 ± 0.31 ^{C}	16.93 ± 0.33 ^{D}	14.87 ± 0.14 ^{E}
Olefins (C2-C4)	6.69 ± 0.18 ^{A}	6.01 ± 0.11 ^{B}	5.73 ± 0.36 ^{BC}	5.19 ± 0.22 ^{C}	4.54 ± 0.09 ^{D}
Oxygenated Compounds	0.23 ± 0.04 ^{A}	1.59 ± 0.14 ^{B}	1.81 ± 0.03 ^{C}	2.13 ± 0.10 ^{D}	2.32 ± 0.14 ^{D}
Total Carbon Closure	91.48 ± 0.88 ^{A}	90.7 ± 0.71 ^{A}	91.85 ± 0.69 ^{A}	93.11 ± 1.89 ^{A}	90.9 ± 0.84 ^{A}
	Aromatics Selectivity (%)				
Benzene	6.06 ± 0.09 ^{A}	4.96 ± 0.08 ^{B}	4.81 ± 0.14 ^{BC}	4.69 ± 0.10 ^{C}	4.5 ± 0.22 ^{C}
Toluene	15.51 ± 0.14 ^{A}	14.29 ± 0.19 ^{B}	13.96 ± 0.17 ^{B}	13.57 ± 0.10 ^{C}	13.22 ± 0.13 ^{D}
Ethyl Benzene	1.08 ± 0.09 ^{A}	1.11 ± 0.06 ^{A}	1.09 ± 0.05 ^{A}	1.03 ± 0.09 ^{A}	0.98 ± 0.07 ^{A}
Xylene	16.89 ± 0.21 ^{A}	16.98 ± 0.13 ^{A}	17.11 ± 0.15 ^{AB}	17.27 ± 0.07 ^{B}	17.3 ± 0.11 ^{B}
C9 Aromatics	15.06 ± 0.19 ^{A}	14.87 ± 0.10 ^{A}	14.53 ± 0.11 ^{B}	14.25 ± 0.16 ^{BC}	13.98 ± 0.12 ^{C}
C10+ Aromatics	40.18	41.37	41.56	41.73	43.74
Naphthalenes	27.34 ± 0.21 ^{A}	30.43 ± 0.33 ^{B}	31.24 ± 0.20 ^{C}	31.69 ± 0.31 ^{CD}	32.11 ± 0.08 ^{D}
Fluorene, Anthracene	12.85 ± 0.15 ^{A}	10.94 ± 0.14 ^{B}	10.32 ± 0.10 ^{C}	10.04 ± 0.18 ^{CD}	9.83 ± 0.11 ^{D}

Chapter 3

Table S1. Detailed product distributions from *in-situ* catalytic pyrolysis of biomass, HZSM-5 catalyst doped with various amounts of Ca.

Component	Overall Carbon Yield (C %)									
	Control	Std. dev	Ca 0.5	Std. dev	Ca 1.0	Std. dev	Ca 2.0	Std. dev	Ca 5.0	Std. dev
Aromatic hydrocarbons	22.35	0.35	22.90	0.28	20.79	0.20	15.44	0.37	9.85	0.35
Phenols	0.06	0.04	0.09	0.03	0.12	0.02	0.64	0.06	1.44	0.11
Guaiacols	0.00	0.00	0.05	0.02	0.13	0.03	0.89	0.14	1.77	0.08
Furans	0.00	0.00	0.12	0.04	0.40	0.12	1.57	0.11	2.89	0.02
Ketones	0.04	0.06	0.04	0.05	0.12	0.04	0.40	0.06	0.86	0.04
Oxygenated compounds	0.10	0.02	0.29	0.01	0.76	0.09	3.50	0.15	6.95	0.25
Total carbon yield	22.45	0.37	23.19	0.27	21.55	0.29	18.94	0.52	16.80	0.60

Table S2. Detailed product distributions from *in-situ* catalytic pyrolysis of biomass, HZSM-5 catalyst doped with various amounts of K.

Component	Overall Carbon Yield (C %)									
	Control	Std. dev	K 0.5	Std. dev	K 1.0	Std. dev	K 2.0	Std. dev	K 5.0	Std. dev
Aromatic hydrocarbons	22.35	0.35	13.09	0.33	4.91	0.27	1.43	0.31	0.11	0.04
Phenols	0.06	0.04	0.48	0.06	1.95	0.06	2.27	0.18	2.57	0.19
Guaiacols	0	0	0.52	0.04	2.08	0.10	2.94	0.10	3.10	0.15
Furans	0	0	0.97	0.09	1.66	0.17	3.60	0.26	4.33	0.24
Ketones	0.04	0.06	0.04	0.05	0.38	0.05	0.63	0.05	0.60	0.16
Oxygenated compounds	0.1	0.02	2.00	0.12	6.07	0.26	9.43	0.59	10.59	0.44
Total carbon yield	22.45	0.37	15.08	0.21	10.98	0.53	10.86	0.28	10.70	0.40

Table S3. Detailed product distributions from *in-situ* catalytic pyrolysis of biomass, HZSM-5 catalyst doped with various amounts of Na.

Component	Overall Carbon Yield (C %)									
	Control	Std. dev	Na 0.5	Std. dev	Na 1.0	Std. dev	Na 2.0	Std. dev	Na 5.0	Std. dev
Aromatic hydrocarbons	22.35	0.35	14.96	0.11	5.52	0.29	2.12	0.23	0.20	0.06
Phenols	0.06	0.04	0.28	0.05	1.91	0.01	2.13	0.09	2.50	0.27
Guaiacols	0	0	0.64	0.06	1.99	0.08	2.75	0.04	3.25	0.09
Furans	0	0	1.10	0.03	1.42	0.11	3.25	0.09	4.09	0.11
Ketones	0.04	0.06	0.00	0.00	0.29	0.03	0.63	0.05	0.77	0.08
Oxygenated compounds	0.1	0.02	2.02	0.08	5.61	0.18	8.74	0.27	10.61	0.21
Total carbon yield	22.45	0.37	16.98	0.04	11.12	0.11	10.86	0.04	10.81	0.15

Chapter 4

Table S1. Ultimate analysis of raw and torrefied samples

Feedstock	Carbon (wt.%)	Std.dev	Hydrogen (wt.%)	Std.dev	Nitrogen (wt.%)	Std.dev	Oxygen (wt.%)
Raw Pine	45.86	0.02	6.60	0.05	0.25	0.04	47.30
RLP	65.52	0.14	5.63	0.04	0.25	0.00	28.60
TP 150	65.90	0.25	5.44	0.03	0.25	0.03	28.42
TP 175	66.29	0.31	5.41	0.11	0.24	0.01	28.07
TP 200	67.34	0.23	5.41	0.11	0.23	0.00	27.03
TP 225	67.78	0.14	5.33	0.03	0.21	0.00	26.68
Raw Switchgrass	43.67	0.17	6.18	0.08	0.59	0.02	49.57
RLS	64.88	0.50	5.69	0.08	0.65	0.00	28.79
TS 150	65.17	0.11	5.62	0.01	0.64	0.01	28.58
TS 175	65.77	0.21	5.68	0.01	0.61	0.00	27.95
TS 200	65.83	0.11	5.63	0.01	0.63	0.01	27.92
TS 225	66.59	0.27	5.57	0.02	0.62	0.01	27.23

Table S2. Major compounds identified and quantified from GC/MS library

Aromatic Hydrocarbons	Phenols	Guaiacols	Syringols
Benzene	Phenol	Phenol, 2-methoxy (guaiacol)	Phenol, 2,6 dimethoxy (syringol)
Toluene	Phenol, 2-methyl (o-cresol)	Phenol, 2-methoxy-4-methyl (creosol)	
Xylene	Phenol, 4-methyl (p-cresol)	Phenol, 4-ethyl 2-methoxy (ethyl guaiacol)	
Ethyl benzene	Phenol, 2,4-dimethyl	Eugenol	
Indane	Phenol, 3,5 dimethyl	Iso-eugenol	
Indene	Phenol, 2,4,6 trimethyl	Phenol, 2-methoxy 4-vinyl	
Naphthalene	Phenol, 3-ethyl	Vanillin	
Naphthalene, 1-methyl	Phenol, 4-ethyl		
Naphthalene, 2,6 dimethyl	Catechol		
Naphthalene, 2-methyl	Phenol, 4-vinyl		
Phenanthrene	Catechol, 4-methyl		
Fluorene			

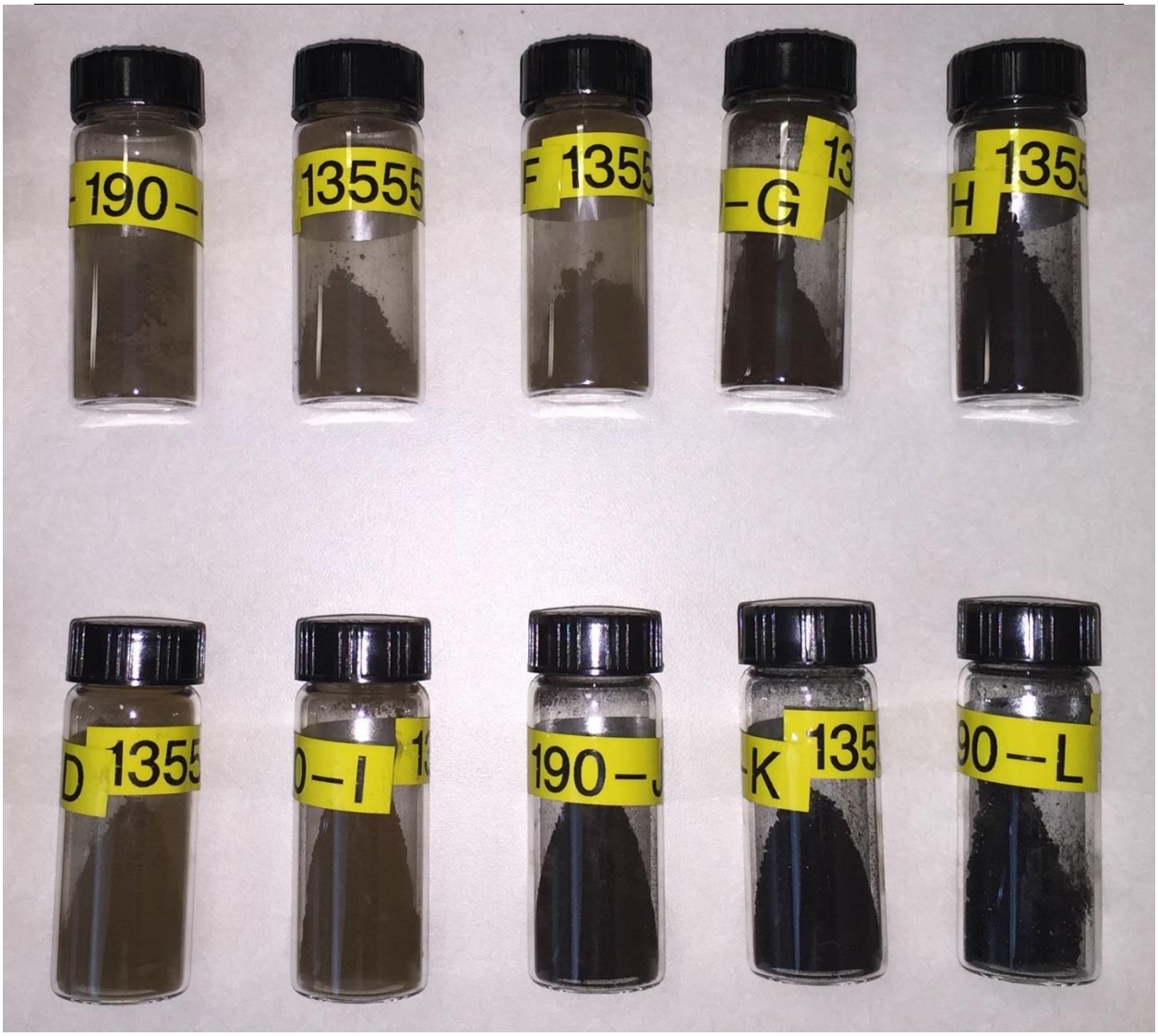

Figure S1. Top row (left to right): RLP, TP 150, TP 175, TP 200, TP 225; Bottom row: RLS, TS 150, TS 175, TS 200, TS 225. Change in the color of the lignin samples could be seen with increasing torrefaction temperature